RECHARGE FROM EPHEMERAL STREAMS: CASE STUDY IN ARIZONA

by

Boumedine Hadj-Kaddour

A Thesis Submitted to the Faculty of the

DEPARTMENT OF HYDROLOGY AND WATER RESOURCES

In Partial Fulfillment of the Requirements
For the Degree of

MASTER OF SCIENCE
WITH A MAJOR IN HYDROLOGY

In the Graduate College

THE UNIVERSITY OF ARIZONA

1 9 8 3

STATEMENT BY AUTHOR

This thesis has been submitted in partial fulfillment of requirements for an advanced degree at The University of Arizona and is deposited in the University Library to be made available to borrowers under rules of the Library.

Brief quotations from this thesis are allowable without special permission, provided that accurate acknowledgment of source is made. Requests for permission for extended quotation from or reproduction of this manuscript in whole or in part may be granted by the head of the major department or the Dean of the Graduate College when in his judgment the proposed use of the material is in the interests of scholarship. In all other instances, however, permission must be obtained from the author.

SIGNED: 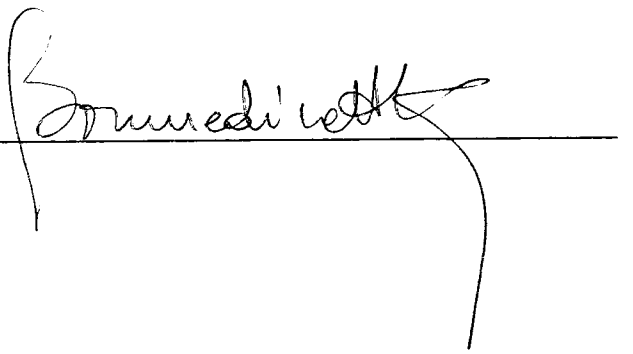

APPROVAL BY THESIS DIRECTOR

This thesis has been approved on the date shown below:

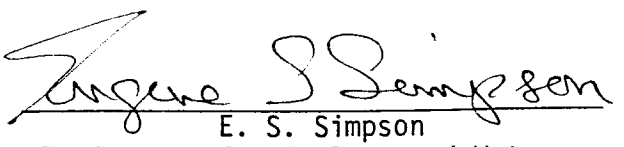

E. S. Simpson
Professor of Hydrology and Water Resources

1 August 1983
Date

ACKNOWLEDGMENTS

The completion of this thesis would not have been possible without the help and guidance of many people. I am especially grateful to my thesis director, Dr. E. S. Simpson, for his continual aid and advice during the course of this study. Dr. N. Buras, Dr. T. E. A. van Hylckama, and Dr. G. Wilson served on my thesis committee, and I thank them for their assistance.

Sincere thanks go to Dr. G. Wilson, Dr. T. E. A. van Hylckama, Dr. M. Fogel, Eilon Adar, Todd Rasmussen, and Mark Olson for their assistance and helpful suggestions, particularly during the early stages of this project. I would also like to thank Sarah Adams for typing the manuscript, and my friends Kamel and Hayett Saka, A. E. K. and Jacqui Mekias, Andrea D. Behrmann and Mark Olson for making my stay in the U.S. an enjoyable experience.

Funding was in part received from King Abdulaziz University project--a project of the United States-Saudi Arabian Joint Commission on Economic Cooperation, for which I am sincerely thankful.

TABLE OF CONTENTS

TABLE OF CONTENTS--Continued

LIST OF ILLUSTRATIONS

LIST OF ILLUSTRATIONS--Continued

LIST OF ILLUSTRATIONS--Continued

LIST OF TABLES

ABSTRACT

Infiltration losses and recharge to groundwater at a section of Rillito Creek at Tucson, Arizona, were analyzed using data from two flood events in December 1959 and January 1960. Assuming infiltration losses are a function of stream discharge and using empirical equations developed by the U.S. Geological Survey, infiltration loss at the section was estimated to be 2.24×10^6 m^3/km.

Estimates of recharge were obtained by two indirect methods: (1) A deconvolution integral in which the impulse response function is derived from the one-dimensional diffusion equation and the output functions are based on well hydrographs. The recharge values ranged between 1.41×10^6 m^3/km and 2.07×10^6 m^3/km depending on values of aquifer diffusivity obtained from the literature (α_1 = 6,000 m^2/day and α_2 = 3,000 m^2/day). (2) A groundwater mound method gave a recharge value ranging between 0.86×10^6 m^3/km and 1.29×10^6 m^3/km depending on the effective porosity values (0.10, 0.15).

Over all, an average of 70 percent of transmission losses reached and recharged the groundwater reservoir. However, this figure should not be generalized because recharge conditions are favorable in the Rillito Creek area.

CHAPTER 1

INTRODUCTION

In most of the arid and semi-arid regions of the western United States, groundwater is regarded as a major, and sometimes the only, source of water supply. Oftentimes water is withdrawn at a rate higher than it is being replenished by natural recharge and being balanced by a decrease in natural discharge. In many of these states (Arizona, California, Nevada) where water has been removed from storage by pumping, the former virgin steady-state condition is no longer valid in the groundwater system. To properly manage groundwater resources, a balance among groundwater extraction, recharge, and discharge should be imposed on the aquifer system (Theis, 1940; Bredehoeft and others, 1982). Of the three components, recharge plays an important role in reaching a new steady state in the aquifer system.

Statement of the Problem

Of all components of the hydrological cycle, one of the most difficult to evaluate is groundwater recharge. This evaluation problem is critical in areas of low precipitation where groundwater resources are especially important and recharge is erratic.

In arid regions, a large fraction of, sometimes most, natural recharge to groundwater is derived from intermittent flood flow in stream channels in alluvial deposits. The evaluation of channel recharge has been approached by many investigators (Smith, 1910;

Burkham, 1970; Anderson, 1972; Davidson, 1973; and Keith, 1981) through analysis of streamflow loss, also called transmission loss, inflow loss, and infiltration loss. Streamflow loss is defined as loss in a stream channel such that the volume of flow passing a particular section of a stream channel is reduced as the flood wave travels downstream. However, not all the water which passes into the streambed material during a flood event reaches the groundwater reservoir as recharge. Among these investigators, Burkham (1970, p. 11), with respect to the Tucson basin, stated that "... the part of the average annual infiltrated water that reaches the groundwater reservoir is not known but probably is more than 90 percent." This statement seems to be pure speculation. Nowhere does Burkham cite a study to verify this percentage. The problem may be posed in the form of a question: What fraction of infiltrated water actually reaches the water table as groundwater recharge?

This report includes the following:

1. Outline of physical laws relating to recharge.
2. Literature review on ephemeral streamflow recharge.
3. Application of the deconvolution integral and the groundwater mound methods to a section of Rillito Creek to obtain estimates of recharge.
4. Estimate of recharge/transmission loss ratio at the above river section.

CHAPTER 2

WATER IN THE VADOSE ZONE

Introduction

It has long been recognized that recharge to the groundwater body must traverse the unsaturated zone, and that groundwater flow must be continuous with the unsaturated flow above the water table (Freeze, 1969).

In the present study I shall use the classification scheme for subsurface water suggested by Davis and De Wiest (1966), illustrated in Figure 1. In this illustration there are no sharp boundaries between the various types of water. Water in the vadose zone, herein of interest, is divided into soil water, intermediate vadose water, and water in the capillary fringe. Most of the following discussion is taken from Davis and De Wiest (1966, p. 39-40). In the soil horizon the soil water is subject to a great variation in quantity and quality in response to evapotranspiration. The water in the intermediate zone, called suspended or vadose water, can be several hundred feet thick in arid regions. The moisture content in this zone can range between near saturation to below the specific retention of the porous media. The lowest horizon of the vadose zone is called the capillary fringe. This horizon is in two parts. The upper part has numerous pockets of air that slows the movement of water, whereas the lower part of the fringe is fully saturated to the groundwater reservoir. The water table is

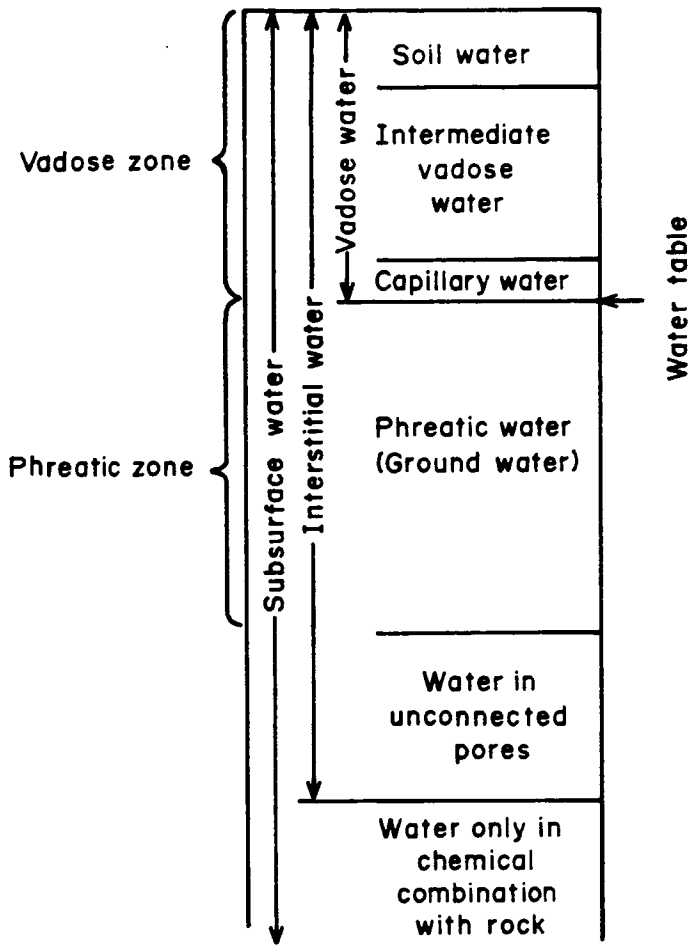

Figure 1. Classification of subsurface water. (After Davis and De Wiest, 1966)

defined as the surface where water pressure is exactly atmospheric. The pressure of water above this surface is below atmospheric (or negative), whereas water below this surface is above atmospheric (or positive).

The processes within the unsaturated zone that can be expected to lead to continuity of flow with the saturated zone are infiltration and recharge. Freeze (1969) defines these two terms as:

> Infiltration is the entry into the soil of water made available at the ground surface, together with the associated downward flow.
>
> Recharge is the entry into the saturated zone of water made available at the water table surface, together with the associated flow away from the water table within the saturated zone.

The rest of this chapter describes the physical phenomena and the mathematics associated with the unsaturated zone.

Background Physics

In order to discuss the potentials and forces in soil water, it is of prime importance to define certain terms such as force, work, energy, potentials, and gradients. Most of the following information is taken from Remson and Randolph (1962).

Force and Work

Force can be described as the cause of a change in the state of rest or state of uniform motion of a body. The relationship is stated by Newton's second law of motion.

$$F = Ma \tag{1}$$

where

F = force, in gram centimeters per square second

M = mass of the body, in grams

a = acceleration, in centimeters per square second.

Work is the product of force and distance, with the body moving in the direction of the force. It is expressed as:

$$W = F \times \cos A \qquad (2)$$

where

F = the force causing the motion, in gram-cm/sec^2

x = the distance that the body moves, in cm

A = the angle between the direction of the acting force and the direction of the moving body

W = the performed work, in gram-cm^2/sec^2

Energy

Energy may be defined as the maximum capacity of a mass of substance for doing work. Energy has the same dimensions as work.

Potential and Gradient

Potential is the work required to take a unit mass or volume from a datum to the point in question. Potential gradient at a point is the rate of change of potential with distance measured in the direction in which this variation is a maximum (Gray, 1958).

Potential in Soil Water

A soil physics terminology committee of the International Soil Science Society (Aslyng et al, 1963) defined the total potential of soil water in a conceptual manner as: "... the amount of work that must be done per unit quantity of pure water in order to transport reversibly and isothermally an infinitessimal quantity of water from a pool of pure water at a specified elevation at atmospheric pressure to the soil water (at the point of consideration)." This definition is incomplete because no change in soil wetness can in practice be carried out reversibly, or that the total potential need not be restricted to isothermal conditions. A most serious difficulty is encountered in attempting to allocate the total potential among the various components or mechanisms which may not be independent (Hillel, 1971).

Soil water is subject to several field forces, which result in a different potential from that of pure water. In unsaturated soils such field forces forming the potential are presumed to be due to: (a) gravitational attraction, (b) hydrostatic pressure differences, (c) osmotic pressure difference, (d) adhesion of water to the soil matrix, (e) temperature gradient, and (f) gradient of chemical potential due to changes in solute concentration. The last two factors are negligible except in a thermodynamic context where the thermal and chemical potentials are included. Hence, the total potential of soil water will be considered as the sum of four separate components.

$$\phi_t = \phi_g + \phi_p + \phi_o + \phi_a + \ldots \qquad (3)$$

where, ϕ_t is the total potential, ϕ_g is the gravitational potential, ϕ_p is the pressure potential, ϕ_o is the osmotic potential, ϕ_a is the adhesion of water potential, and the dots on the right side signify that the aforementioned last two factors are theoretically possible.

Gravitational Potential

The soil water is subject to the earth's gravitational field. The gravitational potential of soil water is the energy (Eg) required to move a mass (M) of water occupying a volume (V) from a datum to a given position (Z) in the field against the attraction of gravity (G). Hence, the gravitational potential energy (Eg) can be written as:

$$Eg = MGZ = \rho_w VGZ \tag{4}$$

where ρ_w is the density of water and G the acceleration of gravity. In terms of potential energy per unit mass, the gravitational potential (ϕ_g) is:

$$\phi_g = GZ \tag{5}$$

or in terms of potential energy per unit volume

$$\phi_g = {}_wGZ \tag{6}$$

Hillel (1971) points out that the gravitational potential is independent of the chemical and pressure conditions of soil water, but dependent only on relative elevation.

Pressure Potential

Soil water can exist at lower or higher pressure than the atmospheric pressure. When the hydrostatic pressure is higher, the pressure potential is considered positive. With reference to the atmospheric pressure (Po), the hydrostatic pressure of water can be expressed as:

$$P = \rho_w GH \tag{7}$$

where H is the submergence depth below the free water surface. Then the potential energy (Ep) of this water is (Hillel, 1971):

$$Ep = P\ dV \tag{8}$$

or per unit volume, the pressure potential is:

$$\phi_p = P \tag{9}$$

In the other case, when the soil water is at pressure lower than atmospheric, the pressure potential is considered negative. This negative pressure potential is often called capillary potential or matrix potential, and it results from the capillary and adsorptive forces due to the soil matrix (Hillel, 1971). These forces attract and bind water in the soil and lower its potential energy below that of bulk water.

Osmotic Pressure

Osmotic pressure potential, the third major type of potential, is due to differences of both soluble salts and anions and cations in

the electrostatic (or Gouy) double layers associated with the solid surfaces of soil particles (Remson and Randolph, 1962). The osmotic effect is only important in the interaction between plant roots and soil moisture, and processes involving vapor diffusion (Hillel, 1971).

Adhesion of Water Potential

Adhesive forces between solid and water are due to chemical forces, to electrostatic attraction of the nucleus of one molecule for the electrons of another, and mainly to the attraction between the positive ends of water dipoles and the negatively charged soil particles. However, as Remson and Randolph (1962) mentioned: "... these adsorptive forces become prominent only when soils are dried far beyond the state of dryness that is normally found in nature."

Flow of Water in Unsaturated Soils

Recharge to the groundwater is continuous with the unsaturated flow above the water table. The processes with the unsaturated flow are in general complicated and difficult to describe quantitatively, since they involve changes in the state and content of soil water during flow.

Movement of Soil Moisture

Soil moisture movement occurs in three different manners: as liquid water, water vapor, and adsorbed water. The latter is important only when the soil is very dry with a large specific surface. In this report movement only as liquid water will be considered. Such movement occurs in response to potential gradients as described earlier.

Redistribution of Soil Moisture

Among several investigators who looked for a physical explanation of the redistribution phenomenon of soil water at the cessation of infiltration are Schofield (1935), Richards (1936), Richards and Weaver (1944), Colman (1944), Youngs (1958), Staple (1962), and Biswas and others (1966).

Staple (1962), measuring at different times the soil water pressure (P) and the water content (θ) of a section of uniform silt loam, showed the existence of scanning curves. Thus, the relation between (θ) and (P) is not single valued when both drying and wetting processes occur. This discrepancy is commonly observed and referred to as hysteresis. Figure 2 illustrates a hypothetical soil water curve. The ABC curve represents the single valued relation between the water content and the pressure for a drying process; however the CDA curve is for a wetting process. The broken curves between ABC and CDA are scanning curves. This phenomenon complicates the mathematics as will be shown later.

Biswas and others (1966) in their study showed that redistribution of soil water after the cessation of infiltration within the soil profiles is dependent upon the initial depth of wetting and the soil water content-soil water pressure-capillary conductivity relationships.

Factors Influencing Redistribution

With respect to the potential gradients and the hysteric nature of the soil, two cases of the redistribution of soil water may result:

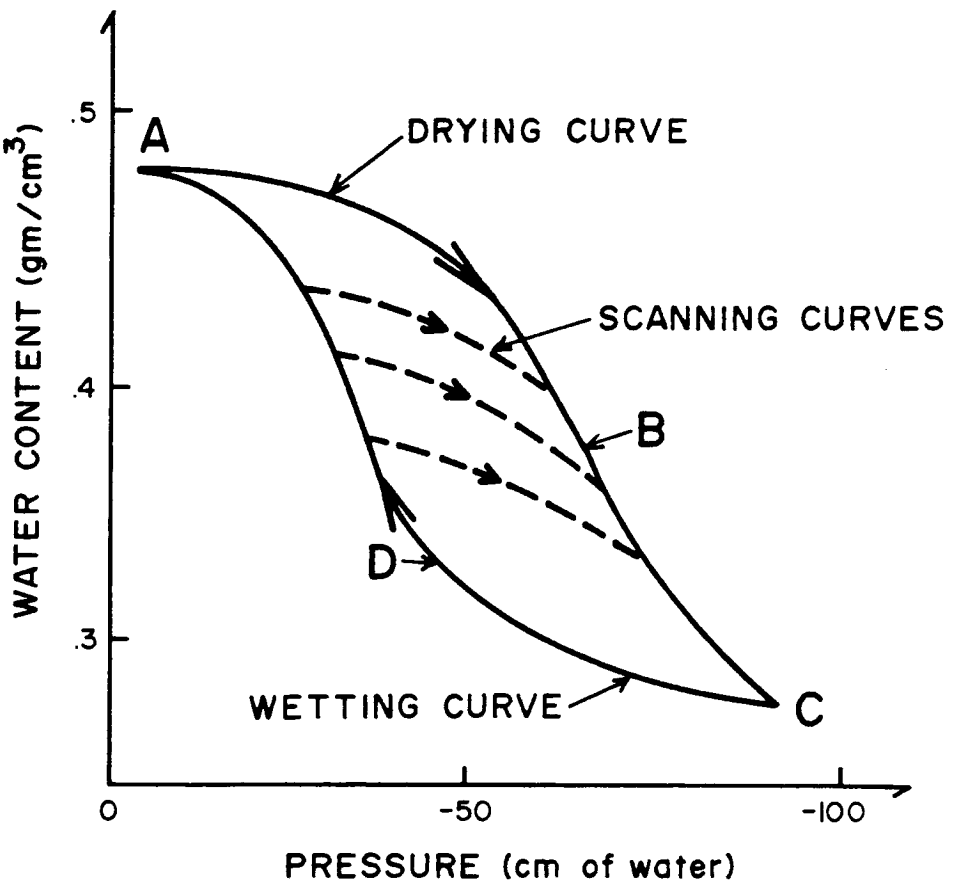

Figure 2. A hypothetical soil water characteristics showing the hysteric equilibrium relations between soil water content and soil water pressure. (After Biswas et al., 1966)

(1) Youngs (1958), using a non-destructive thermo-electric technique, found that the greater the depth of infiltration, the greater the redistribution rate. He also showed that water would first drain from the top of the profile and appear as an advancing bulge below the initially developed infiltration profile. Figure 3 illustrates this case. Using this figure Biswas and others (1966) approached the hysteresis problem mathematically. At time t_o, cessation of infiltration, the area under the curve delineated by t_o is saturated or near saturation. Then, at time t_o the flux of water, drained from the top and passing through the saturated zone, is equal to that entering the transition depth Z_1. This is true in the presence of a positive potential gradient that will drive the water to move downward. If we neglect the evapotranspiration, this flux can be expressed as:

$$-K_d\left(\frac{d\phi}{dZ}\right) = -K_w\left(\frac{d\phi}{dZ}\right)_{z=z_1} \tag{10}$$

where the subscripts d and w stand for drying and wetting stages, respectively. Biswas and others (1966) developed this equation and found good agreement between experimental and predicted theoretical values for glass beads.

Wilson and De Cook (1968) conducted a field study of the distribution of water in the vadose zone using a neutron logger. They examined the evolution of moisture profiles in the intermediate vadose zone after a flood event in the Santa Cruz River (Figure 4). The channel bottom of the river is about 25 meters above the water table

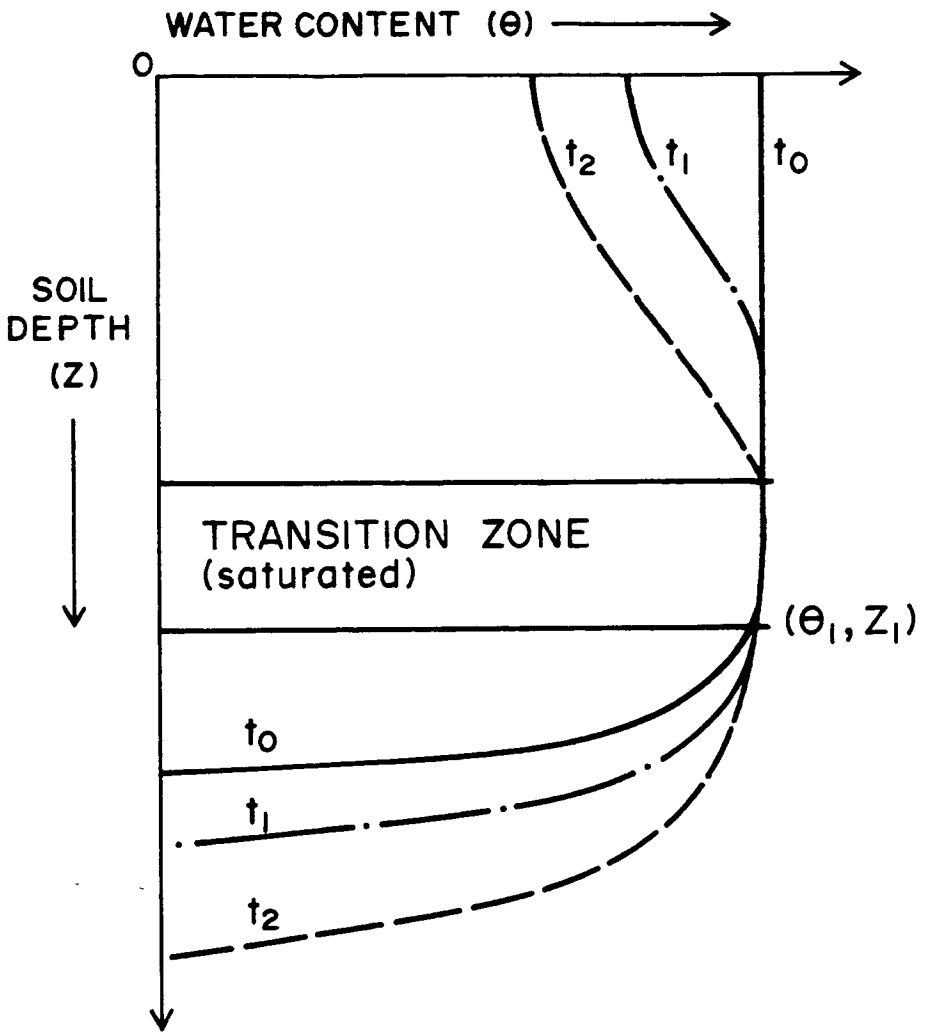

Figure 3. Hypothetical soil water profile during redistribution of water.

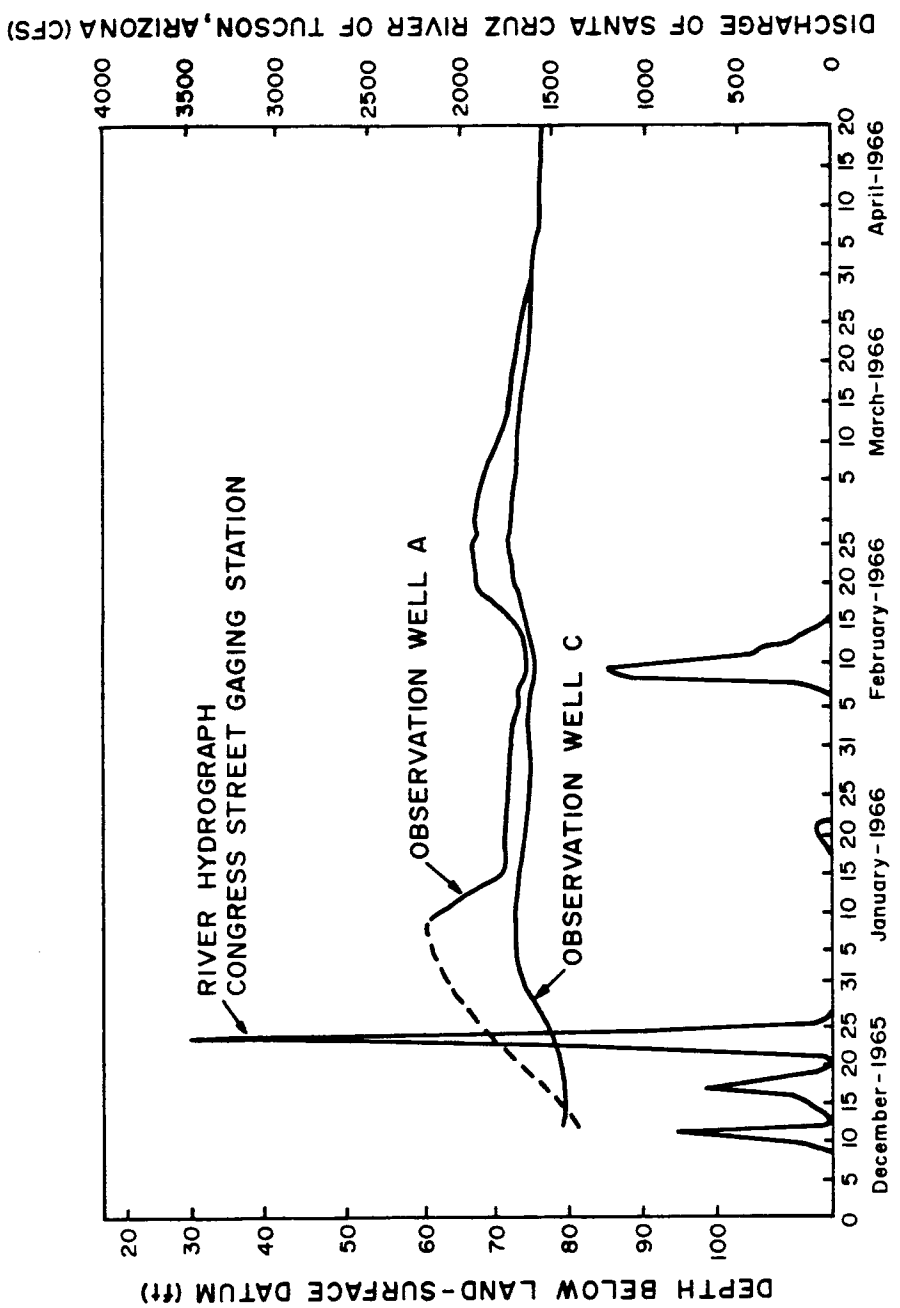

Figure 4. Hydrographs of flow in the Santa Cruz river and well hydrographs nearby. (After Wilson and De Cook, 1968)

aquifer. The existence of saturated or nearly saturated zones in the profile was clearly shown on the logs reported in Figure 5. This illustration, in accordance with the aforementioned theory, shows a downward flow in time.

The conclusion of Wilson and De Cook that the moisture pulse migrated downward and recharged the groundwater reservoir is based on observed recovery of the water table during the dissipation of the pulse and measured potential gradient with piezometers. The direction of water movement is a result of an energy gradient and not necessarily a moisture gradient.

(2) A second case may occur in which the right hand term of equation (10) goes to zero. This can occur when there is either equilibrium between the gravitational and capillary forces or when a negative total potential gradient exists. Under these conditions no moisture recharges the water table.

Before and after a flood event, van Hylckama (1982) made a series of soil moisture measurements by the neutron logging method near Buckeye, Arizona. These results are shown in Figure 6. This illustration indicates that the flood water did not penetrate deeper than about 0.3 meters during the four monitoring days. However, below this depth the moisture content remained remarkedly constant. It is also interesting to note that a certain layer at the depth between 1.15 and 2.0 meters has a much higher moisture content than the layer either immediately above or below it. Such observations are inconclusive and provide only circumstantial evidence because no one knowns exactly what kind of changes took place between the deepest

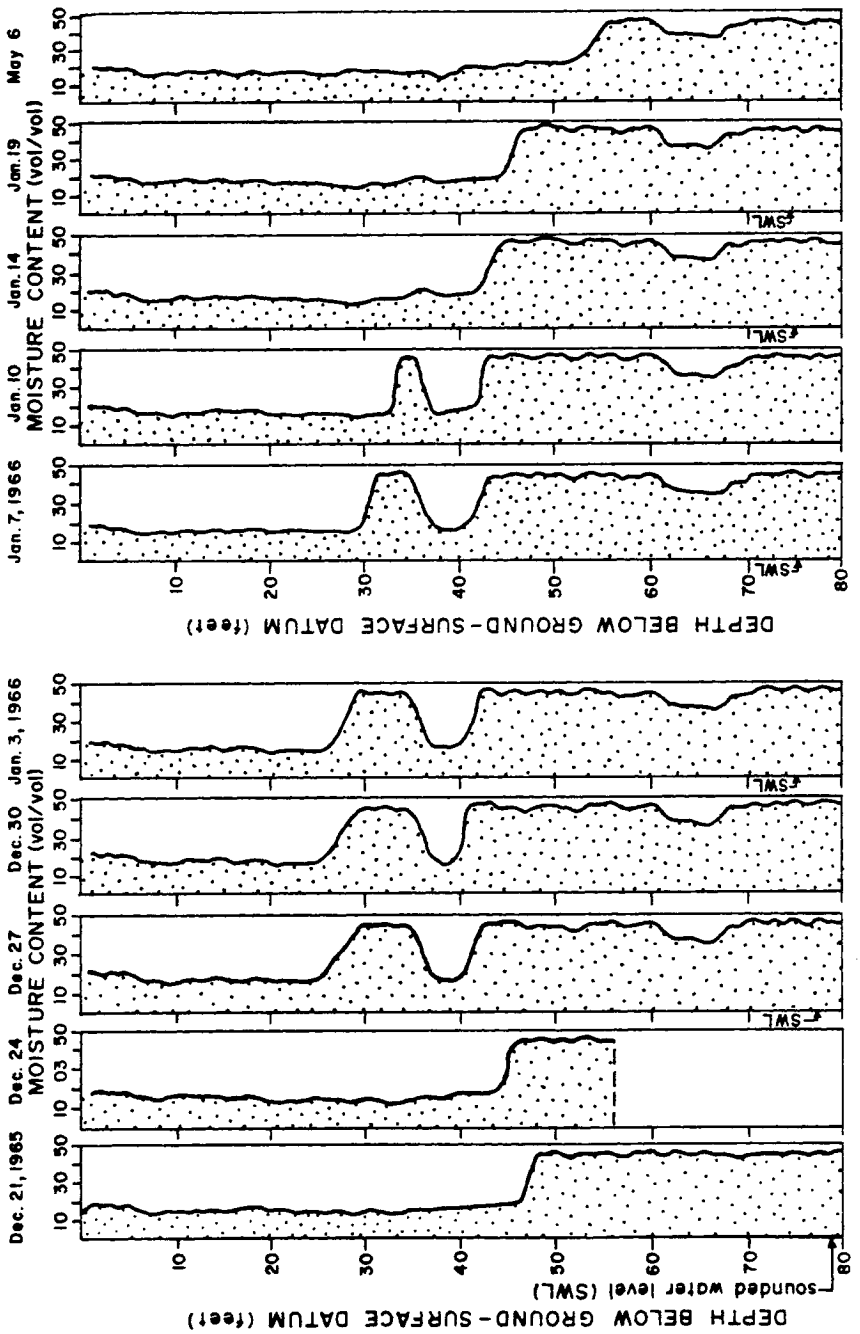

Figure 5. Evolution of the moisture content in the vadose zone. (After Wilson and De Cook, 1968)

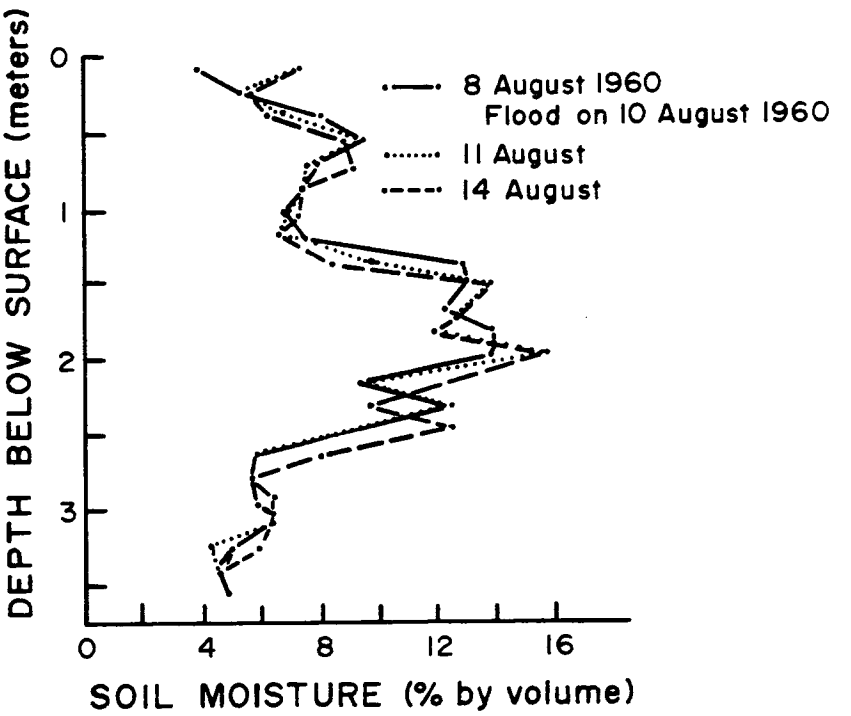

Figure 6. Soil-moisture profiles before and after a flood at the confluence of Waterman Wash and the Gila River, near Buckeye, Arizona. (After T. E. A. van Hylckama, 1982)

point of observation, 3.25 meters below the surface, and the groundwater reservoir. These figures seem to indicate that the small amount of water that enters the soil either evaporates directly from the soil or is transpired by the vegetation.

An illustration of the possibility of non-recharge is given in Figure 7, made by van Hylckama. Moisture contents, in percent by volume, were plotted at weekly or biweekly intervals for the period September 1964 to August 1965. Lines of equal soil moisture content were drawn through these points, and the amount of moisture present at different times and layers was indicated by the darkness of the shading. Nowhere is there any suggestion that any rainfall for the observed period has caused a significant increase in soil moisture below a depth of about 4.0 meters. Again, in the absence of potential measurements these exhibits are inconclusive. One can hypothesize that water had moved horizontally and then downward out of the reach of the neutron logger.

Factors Influencing Recharge

Clear water from mountain snowmelt can infiltrate rapidly, but most flow in arid regions carries high concentrations of suspended solids. With a decrease in the discharge, the silt settles out and may ultimately clog the streambed which results in a lower infiltration rate.

Among several investigators, Matlock (1965) looked at the relationships between silt content, velocity of flow, and the

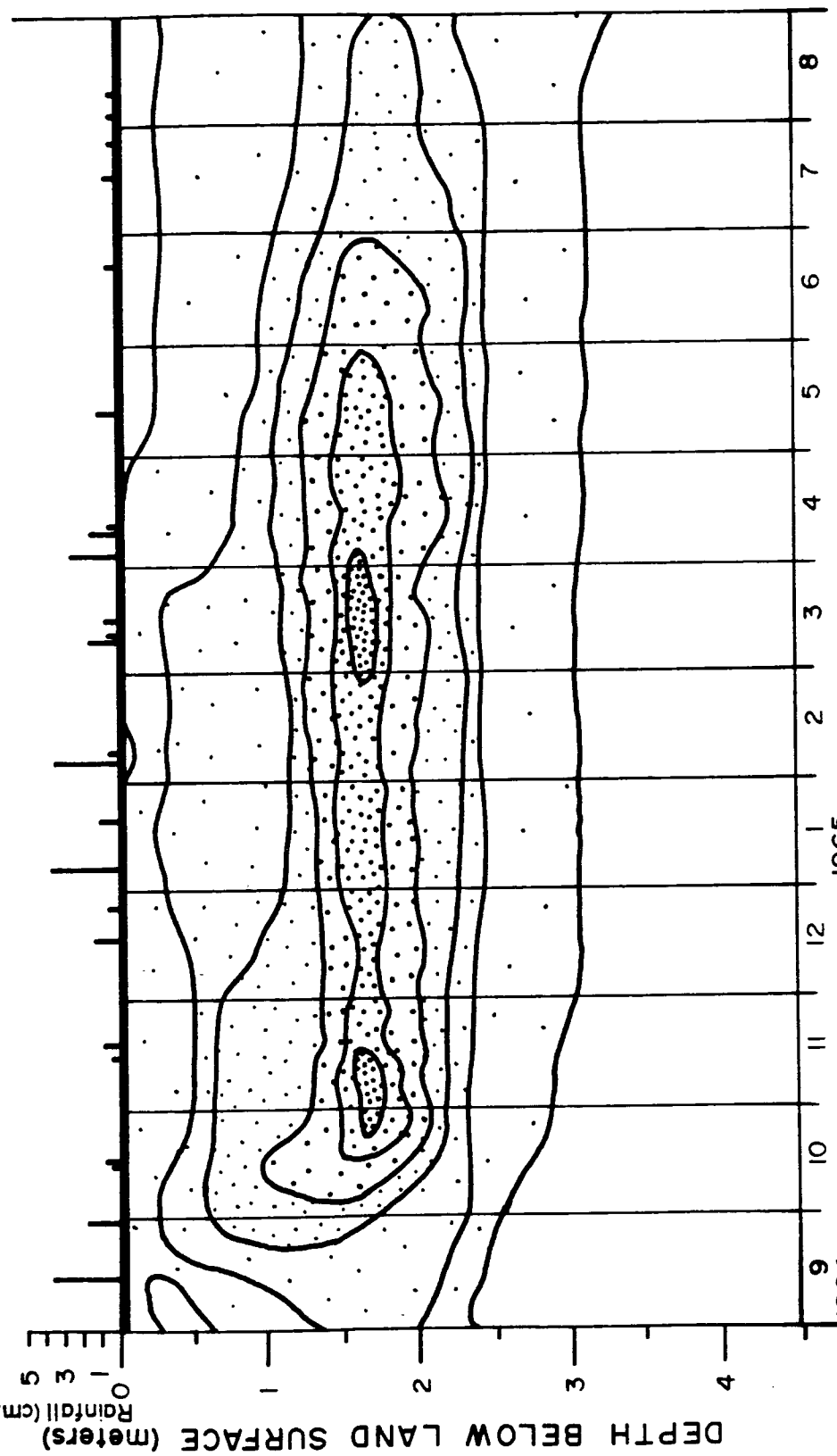

Figure 7. Isolines of soil moisture as measured at the Buckeye test site. The darker the shading the higher the moisture content. (After T. E. A. van Hylckama, 1982)

infiltration rate of a sand bed in alluvial channels. He concluded with the following points:

- Sediment content of flood water is available and depends on the source of the runoff, flow velocity, and streambed conditions.
- When the flow velocity decreases, there is a reduction of the capability to transport the suspended material; therefore, the sediment content decreases.
- Silty flow increases in suspended sediment with downstream distance as additional runoff carrying large amounts of fine material enters the channel from side washes. This increase will result in an immediate decrease in infiltration rate and ultimate bed sealing.
- Infiltration rates vary with the flow velocity in the range of 2 to 5 feet per second. Below 2 feet per second the infiltration rate may be higher for relatively clear water than it is for higher velocities.
- For a constant flow velocity in an alluvial channel, the infiltration rate will have an inverse relationship to the concentration of the suspended sediment. Furthermore, with clear water, particle rearrangement and packing at the bed surface will reduce the infiltration rate and provide a limit.
- The past history of a channel may be the most important single factor in determining the infiltration rate.

Unsaturated Versus Saturated Flow

The creation of an effective potential gradient causes a driving force which results in a soil water flow. The flow takes place in the direction of a decreasing potential and the rate of flow is proportional to this potential gradient if the hydraulic conductivity, $K(\theta)$, is constant. In saturated soils, the moving force is due to a gradient or positive pressure. However, in unsaturated soils the water is subject to a suction whose gradient likewise produces a moving force (Hillel, 1971), and water tends to flow from low suction to where it is high. In cases where suction is constant along a horizontal column there is no moving force.

The main important difference between unsaturated and saturated flow is in the hydraulic conductivity (K). When the pores are filled with water, the soil is said to be at saturation. The hydraulic conductivity, independent of the magnitude of the water potential or pressure, is maximal. On the other hand, when pores are partially filled with air, the soil is unsaturated. In this case, the hydraulic conductivity, sometimes called capillary conductivity, is smaller and is a function of the water content.

General Flow Equation

The flux in an unsaturated porous medium can be expressed in a generalized form of Darcy's law as:

$$\overline{q} = -\overline{\overline{K}}(\theta)\text{grad}(h) \qquad (11)$$

where $\overline{\overline{K}}$, the hydraulic conductivity tensor, is a function of the volumetric moisture content (i.e., volume of water per unit bulk volume) (θ). $K(\theta)$ is usually experimentally determined. The hydraulic head, h, is defined as:

$$h = \frac{P}{\rho w G} + Z \tag{12}$$

where

Z = elevation above the datum

P = pressure in the liquid phase

ρ_w = water density

G = gravity field.

Equation (12) is equivalent to equation (3), with all terms on the right-hand side of equation (3) neglected except gravitational attraction and hydrostatic pressure. The equation of continuity in three dimensions for transient flow of a compressible fluid is:

$$-\left[\frac{\partial(\rho z_x)}{\partial x} + \frac{\partial(\rho q_y)}{\partial y} + \frac{\partial(\rho q_z)}{\partial z}\right] = \frac{\partial}{\partial t}(\rho\theta) \tag{13a}$$

Substituting the appropriate form of Darcy's law (11) into (13a) the equation of continuity leads to:

$$\frac{\partial}{\partial x}(\rho\overline{\overline{K}}(\theta)\frac{\partial h}{\partial x}) + \frac{\partial}{\partial y}(\rho\overline{\overline{K}}(\theta)\frac{\partial h}{\partial y}) + \frac{\partial}{\partial z}(\rho\overline{\overline{K}}(\theta)\frac{\partial h}{\partial z}) = \frac{\partial}{\partial t}(\rho\theta) \tag{13b}$$

where the right-hand terms of the above equation represent the dewatering of a representative elementary volume within the porous medium.

Equation (13b) is a generalized equation of flow used to develop one, two, or three dimensional forms of the steady or transient flow equation for saturated or unsaturated flow of a compressible or incompressible fluid through a heterogeneous porous medium.

CHAPTER 3

RILLITO CREEK STUDY AREA

General Description

Rillito Creek is an ephemeral stream flowing east to west along the northern boundary of the Tucson basin and has long been recognized as a major contributor of recharge (Figure 8). With a total drainage area of 2,377 km^2, Rillito Creek is the largest tributary of the Santa Cruz river. The minor sub-drainage basins, tributaries to Rillito Creek, are: Sabino Creek, 92 km^2; Bear Creek, 42 km^2; Tanque Verde Creek, 111 km^2; Rincon Creek, 116 km^2; and Pantano Wash, 1184 km^2. About 20 percent of the total drainage area is mountainous with elevation above 1800 meters where snowfall is frequent during the winter. Of the rest, 60 percent encompasses most of the alluvial aquifer of the Tucson basin. The study area, as shown in Figure 9, is bounded by Tucson Boulevard on the east (0.80 km east of Campbell Avenue) and by Mountain Avenue on the west (0.70 km west of Campbell Avenue).

Climate

The climate of the Tucson basin is semi-arid with two distinct seasons: a hot summer and a moderate winter. In the higher elevations the temperature often drops below freezing in the winter and snow is common at the summits. In the lower elevations summer temperatures often exceed 38°C and in the winter season oscillate between 22°C

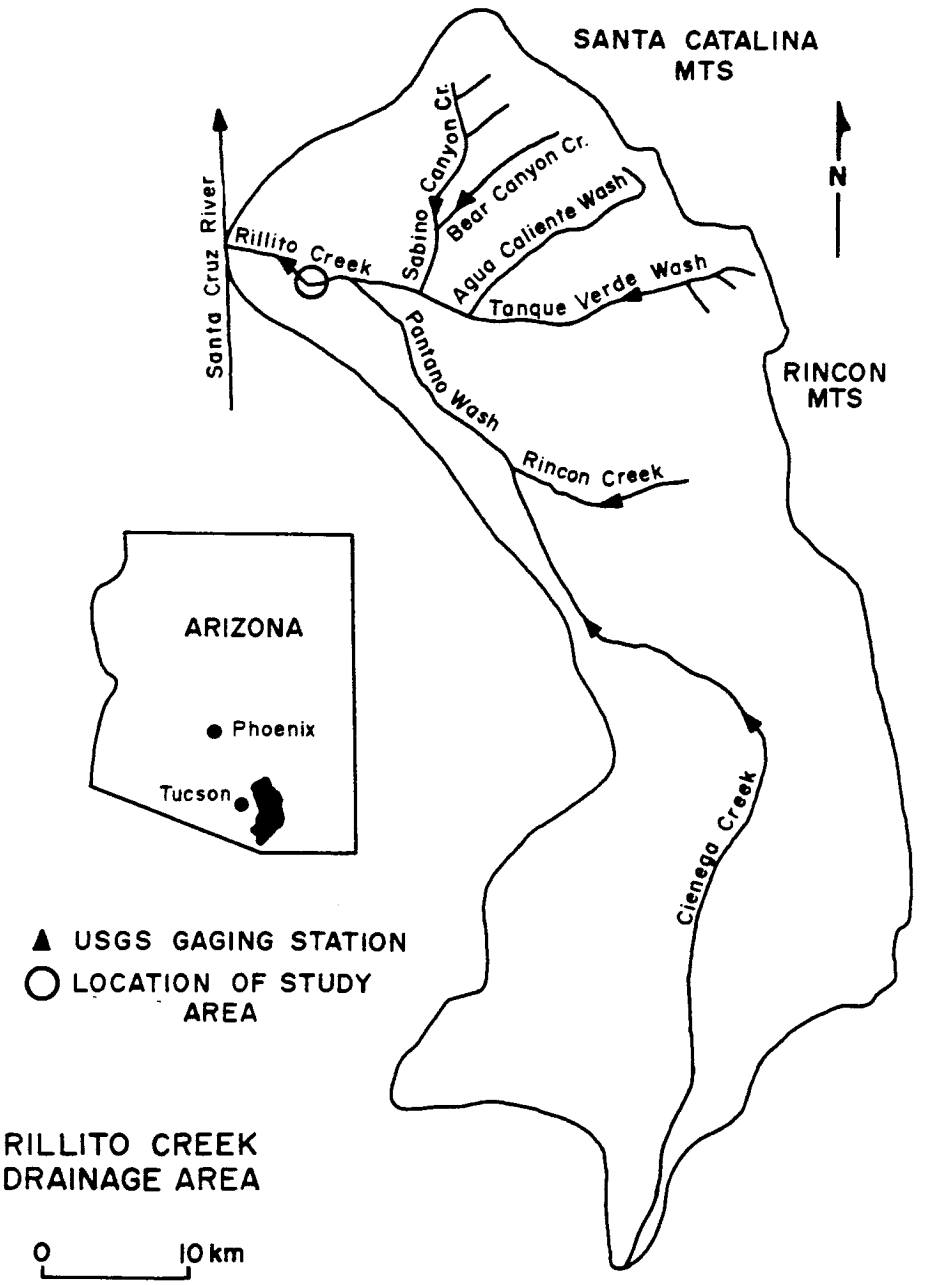

Figure 8. Rillito Creek drainage area and U.S. Geological Survey gaging stations.

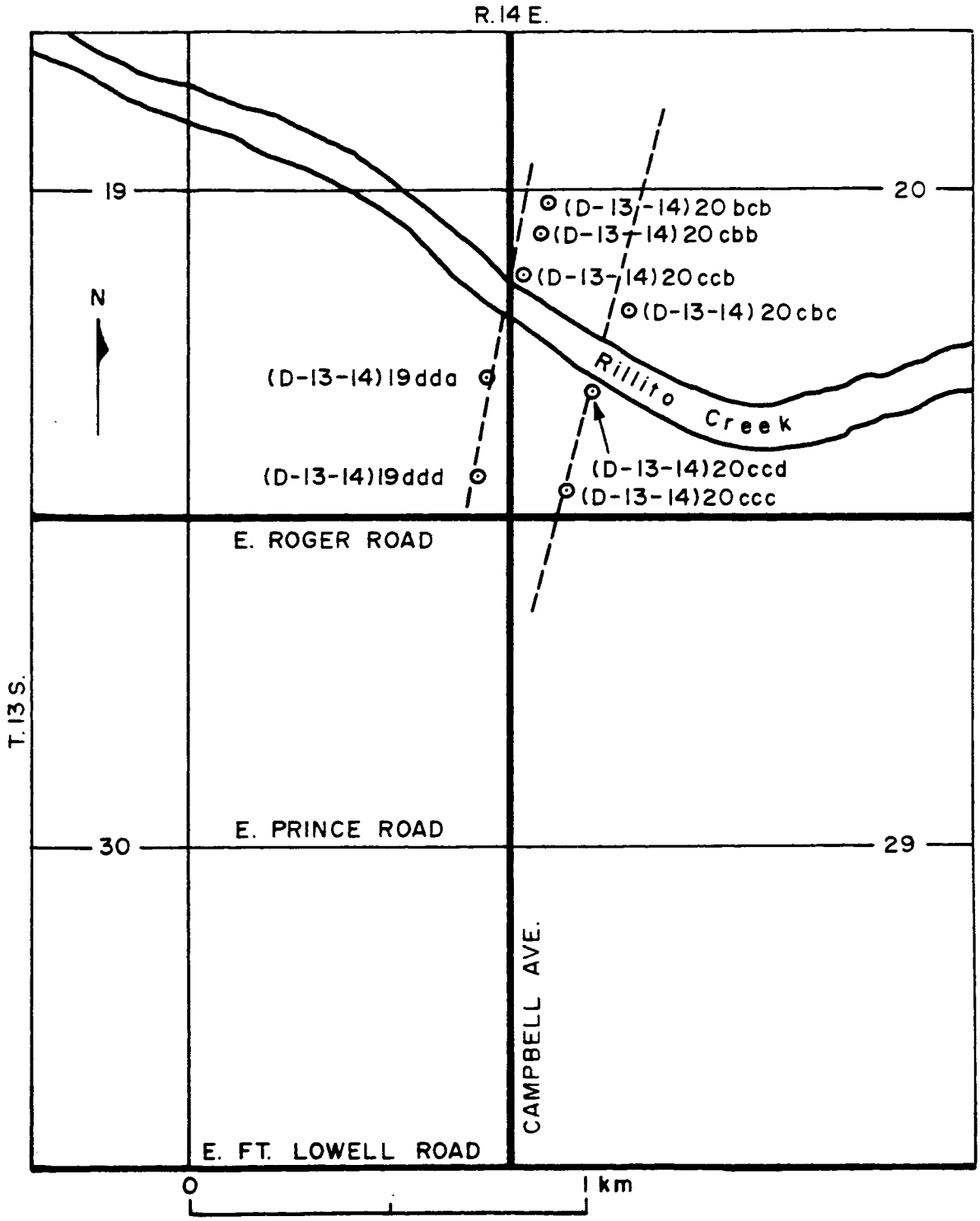

Figure 9. Location of profile lines of well measurements.

during the day and 2° C at night. The annual average precipitation (basin wide) is about 305 mm with extreme variability in time and space. Precipitation is almost equally distributed between the two seasons and increases with elevation. Slightly more than half of the annual precipitation occurs from late June to October as concentrated thunderstorms of short duration. The winter season (November through May) is characterized by low-intensity rainfall events of longer duration. Keith (1981) noted that summer precipitation is less variable than winter precipitation in frequency of occurrence and resulting runoff. Pan evaporation and potential evapotranspiration are 2032 mm and 1067 mm per year, respectively (Davidson, 1973).

Geology

The Santa Catalina-Rincon mountain complex is composed of highly fractured, faulted and folded metamorphic and igneous rocks. Rillito Creek is underlain by Recent alluvial deposits, which in turn are underlain by Quaternary basin fill deposits. The Recent alluvium is about 50 meters thick and the basin fill at the study area is about 125 meters thick (Figure 10) (Pashley, 1966).

Streamflow

Flashy summer rainstorms produce high-volume streamflows of short duration that rapidly dissipate. Winter rainfall of long duration contributes more to recharge (Keith, 1981) than summer rainfall.

Runoff in the Rillito Creek basin for the 1960 water-year, herein of interest, was about 69.08 x 10^6 m^3 (56,000 acre-feet) where

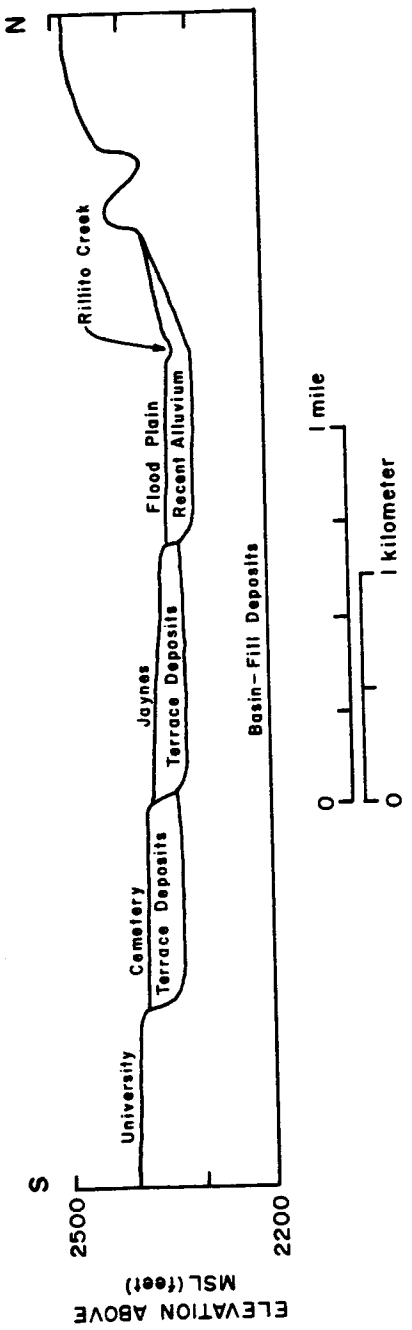

Figure 10. Geologic cross-section of Rillito Creek near Campbell Avenue. (After Pashley, 1966, Fig. 40)

16.65 x 10^6 m^3 (13,500 acre-feet) of this amount went past the Rillito gaging station at Oracle bridge located 4.27 km downstream of the study site. Of the 69.08 x 10^6 m^3, 49.34 x 10^6 m^3 (40,000 acre-feet) was measured at gaging stations on Sabino, Bear, and Rincon Creeks, and Pantano Wash at Vail. An addition 19.74 x 10^6 m^3 (16,000 acre-feet) of ungaged runoff was estimated by the Agriculture Engineering Department (unpublished files). Most of this runoff was derived from urban areas. Streamflow discharge data are available from the U.S. Geological Survey (1960).

Groundwater Levels

Smith (1910), with respect to well hydrographs, stated that "... the crests are due mainly to river flows in the winter, though minor crests were caused by the summer floods of 1907 and 1908." This observation was based partly on well hydrographs and partly on water temperature data. Recently, Keith (1981, p. 62) noted from a comparison of well hydrographs with streamflow data that the "... most obvious trend between streamflow in the Rillito and water-level response is that all significant water-level rises ... occur in response to winter flow." Furthermore, she noted that the recharge is negligible during the summer, even though summer flows accounted for 56 percent of the flow volume between 1931 and 1959 on Rillito Creek.

Daily groundwater level measurements were collected by the Soils, Water, and Engineering Department at and near the University of Arizona Experimental Farm. The locations of the wells are shown in Figure 9 and listed in Table 1. The Bureau of Land Management's

Table 1. Well identification and their normal distances from the centerline of the streambed, Rillito Creek.

Number	Location	Identifying names	Normal distance from the stream (meters)
1	(D-13-14)20bcb	Murphy #1	366.00 m (north)*
2	(D-13-14)20cbb	Murphy #4	198.00 m (north)
3	(D-13-14)20ccb	Murphy #7	49.00 m (north)
4	(D-13-14)20cbc	Murphy #5	140.00 m (north)
5	(D-13-14)19dda	Campbell #1	259.00 m (south)
6	(D-13-14)19ddd	Campbell #4	396.00 m (south)
7	(D-13-14)20ccd	Erwing #4	21.00 m (south)
8	(D-13-14)20ccc	Erwing #2	305.00 m (south)

*Indicates the side of the Rillito Creek.

location indices (Appendix A) also are given. Data for groundwater levels of interest are reported and graphed in Appendix B. Visual inspection suggests that the hydrograph peaks are due mainly to winter flows which confirms both Smith's and Keith's conclusions. The well hydrographs, called output functions in this study, will later be used for recharge computations by two different methods.

Evapotranspiration

Not all of the water which passes into the bed material during a flood event reaches the groundwater aquifer as recharge. Evaporation from the wetted channel after a flood has ceased and water used by the riparian vegetation as evapotranspiration are significant in semi-arid regions.

Sorey (1967) conducted a study on the volume of water lost by evaporation from the wetted streambeds along the Rillito Creek. He estimated an annual streambed evaporation of about 10.2 inches per year which converts to about 1.57×10^4 m^3/km.

Due to the dense concentration of riparian vegetation along the Rillito Creek, substantial streamflow infiltration or underflow may thus be lost through transpiration. The losses due to evapotranspiration along stream channels in the Tucson basin are unknown because specific studies have not been performed. Matlock (1965) reported that phreatophyte transpiration amounted to 23 percent of streamflow infiltration along Rillito Creek. Unfortunately, the method of computation was not discussed and the estimate was based on an unpublished water budget analysis. Despite numerous related studies

within the Tucson basin, the amount of evapotranspiration of infiltrated streamflow remains uncertain.

In addition to the degree of concentration of vegetation species, Olson (1982) mentioned that "... consideration should be given to seasonal variations, the short-term storage capability of the porous media, changes in infiltration rates, and stable isotope evidence" in estimating the evapotranspiration of streamflow infiltration. Hence, it seems that numerous variables affect evapotranspiration losses from streamflow infiltration. At least two major points should be emphasized: independent evapotranspiration estimates should be made for winter and summer flow regimes, and secondly Burkham's (1970) estimate that less than 10 percent is lost as evapotranspiration is questionable. From several sources Olson (1982) estimated that the groundwater recharge amounts to from 10 to 30 percent of streamflow infiltration during the summer, and 70 to 90 percent during the winter precipitation season.

CHAPTER 4

EPHEMERAL STREAMFLOW LOSS

Introduction

The infiltration of floodwaters through an ephemeral stream channel is a principal source of recharge to free surface aquifers in arid regions. This mechanism of recharge has been investigated in many regions by correlations between streamflow events and water level recoveries in nearby wells (Keith, 1981; Burkham, 1970; Foster, 1969; and Gross and others, 1976). Water-table rises occur within hours or a few days of runoff events, even when depths of the unsaturated zones are greater than several tens of meters. Individual streamflow recharge events are too transient to be detected by yearly or even monthly water level measurements, and the water table recovery may be overlooked and thus not taken into account unless there is continuous water level recording or measurements at short time intervals.

Previous Work

Burkham (1970) investigated the infiltration of ephemeral streamflow in the Tucson basin. He related the infiltration to the inflow by the empirical equation:

$$Q_f = C(Q_{inflow})^{0.8} \qquad (14a)$$

where

Q_f = infiltration rate (cfs), the difference between surface water inflow and outflow during corresponding time intervals in a reach

C = a variable coefficient

Q_{inflow} = surface-water inflow rate, in cfs

The coefficient and exponent in equation (14a) were determined by Burkham using the method of least squares. The results of the average annual infiltration loss per mile of channel and the total average annual infiltration loss in each channel reach, in the Tucson basin, are shown in Figure 11.

Lane and others (1971) looked at the same problem of transmission losses. They developed an inflow-outflow equation by using regression analysis on the Walnut Gulch watershed in southeastern Arizona. They concluded that "... the transmission losses, and hence the outflow volume, were found to be correlated significantly only to the volume of the inflow hydrograph."

Flug and others (1980) developed a stochastic event-based model to estimate groundwater recharge in a 23-kilometer section of Rillito Creek. The flow duration from streamflow events is used as an input into a transfer function relating streamflow to groundwater recharge. Their application of this model to the Rillito Creek area gave an expected transmission loss value of 1.40×10^6 m^3/km of channel for the 1958-1959 streamflow data.

The Water Resources Research Center (1980), University of Arizona, reviewed and discussed all the possible components of recharge in arid regions and summarized all the transmission loss data for

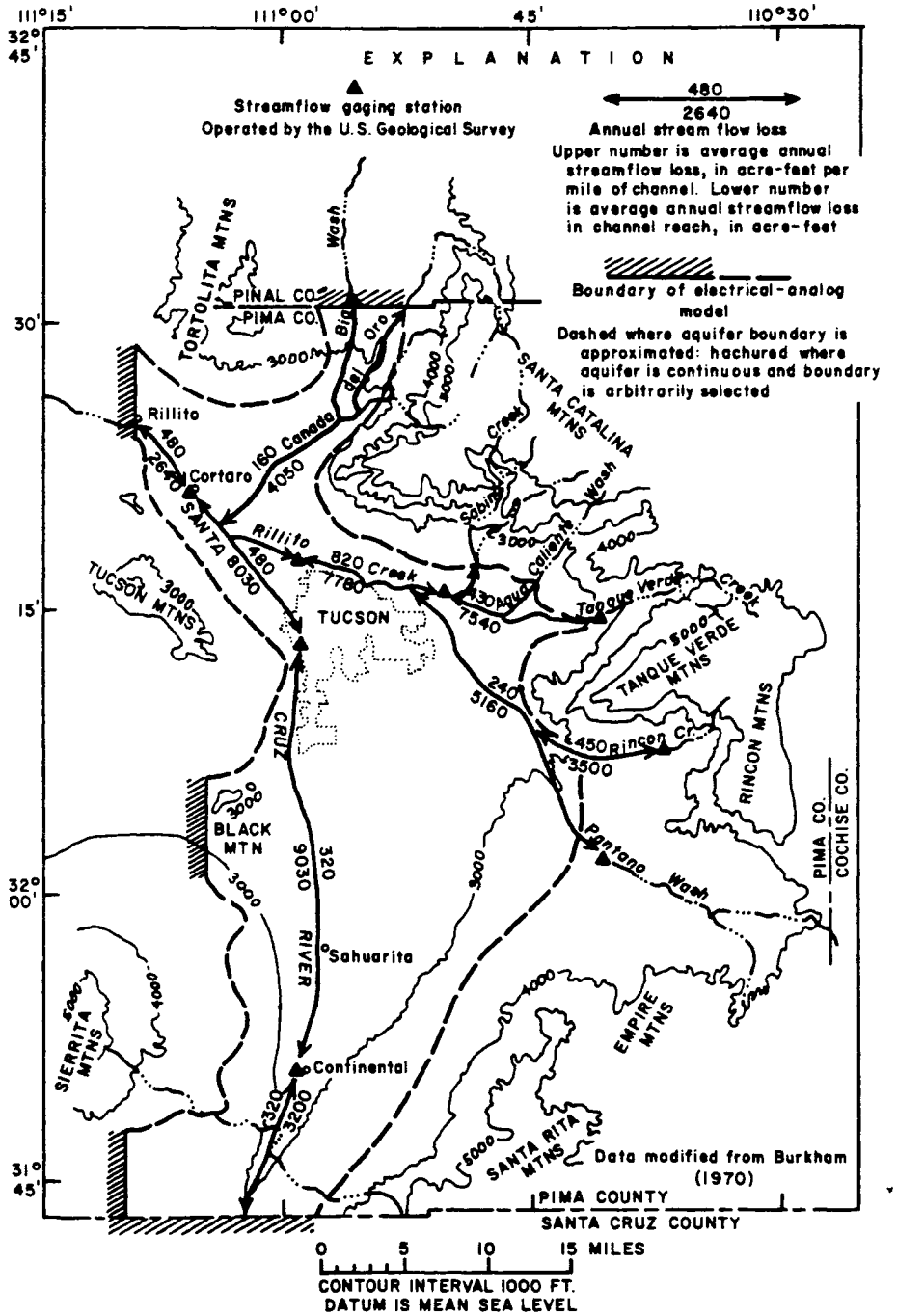

Figure 11. Computed average annual streamflow losses in the Tucson basin. (Burkham, 1970).

alluvial channels in Arizona (Table 2). The wide range in infiltration rates, not only between the different streams but on the same stream, are due mainly to temporal and spatial changes in the distribution of flow events and to temporal changes in channel characteristics. They also reported (Table 3) the amount of recharge as calculated by four models applied to Rillito Creek.

In the Tucson basin, recharge characteristics have been investigated and divided into two regimes: summer and winter (Simpson and others, 1970; Keith, 1981). Summer rainstorms produce high-volume streamflows with peak discharge of short duration and high suspended sediment concentration. Winter flows are characterized by low peak discharge of long duration and low suspended sediment concentration. Most investigators feel that the winter flow regime has the highest transmission losses because of its low sediment concentration and long duration. An additional factor noted by the Water Resources Research Center that may make the winter flows more effective is the lower loss from evapotranspiration.

Evans and Warrick (1970) studied streamflow infiltration and noted that "... some of the infiltrated water will return to the root or soil surface where it is removed by evaporation or transpiration." However, no study was performed to quantify these amounts. In a subsequent chapter of this report, I will attempt to relate the transmission losses to the recharge in the Rillito Creek area for the 1960 water-year.

Table 2. Summary of transmission loss data for alluvial channels in the Tucson basin. (After Water Resources Research Center, 1980)

Stream	Infiltration Rate*	Flow Loss*	Comments	Reference
Santa Cruz, Continental-Tucson	3-6.7 ft/d (.91-2.04 m/day)	-	Calculated from streamflow losses	Matlock (1965)
"	-	(2.45×10^5 m^3/km/yr) 320 AF/mi/yr; 40 percent of inflow	Calculated from streamflow losses	Burkham (1970)
Santa Cruz, Tucson-Cortero	6.4-7.4 ft/d (1.95-2.26 m/day)	-	Calculated from streamflow losses	Matlock (1965)
Rillito	1.1-3.7 ft/day (.34-1.13 m/day)	-	Snowmelt runoff; lower rate in area of high water table	Turner and others (1943)
"	2.4-6.5 ft/d (.73-1.98 m/day)	-	Snowmelt runoff; calculated from seepage runs	Matlock (1965)
"	2.8 ft/d (.85 m/day)	1,410 AF/mi (1.08×10^6 m^3/km) 14 AF/mi/d (1.06×10^4 m^3/km/day)	Snowmelt runoff; calculated from ground water level changes	Matlock (1965)
"	-	1,770-2,840 AF/mi ($1.36-2.18 \times 10^6$/m^3/km)	Snowmelt runoff, calculated using convolution/deconvolution; range due to range in diffusivity estimates	Moench and Kisiel (1970)

Table 2 -- continued

Stream	Infiltration Rate*	Flow Loss*	Comments	Reference
Rillito	-	1,820 AF/mi (1.39 x 10^6 m^3/km)	Snowmelt runoff; calculated from a calibrated flow duration model	Flug and others (1980)
"	-	56 percent of inflow; 820 AF/mi/yr average (.63 x 10^6 m^3/km/yr)	Calculated from stream-	Burkahm (1970)
Rillito Creek-Cortero	4.3-11 ft/d (1.31-3.35 m/day)	-	Calculated from streamflow losses	Matlock (1965)
Rillito and Santa Cruz River-Cortero	-	30 percent of inflow; 480 AF/mi/yr average (.37 x 10^6 m^3/km/yr)	Calculated from streamflow losses	Burkham (1970)
Pantano Wash	-	72 percent of inflow; 240 AF/mi/yr average (.18 x 10^6 m^3/km/yr)	Calculated from streamflow losses	Burkham (1970)
Pantano Wash	3.2-4.1 ft/d (.97-1.25 m/day)	-	Calculated from streamflow losses	Matlock (1965)
Tanque Verde Creek	-	45 percent of inflow; 430 AF/mi/yr average (.33 x 10^6 m^3/km/yr)	Calculated from streamflow losses	Burkham (1970)

Table 2 -- continued

Stream	Infiltration Rate*	Flow Loss*	Comments	Reference
Rincon Creek	-	92 percent of inflow; 450 AF/mi/yr average ($.34 \times 10^6$ m^3/km/yr)	Calculated from stream-flow losses	Burkham (1970)
Canada del Oro	-	60 percent of inflow; 160 AF/mi/yr average ($.12 \times 10^6$ m^3/km/yr)	Calculated from stream-flow losses	Burkham (1970)
Tucson area streams	3.3 ft/d (1.00 m/day)	-	Average for all streams	Matlock (1965)

*ft/d = feet per day
AF/mi = acre-feet per mile
AF/mi/yr = acre-feet per mile per year
m/day = meters per day
m^3/km = cubic meters per kilometer

Table 3. Recharge as calculated by four models applied to Rillito Creek. (After Water Resources Research Center, 1980)

Model (reference)	Data Used	Recharge*	Comments
Recharge mound calculation (reported in Moench and Kisiel, 1970)	Water levels, specific yield	1.68×10^6 m^3/km 2,200 AF/mile	Evapotranspiration losses that occurred were subtracted from total recharge.
Convolution/deconvolution (Moench and Kisiel, 1970)	Water levels, aquifer diffusivity	$1.36 - 2.18 \times 10^6$ m^3/km 1,770 - 2,840 AF/mile	Range due to range in estimate of diffusivity (α)
Inflow-loss (Burkham, 1970)	Inflow and loss/mile equation	1.99×10^6 m^3/km	see text
Event-based model (Flug and others, 1980)	flow duration	$1.39 - 2.08 \times 10^6$ m^3/km 1,820 - 2,715 AF/mile	Low value is from duration data for year preceding recharge event; high value is from duration data for the year of the recharge event

*AF/mile = acre-feet per mile channel reach
m^3/km = cubic meters per kilometer channel reach

Transmission Loss in Study Area

In order to determine transmission loss at the study section of Rillito Creek, the drainage area was divided into channel sections as shown in Figure 12. Burkham (1970), as discussed earlier, developed streamflow loss equations for different reaches in the Tucson basin. The calculation of the transmission loss is based on Burkham's equations for the different corresponding reaches except for the reach from point D to the Rillito Creek gaging station for reasons stated below. The results of the transmission losses for each reach are given in Table 4. The outflow in acre-feet (discharge passing the point of consideration) is calculated as follows: the discharge recorded at, say, Sabino Creek gaging station is used as inflow in Burkham's equation corresponding to the reach going from Sabino Creek gaging station to point A for computing the loss of that reach. Similarly, the loss is computed for the reach from Bear Creek gaging station to point A. At point A the inflow is the sum of the discharges recorded from the gaging stations minus the losses over their respective reaches. Similar calculations are performed for the Pantano Wash reach. Finally at point D, in addition to the computed inflow, 16,000 acre-feet were added for urban runoff and 13,480 acre-feet that went past the Rillito Creek gaging station was subtracted. The calculated transmission loss for the 7.2 mile reach (point D to Rillito gaging station) is about 15,984 acre-feet, or 2,220 acre-feet per mile which converts to 1.70×10^6 m^3/km. An example of transmission loss computation is given in Appendix C.

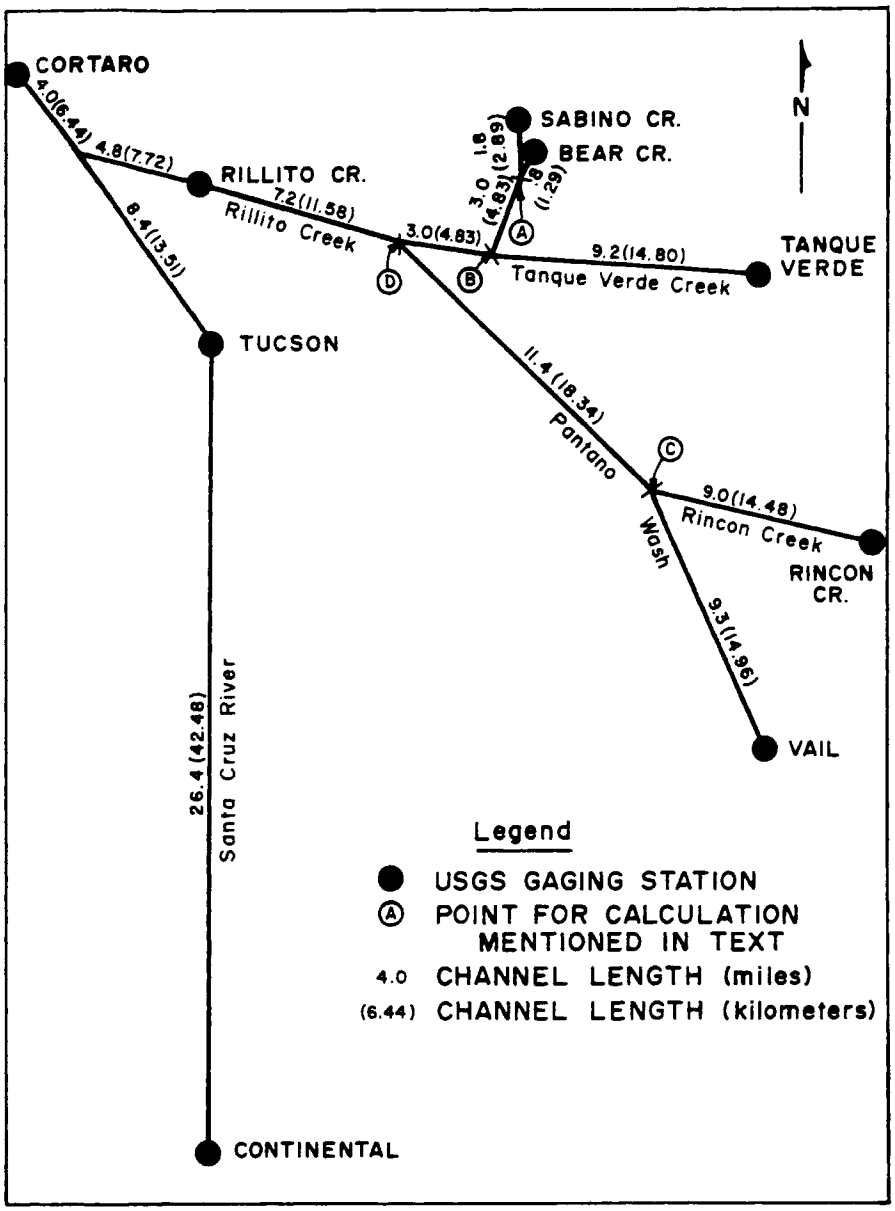

Figure 12. Stream reaches in the Rillito Creek area, Tucson basin. (Modified from Matlock, 1965)

Table 4. Transmission loss computations in Rillito Creek.

Reach Identification	Length (miles)	Equation used*	Inflow (acre-feet)	Transmission losses (acre-feet/reach)	Outflow (acre-feet)	Number Days Above 7 cfs
Sabino Creek to Point A	1.8	$0.18L(Q_{inflow})^{0.8}$	15,246[a]	2,204	13,042	136
Bear Breek to Point A	.8	"	5,597[a]	388	5,209	73
Point A to Point B	3.0	"	18,251	4,242	14,008	-
Tanque Verde to Point B	9.2	"	8,071[a]	6,383	1,688	85
Point B to Point D	3.0	"	15,696	3,760	11,936	-
Rincon Creek to Point C	9.0	$0.11L(Q_{inflow})^{0.8}$	5,464[a]	2,668	2,796	81
Vail to Point C	9.3	"	2,907[a]	1,357	1,550	29
Point C to Point D	11.4	"	4,346	2,818	1,528	-

Table 4 -- continued

Reach Identification	Length (miles)	Equation used*	Inflow (acre-feet)	Transmission losses (acre-feet/reach)	Outflow (acre-feet)	Number Days Above 7 cfs
Urban Runoff at Point D	-	None	16,000[b]	-	-	-
Point D to Rillito Creek	7.2	None	29,464	15,984	13,480[a]	37

* L represents channel length in Burkham's equations.
a. Flow discharge recorded at the U.S. Geological Survey gaging stations.
b. Estimated for urban runoff (Agriculture Engineering Department, University of Arizona).

Burkham in his study reported a transmission loss value of about 820 acre-feet per mile (0.63 x 10^6 m^3/km) in the Rillito Creek area. Most of this discrepancy possibly is due to the fact that Burkham did not take urban runoff into account.

For the 1960 water-year, the Water Resources Research Center (1980) generated a recharge-per-mile value by the use of Burkham's equation and the discharge (13,500 acre-feet) recorded at the Rillito Creek gaging station in the following way. Using Burkham's average inflow and outflow volumes (13,900 and 6,210 acre-feet, respectively) for the Rillito Creek reach, they computed the inflow for the studied period on the assumption that the following ratio is satisfied.

$$\frac{\text{study period inflow}}{13,900} = \frac{13,500}{6,210}$$

Converting the study period inflow to an average cubic-feet-per second and using it in Burkham's loss/mile equation for reach 5.

$$Q_f = 0.18(Q_{inflow})^{0.8} \qquad (14b)$$

The transmission loss amounted to about 2,600 acre-feet per mile (1.99 x 10^6 m^3/km).

Here again the discharge from urban runoff and from small ungaged tributaries were not taken into account. An addition of 16,000 acre-feet for urban runoff to the study period inflow converts to about 64 cubic feet per second. The use of Burkahm's loss/mile equations for reach 5 leads to a transmission loss of about 3,630 acre-feet per mile.

The streamflow loss values ranging from 2.78×10^6 m^3/km to 1.70×10^6 m^3/km will be used in the present study.

CHAPTER 5

ESTIMATION OF RECHARGE BY VOLUMETRIC ANALYSIS

By assuming that the porous medium is homogeneous and isotropic and having a sufficient number of piezometers (water level data) in the vicinity of the stream, it is possible to estimate the volume of the porous material that becomes saturated owing to the flood. However, certain difficulties may be encountered in estimating the effective porosity for computing the volume of recharge expressed as:

$$Q_{recharge} = n_e V_s \tag{15}$$

where

n_e = effective porosity, dimensionless

V_s = saturated volume, in cubic meters.

This method disregards the natural decline of the water table that would occur without the flood. This is particularly important if the unsaturated zone is thick and the mound decay time is long (Besbes, 1978).

Drainage of Recharge Mound

Experience shows that the decay curve of the water table in a non-perturbed flow regime has an exponential shape. Hence, by analogy, one can write the decay equation for a recharge mound as follows (Besbes, 1978):

$$h_t = h_0 e^{-\alpha t} \tag{16}$$

where

h_t = hydraulic head at a point in the recharge mound at time t

h_0 = hydraulic head at time t=0, when the infiltration ceases (meters)

α = decay coefficient which represents the flow properties over the entire system (day $^{-1}$).

The base level, or water table, is the asymptote to which the hydraulic head approaches when t gets larger if the infiltration is zero. Besbes (1978) illustrates the method by using a hypothetical well hydrograph in Figure 13. He applies the discharge equation to this graph and writes the following equations:

$$h_1 = h_o\, e^{-\alpha(t_1 - t_o)} = h_o'\, e^{-\alpha(t_1' - t_o')} \tag{17a}$$

$$h_2 = h_o\, e^{-\alpha(t_2 - t_o)} = h_o'\, e^{-\alpha(t_1' - t_o')} \tag{17b}$$

Hence, $t_1' - t_1 = t_2' - t_2$.

From the above equation, we can conclude that the horizontal distance between the two successive discharge curves is constant for a given time period. Besbes (1978) in his recharge study called this distance the drainage lag of the aquifer, and it can be determined graphically from well hydrographs.

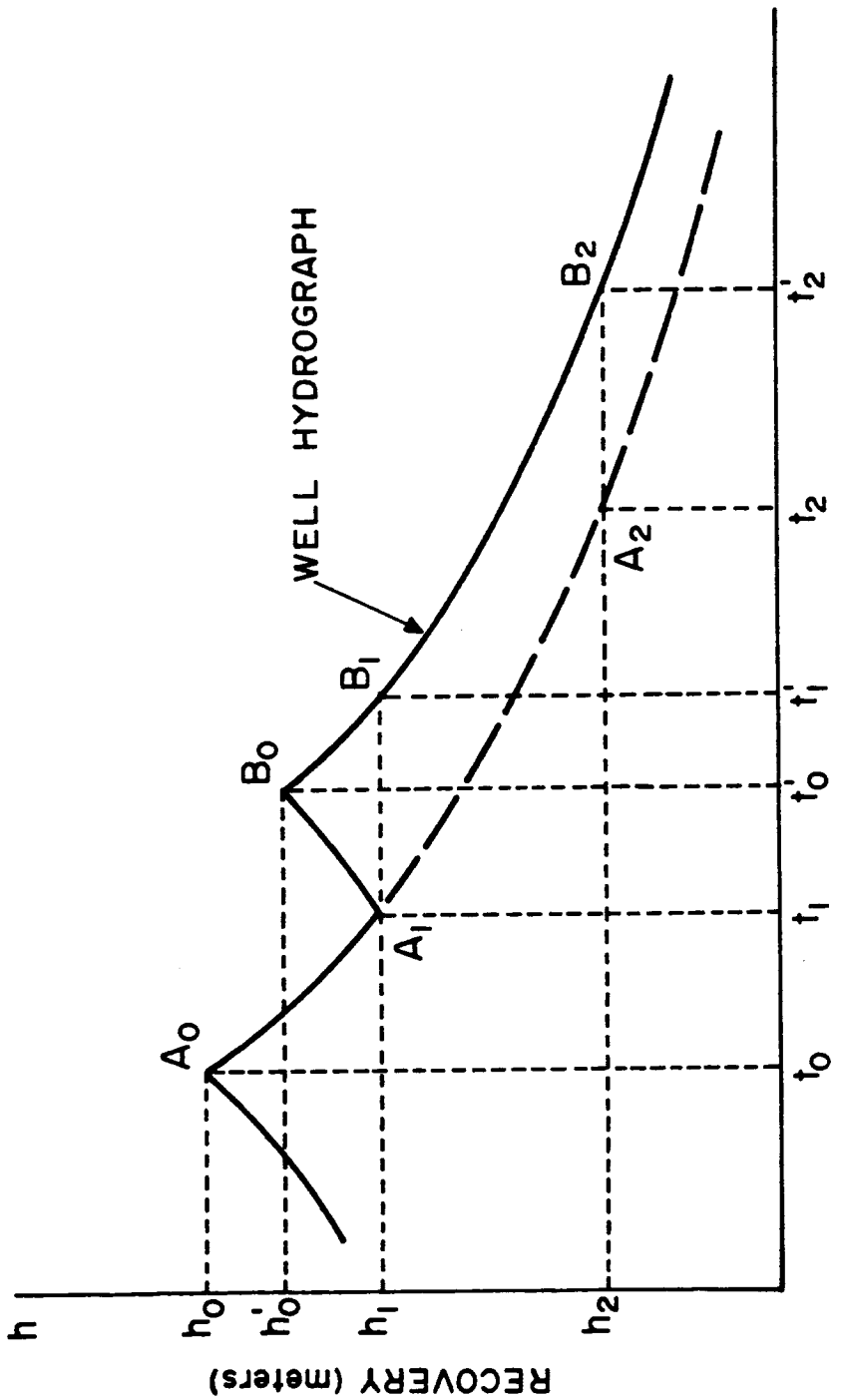

Figure 13. Delayed drainage in recharge mound. (After Besbes, 1978)

Groundwater Mound Method

The application of this method can separate the effects on the aquifer of occurring recharge events and determine the corresponding effective recovery at each time by taking into account the delayed water transfer through the vadose zone.

The infiltrated water during a flood event is a function of the thickness of the vadose zone and its characteristics (permeability and porosity) and the residence time. In addition to this delay, there is another one due to the lateral propagation of the flood wave in the saturated media (Besbes, 1978; Besbes et al, 1978). The maximum net recovery values determined for the same flood event will not be synchronized at all the locations of the aquifer. In other words, the time at which the variation of the aquifer reservoir is computed becomes an important factor.

For each identified flood event, one can establish an iso-recovery map which will allow determination of the evolution in time of the saturated soil volume by the considered flood event. However, due to the lack of spatial data distribution, it was not possible to draw such a map. But since the wells with enough data are on the same profile line, a new method was considered.

By trial and error, I estimated the depth to the water table (called base flow) in the well hydrographs. This depth value is no more than the asymptote that determines the h values in the exponential decay equation, whereas the decay coefficients are calculated from well hydrographs by taking two observed points and their corresponding time of the discharge curve and using the discharge equation.

For each given well, the base level or depth to the water table is calculated by the exponential decay curve, and the maximum recovery for the first flood is read from the well hydrograph. Knowing the normal distance of the well from the centerline of the streambed, the base level, and the maximum recovery of the first flood for each well, I have constructed the first groundwater mound cross-section by joining these values with each other. Similar steps are taken to construct the second groundwater mound cross-section owing to the second flood. The two groundwater cross-sections are illustrated in Figure 14. This illustration shows that the base level slopes positively about 1.4 percent on the north side of the Rillito Creek toward the Catalina mountains. The difference in base level slopes between the north and south sides of Rillito Creek is probably due to the mountain front recharge.

After graphing the two groundwater mound cross-sections, I planimetered the cross-section areas (A_1 = 7,700 m^2 and A_2 = 6,800 m^2) which are assumed to be saturated owing to the floods (Figure 14). Furthermore, assuming that the porous medium is homogeneous and isotropic, these cross-sections can be extended over one kilometer in the third direction along the stream channel. Due to the short time interval (17 days) between the two floods the total saturated soil volume (V_s), in cubic meters per one kilometer, is calculated as follows:

$$V_s = 10^3\left(\sum_{i=1}^{2} W_i A_i\right)$$

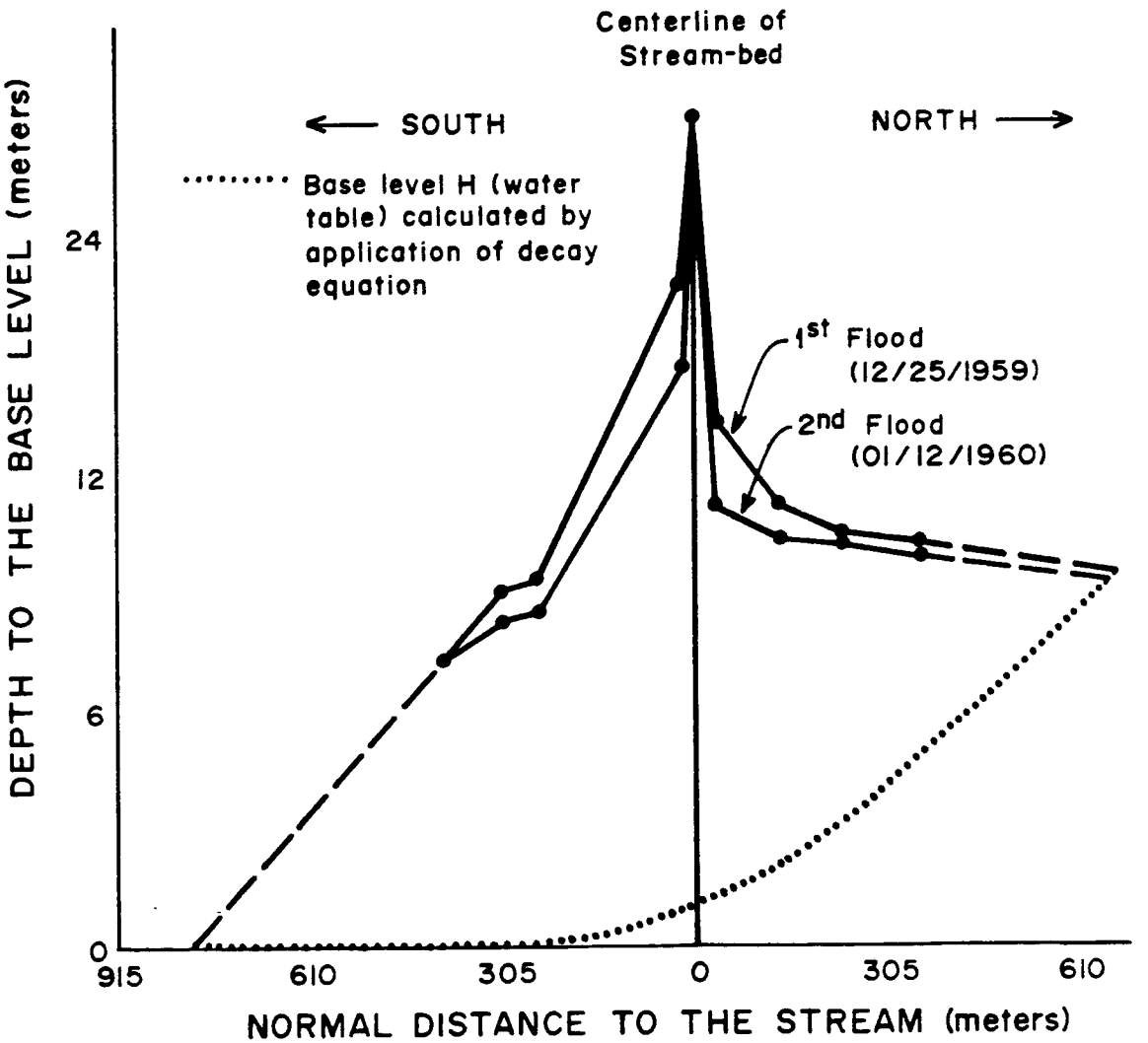

Figure 14. Cross-section of two groundwater mounds (1960 water-year).

where, 10^3 is the factor for conversion of units and W_i is the weight given each flood. From each well hydrograph, a ratio between the maximum recovery of the two floods is calculated and an average ratio is derived. A weight of 100 percent is given to the first flood and 10 percent to the second flood.

The application of equation (15), recalled here,

$$Q_{recharge} = n_e V_s$$

gives a total estimated recharge ranging between 0.86 x 10^6 m^3 and 1.29 x 10^6 m^3 per one kilometer reach depending on the effective porosity used. The two values of the effective porosity used in the computation are 0.10 and 0.15, respectively (Foster, 1969). These estimated recharge values are retained as minimum figures because of the neglected lateral movement in the water table.

CHAPTER 6

ESTIMATION OF RECHARGE BY DECONVOLUTION INTEGRAL

Definition

The deconvolution integral is a mathematical technique used to identify the convolution (or Duhamel) integral relation between the input and the output of a lumped stationary deterministic linear system (Neuman et al, 1976). Mathematically, the convolution integral is expressed as follows:

$$s(t) = \int_0^t H(t-\tau)\, Q(\tau)\, d\tau \qquad (18)$$

where $s(t)$ and $Q(\tau)$ are respectively the output and the input related by a response function, $H(t-\tau)$, of a given linear system.

If we assume that the water flow in a saturated or unsaturated porous medium is linear and that the transmissivity of the aquifer does not change with time, we can write a linear relationship between the magnitude of the recharge from the stream and the magnitude of the recovery of the water table in the aquifer. This relation will have the form of equation (18) in which: $s_i(t)$ represents the net recovery of the water table at well (i), as a function of time. $Q(t)$ is the recharge from the stream at time t; and $H(t-\tau)$ is an operator whose application on the input gives the output of the system. This operator is often called the impulse response function of the system.

Theory

Recalling the flow equation in one dimension and expanding the right-hand term,

$$\frac{\partial}{\partial x}(\rho K(\theta)\frac{\partial h}{\partial x}) = \frac{\partial \theta}{\partial t} + \frac{\partial \rho}{\partial t} \tag{19}$$

where

$\theta\ \partial\rho/\partial t$ is the mass rate of water produced by an expansion of the water under a change in its density

$\rho\ \partial\theta/\partial t$ is the mass rate of water produced by the compaction of the porous medium as reflected by the change of its water content (θ)

For saturated flow becomes the porosity.

The change in ρ and the change in θ are both induced by a change in the hydraulic head h. Then the volume of water resulting from a unit decline in head is S_s, called the specific storage and expressed as:

$$S_s = \rho G(\alpha + \theta\beta) \tag{20}$$

where, and are respectively the compressibility coefficients of the solid matrix and the water, and G is the gravity.

Therefore, the mass rate of water produced would be:

$$\rho\ S_s \frac{\partial h}{\partial t} \tag{21}$$

By substituting expression (21) into the flow equation (13b) and rearranging, we can write the following one dimensional equation for

saturated flow. For derivation details of equation (13) into equation (22), the reader may refer to Freeze and Cherry (1979, p. 49-66).

$$\frac{\partial^2 h}{\partial x^2} = \frac{S_s}{K} \frac{\partial h}{\partial t} \tag{22}$$

For a horizontal confined aquifer of thickness D, storage coefficient S = S_sD, and transmissivity T = KD, equation (22) can be rewritten as:

$$\frac{\partial^2 h}{\partial x^2} = \frac{S}{T} \frac{\partial h}{\partial t} \tag{23}$$

By letting the aquifer diffusivity, α = KD/S, we can write the one dimensional diffusion equation as:

$$\frac{\partial^2 h}{\partial x^2} = \frac{1}{\alpha} \frac{\partial h}{\partial t} \tag{24}$$

Equation (24) is used for deriving a unit instantaneous pulse at the source illustrated in Figure 15. This illustration, taken from Moench and Kisiel (1970), shows a cross-section through an unconfined aquifer perpendicular to a streambed of finite width. This homogeneous and isotropic aquifer underlain by an impermeable base, is infinite in horizontal extent and obeys the Dupuit-Forcheimer assumptions. The application of the aforementioned diffusion equation to the rise and fall of the groundwater mound underneath a stream channel is based on the initial and boundary conditions set by Moench and Kisiel.

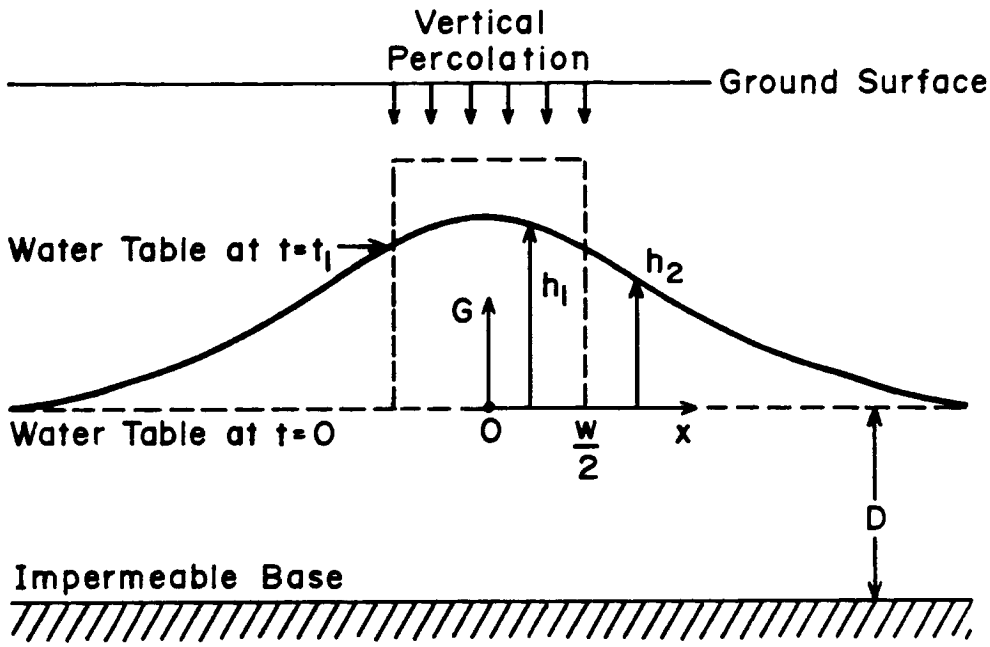

Figure 15. Cross-section of the aquifer below the source of recharge, showing the shape of the groundwater mound at time t_1, due to a pulse of unit amplitude and width W, applied at t = 0. (After Moench and Kisiel, 1970).

With respect to Figure 15 and time greater than zero, the one dimensional diffusion equation for regions adjacent to the streambed can be expressed as:

$$\frac{\partial^2 h_1}{\partial x^2} = \frac{1}{\alpha}\frac{\partial h_1}{\partial t} \; ; \qquad 0 \leq x \leq w/2 \tag{25a}$$

$$\frac{\partial^2 h_2}{\partial x^2} = \frac{1}{\alpha}\frac{\partial h_2}{\partial t} \; ; \qquad x > w/2 \tag{25b}$$

and for initial and boundary conditions

$h_1 = h_0$	$0 \leq x \leq w/2$	$t = 0$
$h_2 = 0$	$x > w/2$	$t = 0$
$\frac{\partial h_1}{\partial x} = 0$	$x = 0$	$t > 0$
$h_1 = h_2$	$x = w/2$	$t > 0$
$\frac{\partial h_1}{\partial x} = \frac{\partial h_2}{\partial x}$	$x = w/2$	$t > 0$
$h_2 \rightarrow 0$	$x \rightarrow 0$	

where

h_0 = amplitude of the initial pulse, in meters

h_1 = rise of water table within the zone of recharge, in meters

h_2 = rise of the water table external to the zone of recharge, in meters

x = horizontal normal distance from centerline of stream, in meters

α = KD/S, aquifer diffusivity, in square meters per day

K = hydraulic conductivity of the aquifer, in meters per day

W = width of the stream bed, in meters

D = aquifer thickness, in meters

S = coefficient of storage of the aquifer, dimensionless

t = time, in days

The solution to this problem is (Glover, 1961; Polubarinova-Kochina, 1962, p. 535; reported by Moench and Kisiel, 1970):

$$H(x,t) = \frac{h_2(x,t)}{h_0(0,0)} = \frac{1}{(\pi)^{1/2}} \int_{u_1}^{u_2} \exp(-u^2)du \qquad (26)$$

where

$u_1 = (x-w/2)/(4\alpha t)^{1/2}$

$u_2 = (x+w/2)/(4\alpha t)^{1/2}$

Using the error function expression, equation (26) can be simplified to (Crank, 1979, p. 14):

$$H(x,t) = 1/2(\mathrm{erf}(u_2)-\mathrm{erf}(u_1)) \qquad (27)$$

The above equation (27), which represents a unit instantaneous pulse at the source, will be used later in this chapter to calculate the response function for the aquifer system. The response function has the effect of distributing the system response to the input (recharge) pulse over time. Once the system properties are fixed (i.e., α and w), the shape and magnitude of the response function depends on normal distance of the well from the source.

The continuous form of the convolution integral can be discretized and expressed in the following form:

$$s(i) = \sum_{j=1}^{i} Q(i-j+1)\, H(j)\Delta j \qquad (28)$$

where, the s(i) are water level measurements from a single well at equal time intervals Δj, and the H(j) are calculated for discrete values of time from the impulse response function.

The input function Q(i) can be obtained by the method of synthetic division for unique values. By letting $\Delta j=1$, time unit, and j=1, Moench and Kisiel write the following solution of Q(i) from equation (28):

$$Q(i) = s(i) - \sum_{j=z}^{i} H(j)\, Q(i-j+1)\, \frac{1}{H(1)} \qquad (29)$$

However, this derived input function Q(i), as Moench and Kisiel noted, "... is a measure of the time variation of the rate at which the water table directly under the source of recharge would rise under the hypothetical situation in which no lateral flow occurs."

Results

The impulse response function derived for a unit instantaneous pulse at the source is computed from equation (27) for each of six wells. Two aquifer diffusivities are used in this computation, α_1 = 6,000 m^2/day and α_2 = 3,000 m^2/day (Anderson, 1972). The shape of the impulse response function (IRF) for well Murhpy #7 is shown in

Figure 16. The functions for the other wells are reported in Appendix B. The IRF's get flatter as the distance from the stream increases. The time to where the IRF is maximum gets larger as the normal distance increases and the maximum value of the IRF decreases.

The input functions are computed by deconvolution for Erwing #4 and #2, Murphy #4, #5, and #7, and Campbell #1 (see Figure 10 and Table 1) at their corresponding normal distances from the stream by the use of equation (29). Figures 17, 18, 19, and 20 represent the output function and three input functions at different stages of computation for well Murphy #7.

Due to the instability of the deconvolution integral and to the high frequency random errors in the output data (water level data), the input function showed some oscillation as illustrated in Figure 18. However, the general trend of the output function is more or less maintained throughout the input function. Since the shape of the input function is highly sensitive to minor variations in the level of noise, the question that arises is what degree of smoothness should be imposed on the solution without impairing the true physical nature of the input function. For simplicity, a 5-day weighted moving average was selected as a means to decrease the level of noise in the computation of the input function. The application of this "filter" considerably decreased the level of noise. Figure 19 represents the input function from Murphy #7 filtered by the aforementioned process.

Figure 19 shows negative values. These negative values reflect the consequences of computations at the tail of the well hydrographs when the position of zero value is in doubt. Moench and Kisiel (1970)

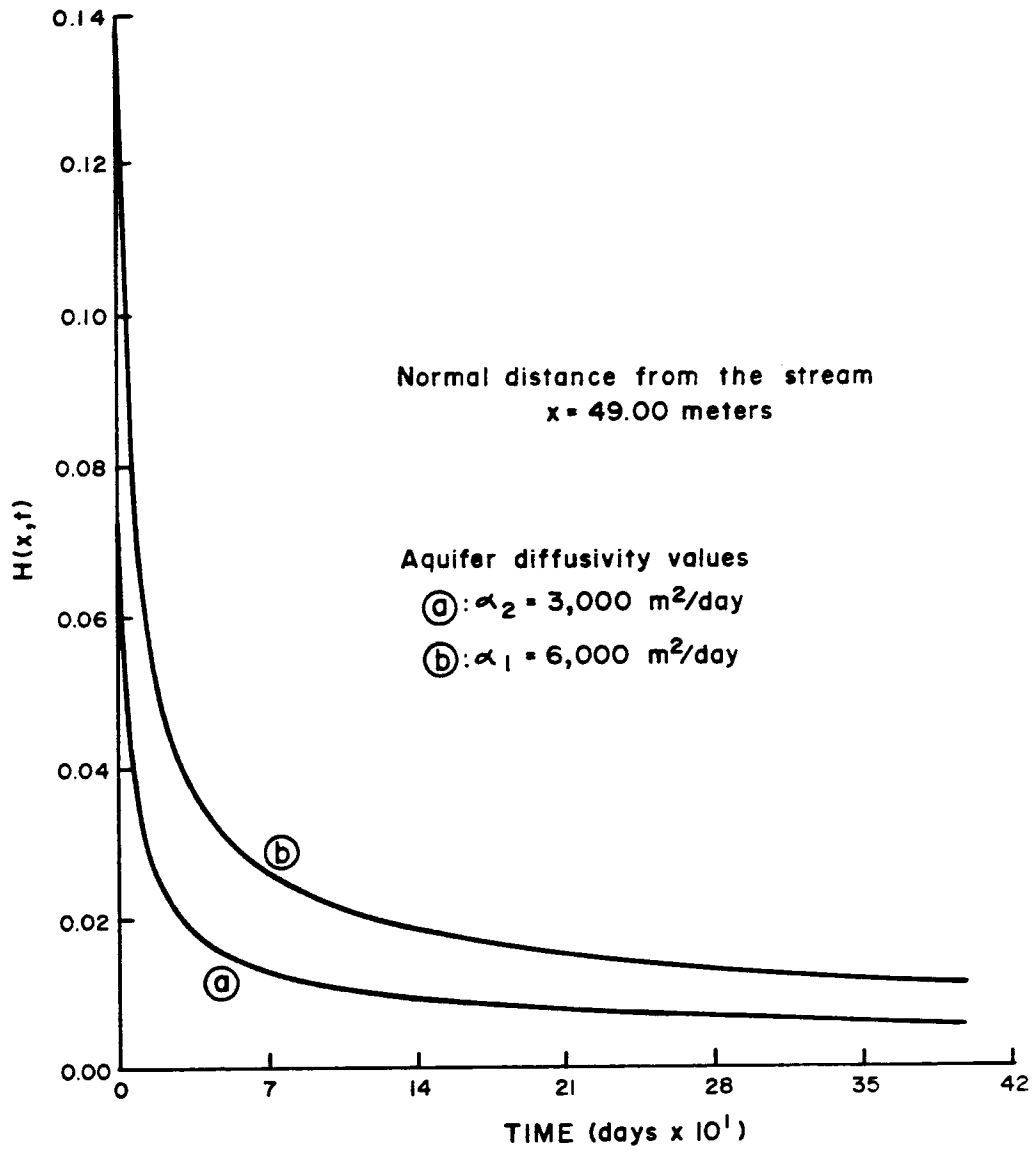

Figure 16. Impulse response functions for well Murphy #7 using two aquifer diffusivity values (α_1, α_2).

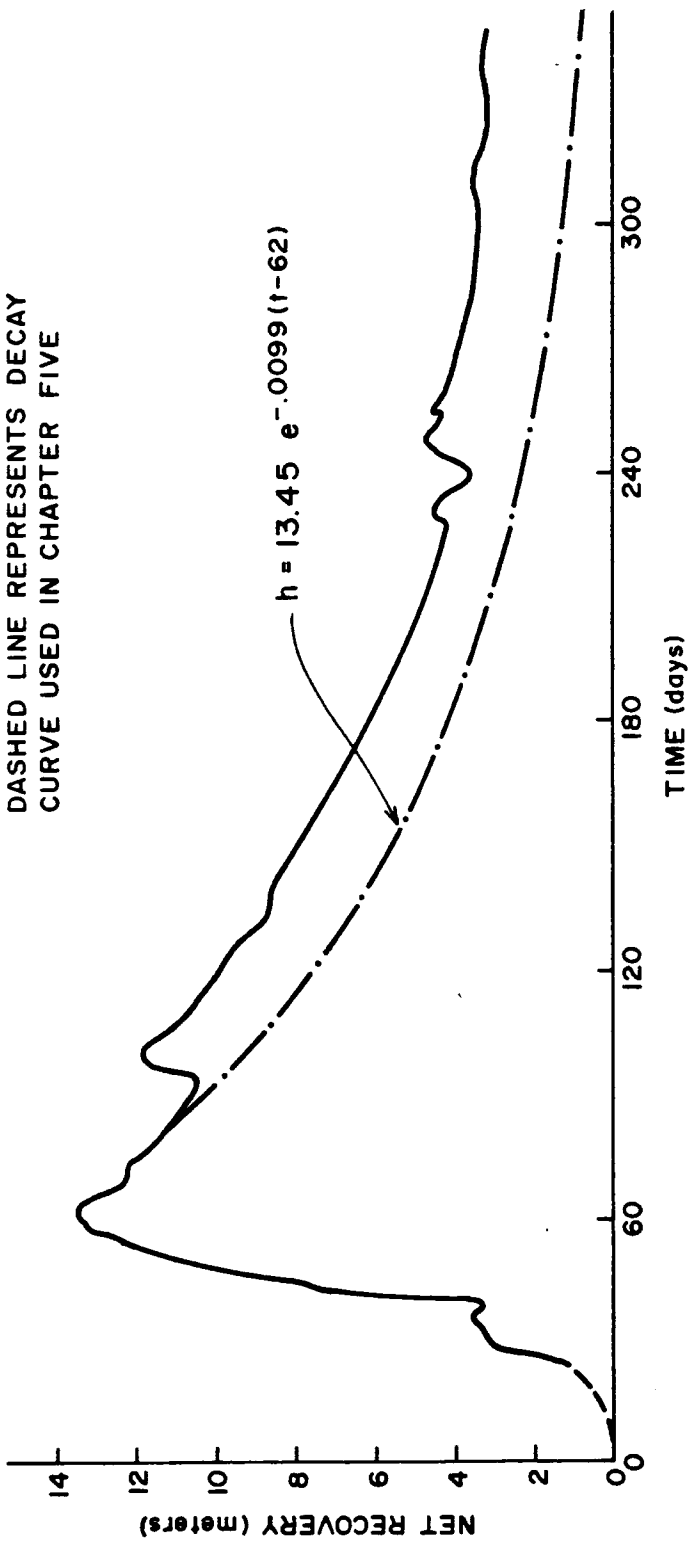

Figure 17. Well hydrograph for well Murphy #7 (49 meters north of stream).

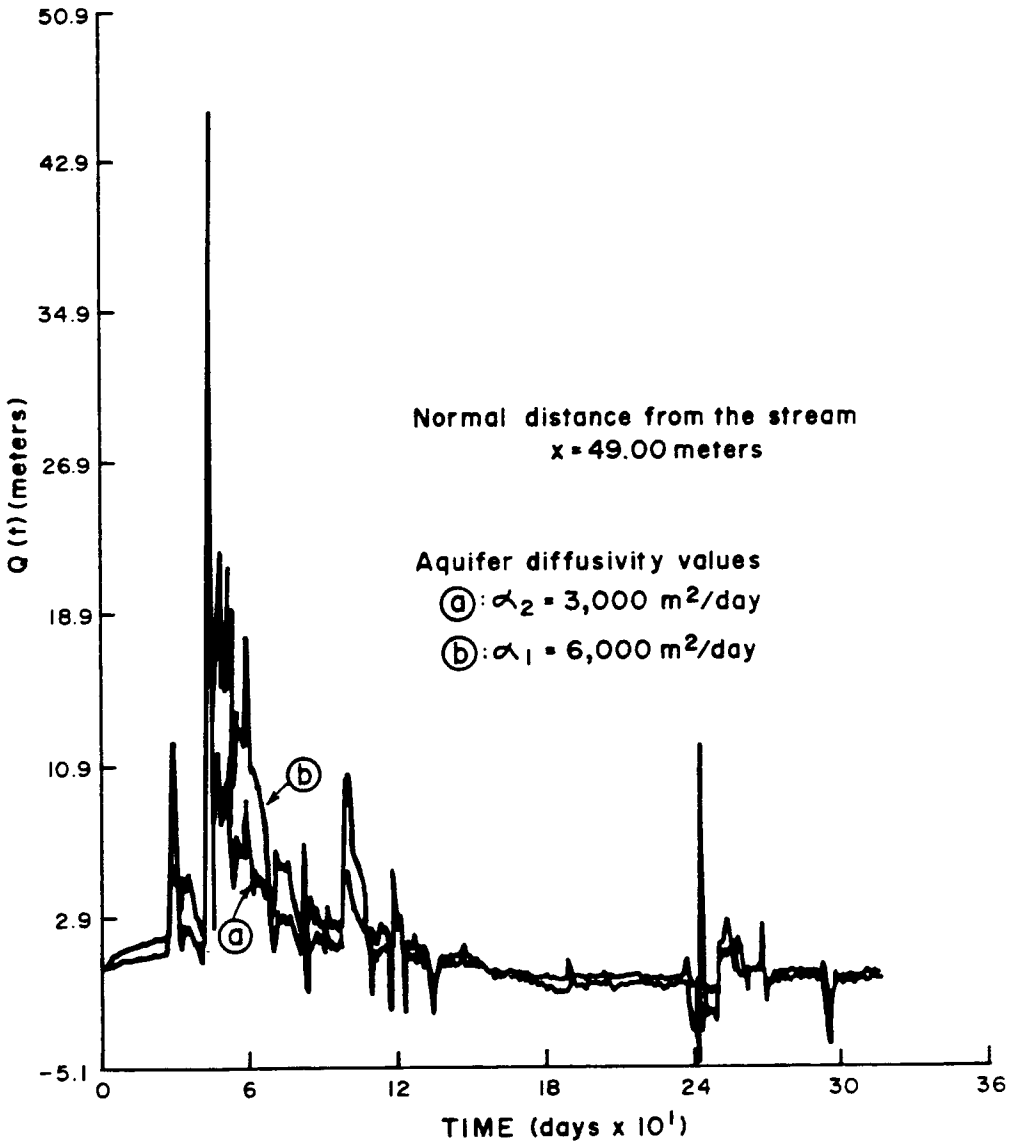

Figure 18. The system input functions for well Murphy #7 without noise filter and with negative values.

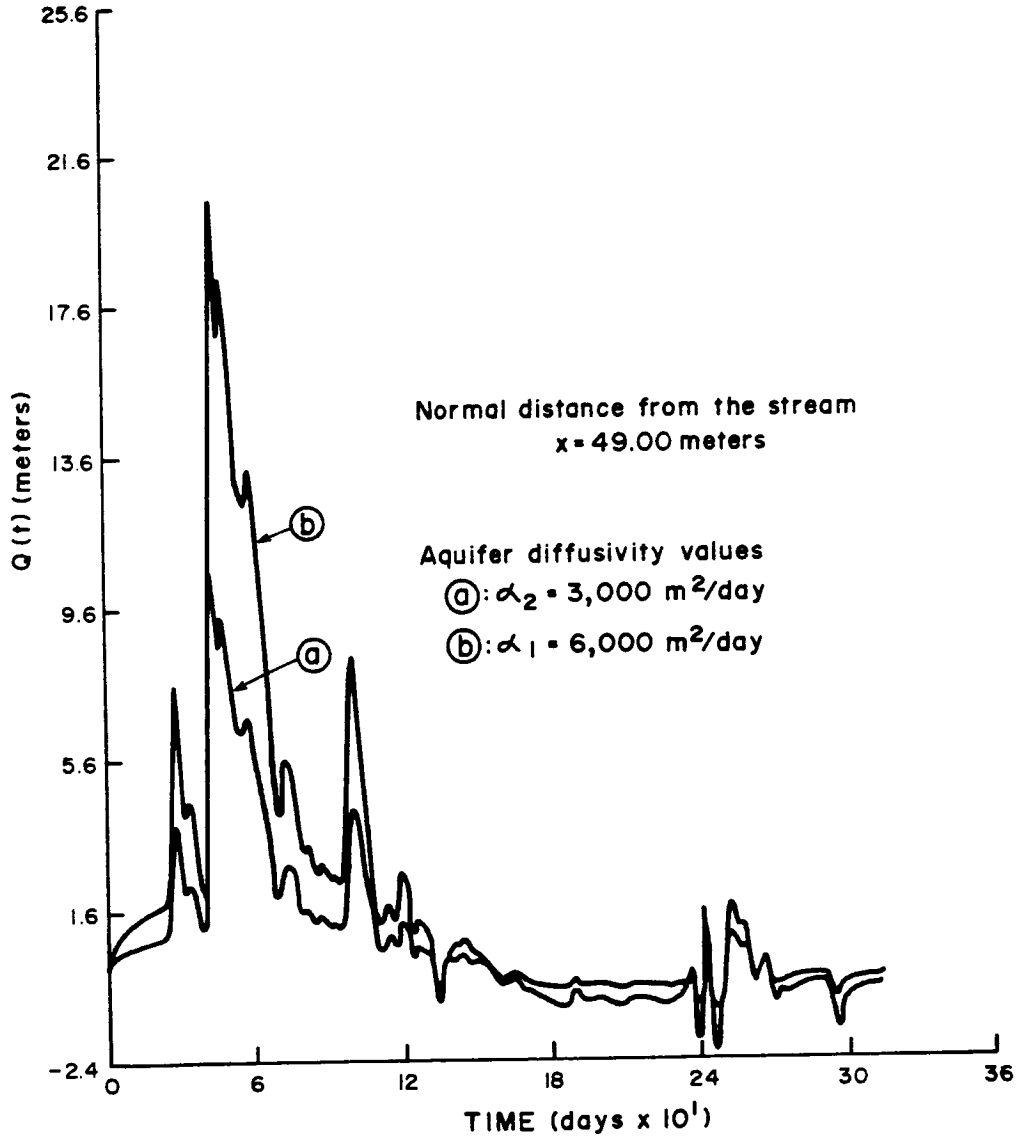

Figure 19. The system input functions for well Murphy #7 after being filtered and with negative values.

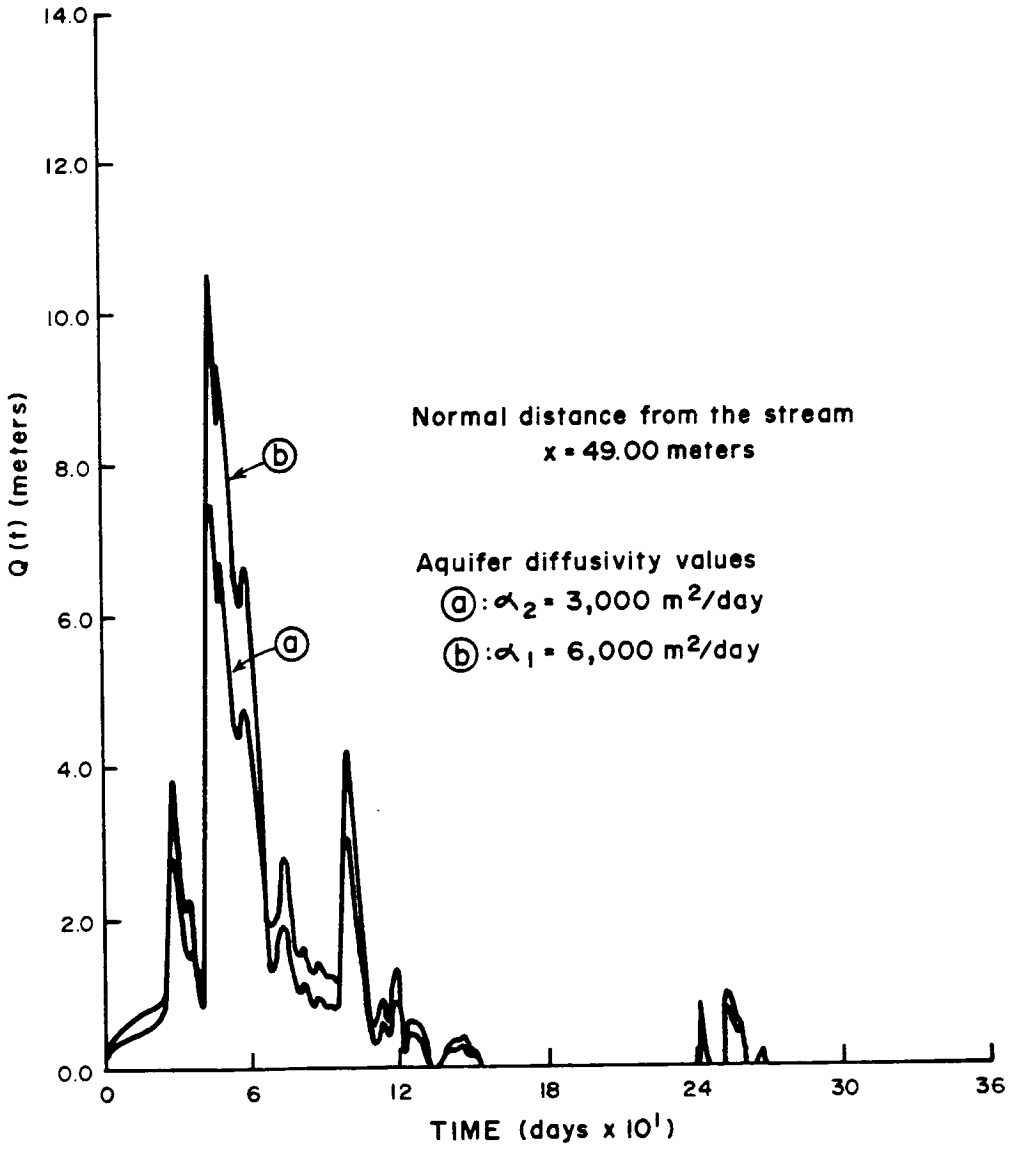

Figure 20. The filtered system input functions for well Murphy #7 without negative values.

stated that "... under ideal conditions of zero pumpage and evapotranspiration, the input function would rapidly approach zero when recharge ceases and remains there." The negative values of the input function were not included in the computation of recharge and they were deleted from the recharge hydrograph as shown in Figure 20 and for the functions in Appendix B.

Overall, the pattern of peaks and valleys of the input functions is closely similar to those in the output functions except in two cases. For well Erwing #2 (Appendix B), a high level of oscillation showed in the input function. This behavior may in part be due to the high frequency random errors detected in the output data. Secondly, for well Murphy #1 a high level of instability was detected in the deconvolution process. This instability could be due to the fact that the well is far from the stream (366.00 meters) and also to the high frequency random errors involved in the water level measurements. Well Murphy #1 was rejected from the computation in the deconvolution method.

The total recharge, R_i, at well (i) is calculated by summing the discrete input function over its positive values and using the following expression:

$$R_i = 10^3(SIF)_i(W)(S)$$

where R_i, in cubic meters per kilometer, is the total recharge during the time period of interest over the width, W = 60 meters, of the source and along a kilometer channel reach, $(SIF)_i$ is the system input function for well (i) integrated over positive values, in meters; 10^3

is a factor for conversion of units. Finally, (S) is the storage coefficient taken equal to 0.15 (Foster, 1969).

The recharge values computed from different wells by the deconvolution method are reported in Table 5. For the upper aquifer diffusivity value, α_1 = 6,000 m^2/day, the recharge values lie between 2.07 x 10^6 m^3/km and 1.84 x 10^6 m^3/km. For the lower aquifer diffusivity value, α_2 = 3,000 m^2/day, the recharge values fall between 1.71 x 10^6 m^3/km and 1.41 x 10^6 m^3/km. The range of results is narrow and could be due to the assumptions made in deriving the impulse response function, to the measurement errors in the output data, and perhaps to effects of pumpage from adjacent wells. Average total recharge of 1.62 x 10^6 m^3/km and 1.89 x 10^6 m^3/km, calculated respectively for the two aquifer diffusivity values (α_1 and α_2) are retained in the present study. These figures are in close agreement with Moench and Kisiel who calculated recharge to be 1.36 x 10^6 m^3/km and 2.18 x 10^6 m^3/km. The slight discrepancy is probably due to the step time differences, 5 days in Moench and Kisiel versus 1 day in the present study. An additional factor could be the improvement in available computer facilities.

Table 5. Recharge values as calculated by the deconvolution method.*

Well	Aquifer diffusivity (m^2/day)	SIF** (meters)	Distance from stream (meters)	Recharge m^3/km	Recharge Acre-ft/mi
Erwing #4	6,000	327	21.00	1.96×10^6	2,579
	3,000	253		1.52×10^6	2,016
Murphy #5	6,000	315	140.00	1.92×10^6	2,503
	3,000	234		1.41×10^6	1,863
Murphy #7	6,000	339	49.00	2.07×10^6	2,698
	3,000	242		1.48×10^6	1,924
Murphy #4	6,000	331	198.00	2.02×10^6	2,631
	3,000	257		1.57×10^6	2,042
Campbell #1	6,000	302	259.00	1.84×10^6	2,402
	3,000	245		1.49×10^6	1,946
Erwing #2***	6,000	330	305.00	2.01×10^6	2,626
	3,000	280		1.71×10^6	2,227

*A storage coefficient of .15, an unsaturated thickness of 46.00 meters, and a channel width (W) of 60 meters are used in the computation (Foster, 1969).

**SIF = System input function integrated over positive values.

***Instability detected.

CHAPTER 7

RECHARGE/INFILTRATION RATIO

For the 1960 water-year, the streamflow loss computed by Burkham's loss equations (Burkham, 1970) amounted to an average of about 2.24 x 10^6 m^3 along one kilometer channel reach of the Rillito Creek. An average effective recharge value between 1.89 x 10^6 m^3/km and 1.62 x 10^6 m^3/km by the deconvolution method, and an average recharge of 0.90 x 10^6 m^3/km by the graphical groundwater mound method were estimated. The streamflow loss figure does not account for evapotranspiration losses and direct evaporation from the surface flows and wetted stream bed, and thus represents a maximum value of potential recharge to groundwater. However, the recharge values computed by the deconvolution method estimates the amount of water that, in fact, does reach the groundwater reservoir. Then, an inflow-loss and effective recharge relationship can be performed in terms of percentage.

With regard to the computed recharge values, the amount of streamflow loss that effectively reaches the aquifer goes from 60 to a maximum of 87 percent with an average of 70 percent. The remainder, 30 percent, accounts for the evaporation from wetted stream beds, for the amount transpired by the phreatophytes, and for a certain amount of water stored temporarily in the vadose zone.

Conditions at Rillito Creek are favorable for recharge to the aquifer during the winter season; therefore, the figure of 70 percent should not necessarily be applied to other streams.

CHAPTER 8

CONCLUSION

In arid and semi-arid regions, a main source of recharge to unconfined aquifers results from infiltration along ephemeral streamflow channels. However, after a flood event, a portion of the infiltrated water is not removed by gravity drainage, but is held against the force of gravity by molecular attraction or capillarity. In an aquifer this water is present at all times above the water table before and after recharge, and the exact amount is difficult to estimate. The stored water in the vadose zone will either become recharge after being pushed downward by the next occurring flood event or be lost as evapotranspiration. The amount of water transpired by the riparian vegetation can be significant in semi-arid regions, but is still unknown. Since on a unit distance (i.e., one kilometer channel reach) basis, the aquifer is mainly recharged by streamflow losses, the accurate determination of the fraction that reaches the zone of saturation is important to the management of the groundwater reservoir.

The application of Burkham's (1970) loss equations on the Rillito Creek for the 1960 water-year lead to an average transmission loss value of about 2.24×10^6 m^3/km. However, this potential value includes the evaporation from the wetted channel, the amount of water transpired by the vegetation along the stream channel, and the amount of water held in the vadose zone.

The groundwater mound method is used to determine the saturated soil volume owing to a flood. This method is subject to error because it does not account for the small floods and for the lateral flow in the aquifer. The estimated recharge with this method is sensitive to the estimation of a regional effective porosity.

Natural recharge is also examined by the deconvolution of water level measurements (system responses) following several flood events. The impulse response function of a unit instantaneous pulse is derived under the assumptions that the system is linear and no lateral flow occurs. By discretizing the deconvolution integral, the recharge is computed using water level data for each of six wells. The results, reported in Table 5, are in close agreement with the suggested values from the literature. Due to the instability of the method some limitations arise. The wells should be in the vicinity of the stream, within a maximum distance of about 200 meters, and the water level measurements should be accurate and continuous.

The attempted relationship between inflow-loss and effective recharge resulted in an average of 70 percent transmission loss that actually reaches the water table in contrast to the 90 percent suggested by Burkham.

In conclusion, the streamflow losses amounted to an average of about 2.24×10^6 m^3/km and an average effective recharge of 1.57×10^6 m^3/km along the Rillito Creek for the 1960 water year.

CHAPTER 9

SUGGESTIONS FOR FUTURE STUDY

Suggestions for future study fall in three major parts.

1. Data Collection

Inexpensive water level recorders based on modern electronic technology be developed to facilitate an increase in the data collection network and to provide computer-compatible data at close time intervals or continuously.

Collection of surface and sub-surface water samples for chemical and isotope analysis, particularly before, during, and after a flood event.

Collection of evapotranspiration data for different time periods and vegetation species.

2. Streamflow Recharge Studies

The use of natural isotopes for measurement of groundwater recharge. The naturally occurring isotopes deuterium, tritium, carbon-13, carbon-14 and oxygen-18 can be used to obtain both qualitative and quantitative hydrologic information.

Monitoring and investigating the moisture content in the vadose zone for more information about the evolution of recharge impulse after a flood event in time and space.

More refined models should be used for improving the response function of the aquifer being studied.

3. Integrated Approach

Qualitative and quantitative research on the streamflow losses and effective recharge should be undertaken by coupling different approaches. Isotopic, hydrochemical, physical, and hydraulic information should be considered for building an integrated model.

APPENDIX A

WELL NUMBERING SYSTEM

The well location system used in this report is the same as that used by the U.S. Geological Survey. The following explanation is taken from Davis (Fig. 4, p. 13, 1967):

> The well numbers used by the U.S. Geological Survey in Arizona accord with the Bureau of Land Management system of land subdivision. The land survey in Arizona is based on the Gila and Salt River meridian and base line, which divides the state into four quadrants. These quadrants are designated counterclockwise by the capital letters A, B, C, and D. All land north and east of the point of origin is in A quadrant, and that south and east in D quadrant. The first digit of a well number indicates the township, the second the range, and the third the section in which the well is situated. The lowercase letters a, b, c, and d after the section number indicate the well location within the section. The first letter denotes a particular 160-acre tract. These letters also are assigned in a counterclockwise direction, beginning the northeast quarter. If the location is known within a 10-acre tract, three lowercase letters are shown in the well number. In the example shown (Fig. A-1), well number (D-4-5)19caa designates the well as being in the NE¼NE¼SW¼ sec. 19, T4S,R5E. Where there is more than one well within a 10-acre tract, consecutive numbers beginning with 1 are added as suffices.

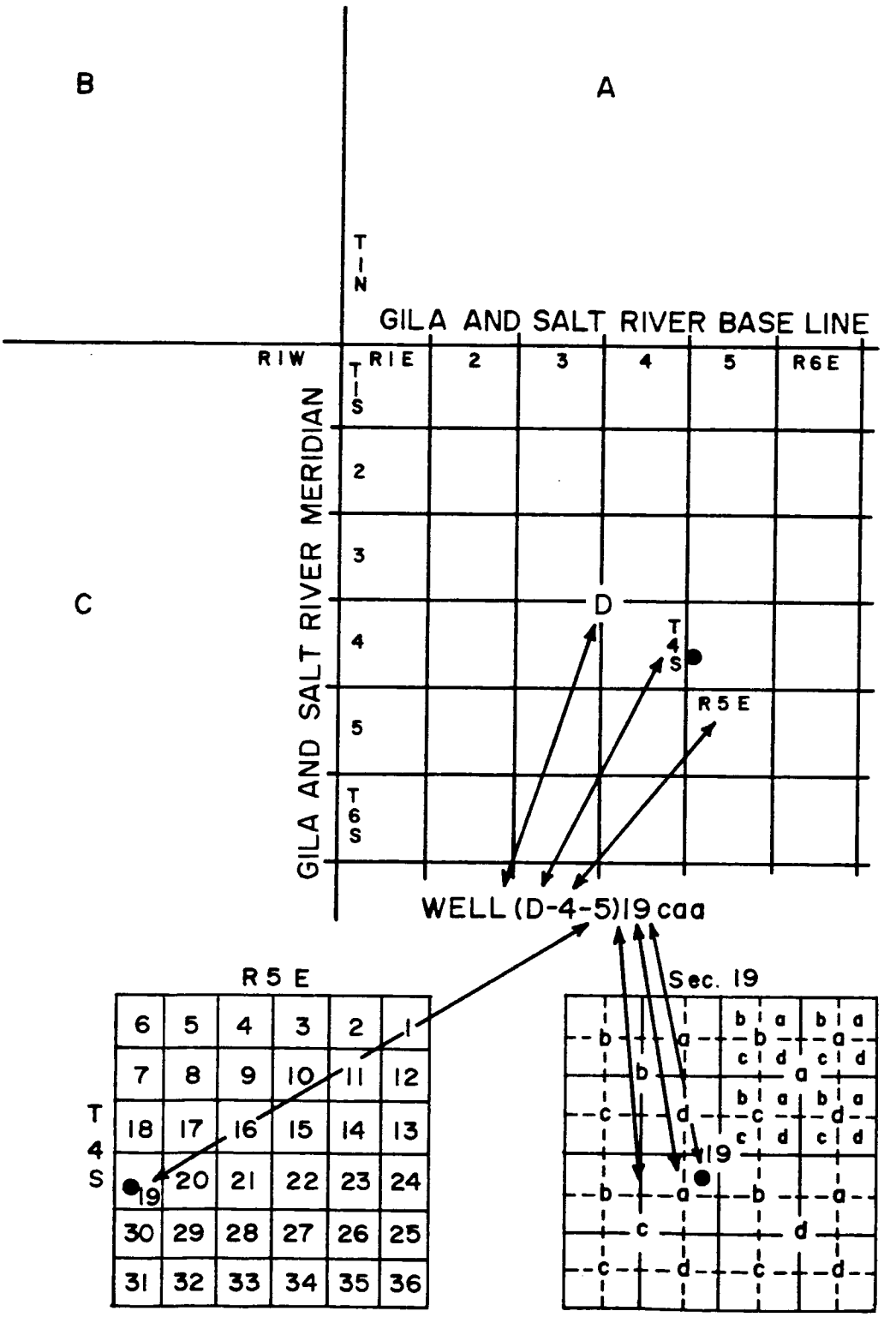

Figure A-1. U.S. Geological Survey well-numbering system. -- From Davis (1967, Fig. 4).

APPENDIX B

WATER LEVEL DATA AND DECONVOLUTION CALCULATIONS

The water level measurements, recorded by the Agricultural Engineering Department, University of Arizona, at different wells in the Rillito Creek area are tabulated herein. For each well a hydrograph is constructed, and from the deconvolution process the impulse response function and the system input function are graphed.

Table B-1. Well Murphy #7, daily elevations of water table above mean sea level (December 1959 to October 1960).

Date	Water level (feet)	Water level (meters)	Date	Water level (feet)	Water level (meters)
12/26/59	2284.36	696.27	2/01/60	2323.97	708.34
12/27/59	2285.55	696.63	2/02/60	2324.04	708.37
12/28/59	-	-	2/03/60	2324.10	708.38
12/29/59	2288.60	697.56	2/04/60	2323.94	708.34
12/30/59	2290.01	697.99	2/05/60	2323.66	708.25
12/31/59	2290.37	698.10	2/06/60	2322.64	707.94
			2/07/60	2321.22	707.41
1/01/60	2290.04	698.00	2/08/60	2320.40	707.26
1/02/60	2290.22	698.06	2/09/60	2320.48	707.28
1/03/60	2290.73	698.21	2/10/60	2320.40	707.29
1/04/60	2291.08	698.32	2/11/60	2320.40	707.26
1/05/60	2291.63	698.49	2/12/60	2320.28	707.22
1/06/60	2291.60	698.48	2/13/60	2320.27	707.21
1/07/60	2291.55	698.46	2/14/60	2320.17	707.19
1/08/60	2291.38	698.41	2/15/60	2319.66	606.03
1/09/60	2290.87	698.26	2/16/60	2319.09	706.86
1/10/60	2291.06	698.31	2/17/60	-	-
1/11/60	2291.44	698.43	2/18/60	2317.89	706.49
1/12/60	2293.21	698.97	2/19/60	2317.55	706.39
1/13/60	2304.07	702.28	2/20/60	2317.17	706.27
1/14/60	2304.22	702.32	2/21/60	2316.85	706.17
1/15/60	2305.67	702.77	2/22/60	2316.67	706.12
1/16/60	2308.32	703.57	2/23/60	2316.37	706.03
1/17/60	2311.80	704.63	2/24/60	2316.07	705.94
1/18/60	2213.19	705.06	2/25/60	2315.84	705.87
1/19/60	2314.42	705.42	2/26/60	2315.80	705.85
1/20/60	2317.22	706.29	2/27/60	2315.44	705.74
1/21/60	2316.99	706.22	2/28/60	2315.22	705.68
1/22/60	2318.94	706.81	2/29/60	2314.78	705.54
1/23/60	2318.62	706.71			
1/24/60	2319.30	706.92	3/01/60	2314.79	705.55
1/25/60	2302.02	707.14	3/02/60	2314.56	705.48
1/26/60	2320.52	707.29	3/03/60	2314.32	705.40
1/27/60	2321.11	707.47	3/04/60	2314.12	705.34
1/28/60	2323.15	708.09	3/05/60	2313.94	705.29
1/29/60	2323.39	708.17	3/06/60	2313.73	705.22
1/30/60	2323.61	708.24	3/07/60	2314.40	705.43
1/31/60	2323.74	708.27	3/08/60	2316.19	705.97

Table B-1 -- continued

Date	Water level (feet)	Water level (meters)	Date	Water level (feet)	Water level (meters)
3/09/60	2317.14	706.26	5/23/60	2301.78	701.58
3/10/60	2317.90	706.49	5/31/60	2300.17	701.09
3/11/60	2318.30	706.62			
3/12/60	2318.57	706.70	6/06/60	2299.31	700.83
3/13/60	2318.70	706.74	6/13/60	2298.20	700.49
3/14/60	2318.73	706.75	6/20/60	2297.30	700.22
3/15/60	2318.57	706.70	6/27/69	2296.27	699.90
3/16/60	2318.34	706.63			
3/19/60	2316.15	705.96	7/05/60	2295.49	699.66
3/20/60	2315.73	705.83	7/12/60	2294.15	699.25
3/21/60	2315.36	705.72	7/17/60	2293.78	699.14
3/22/60	2315.00	705.61	7/23/60	2294.52	699.37
3/23/60	2314.67	705.51	7/25/60	2294.01	699.52
3/24/60	2314.61	705.49	7/28/60	2291.62	698.48
3/25/60	2315.37	705.72	7/29/60	2294.65	699.41
3/26/60	2314.14	705.35			
3/27/60	2313.92	705.28	8/05/60	2294.68	699.42
3/28/60	2313.65	605.20	8/10/60	2295.45	699.65
3/29/60	2313.35	605.11	8/12/60	2294.60	699.39
3/30/60	2313.11	605.03	8/15/60	2294.31	699.30
3/31/60	2312.91	704.97	8/17/60	2294.40	699.33
			8/22/60	2294.21	699.27
4/01/60	2312.65	704.89	8/23/60	2293.73	699.13
4/02/60	2312.40	704.82	8/25/60	2293.14	698.95
4/03/60	2312.28	704.78	8/27/60	2292.43	698.73
4/04/60	2312.10	704.73			
4/05/60	2311.86	704.65	9/03/60	2291.49	698.44
4/06/60	2311.71	704.61	9/10/60	2291.95	698.28
4/07/60	2311.52	704.55	9/20/60	2290.95	698.28
4/08/60	2311.31	704.49			
4/09/60	2311.14	704.43	10/03/60	2290.24	698.06
4/10/60	2310.93	704.37			
4/11/60	2310.67	704.29			
4/12/60	2310.00	704.09			
4/13/60	2309.09	703.81			
4/14/60	2308.65	703.67			
4/15/60	2308.46	703.62			
4/25/60	2307.62	703.36			
5/02/60	2306.29	702.96			
5/09/60	2304.45	602.39			
5/16/60	2303.28	702.04			

Table B-2. Well Erwing #4, daily elevations of water table above mean sea level (December 1959 to November 1960).

Date	Water Level (feet)	Water Level (meters)	Date	Water Level (feet)	Water Level (meters)
12/26/59	2304.03	702.27	2/01/60	2335.14	711.75
12/27/59	2305.69	702.77	2/02/60	2335.83	711.97
12/28/59	-	-	2/03/60	2335.17	711.76
12/29/59	2308.25	703.55	2/04/60	2335.14	711.75
12/30/59	2310.59	704.27	2/05/60	2334.94	711.69
12/31/59	2311.47	704.53	2/06/60	2334.68	711.61
			2/07/60	2334.18	711.46
1/01/60	2310.74	704.31	2/08/60	2333.88	711.36
1/02/60	2310.92	704.37	2/09/60	-	-
1/03/60	2311.26	704.47	2/10/60	2333.22	711.16
1/04/60	2312.53	704.86	2/11/60	2333.19	711.15
1/05/60	2312.53	704.86	2/12/60	2333.05	711.11
1/06/60	2311.74	704.62	2/13/60	2333.04	711.11
1/07/60	2311.00	704.39	2/14/60	2332.95	711.08
1/08/60	2311.59	704.57	2/15/60	2332.72	711.01
1/09/60	2311.49	704.54	2/16/60	2332.47	710.93
1/10/60	2311.73	704.61	2/17/60	2331.86	710.75
1/11/60	2312.01	704.70	2/18/60	2331.41	710.61
1/12/60	2314.45	705.44	2/19/60	-	-
1/13/60	2321.40	707.56	2/20/60	2330.57	710.36
1/14/60	2323.47	708.19	2/21/60	2330.27	710.26
1/15/60	2325.76	708.89	2/22/60	2330.07	710.20
1/16/60	2327.43	709.40	2/23/60	2329.62	710.07
1/17/60	2331.06	710.51	2/24/60	2329.09	709.90
1/18/60	2330.14	710.22	2/25/60	2329.04	709.89
1/19/60	2330.94	710.47	2/26/60	2328.59	709.75
1/20/60	2331.43	710.62	2/27/60	2328.33	709.67
1/21/60	2331.94	710.77	2/28/60	2328.17	709.62
1/22/60	2332.32	710.89	2/29/60	2327.90	709.54
1/23/60	2332.73	711.01			
1/24/60	2333.13	711.14	3/01/60	2327.82	709.52
1/25/60	2333.67	711.30	3/02/60	2327.44	709.40
1/26/60	2334.00	711.40	3/03/60	2327.40	709.39
1/27/60	2334.35	711.51	3/04/60	2327.22	709.33
1/28/60	2334.58	711.58	3/06/60	2326.78	709.20
1/29/60	2334.70	711.61	3/07/60	2327.18	709.32
1/30/60	2334.94	711.69	3/08/60	2327.39	709.39
1/31/60	2335.00	711.71	3/09/60	2327.82	709.52

Table B-2 -- continued

Date	Water Level (feet)	Water Level (meters)	Date	Water Level (feet)	Water Level (meters)
3/10/60	2328.05	709.59	5/02/60	2321.14	707.48
3/11/60	2328.27	709.65	5/09/60	2320.24	707.21
3/12/60	2328.77	709.81	5/23/60	2318.79	706.77
3/13/60	2329.02	709.88	5/31/60	2317.91	706.50
3/14/60	2329.13	709.92			
3/15/60	2329.28	709.96	6/13/60	2316.69	706.13
3/16/60	2329.32	709.97	6/20/60	2315.76	705.84
3/17/60	2328.95	709.86	6/27/60	2315.61	705.80
3/18/60	2328.50	709.72			
3/19/60	2328.17	709.62	7/05/60	2315.16	705.66
3/20/60	2327.84	709.52	7/12/60	2313.57	705.17
3/21/60	2327.46	709.41	7/17/60	2314.17	705.36
3/23/60	2326.93	709.25	7/25/60	2313.86	705.26
3/25/60	2326.37	709.08	7/29/60	2313.99	705.30
3/26/60	2326.12	709.99			
3/27/60	2325.93	708.94	8/05/60	2313.74	705.23
3/28/60	2325.79	708.90	8/12/60	2313.74	705.23
3/29/60	2325.58	709.83	8/15/60	2313.86	705.26
3/30/60	2325.50	708.81	8/17/60	2313.48	705.15
3/31/60	2325.36	708.77	8/22/60	2313.41	705.13
			8/23/60	2313.63	705.19
4/01/60	2325.17	708.71			
4/02/60	2324.95	708.64	9/26/60	2311.86	704.65
4/03/60	2324.72	708.57			
4/04/60	2324.70	708.56	10/10/60	2311.19	704.45
4/05/60	2324.46	708.49	10/17/60	2311.21	704.46
4/06/60	2324.40	708.48			
4/07/60	2324.27	708.44	11/01/60	2310.58	704.26
4/08/60	2324.13	708.39	11/07/60	2310.56	704.25
4/09/60	2324.98	708.35	11/14/60	2310.44	704.22
4/10/60	2323.85	708.31	11/22/60	2310.18	704.14
4/11/60	2323.75	708.28			
4/12/60	2323.67	708.25			
4/13/60	2323.43	708.18			
4/14/60	2323.21	708.11			
4/15/60	2323.21	708.11			
4/25/60	2322.90	708.02			

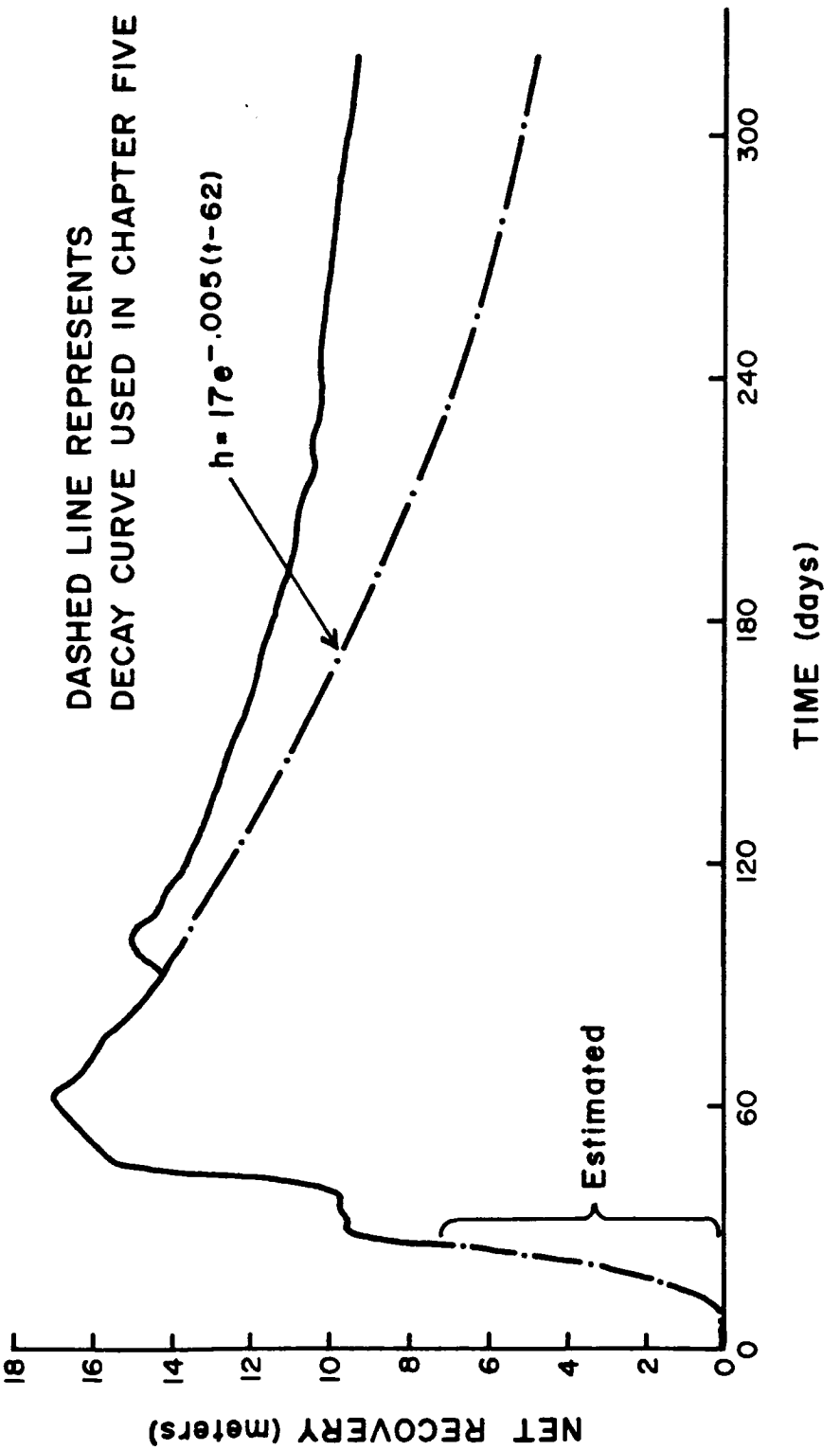

Figure B-1. Well hydrograph for Erwing #4.

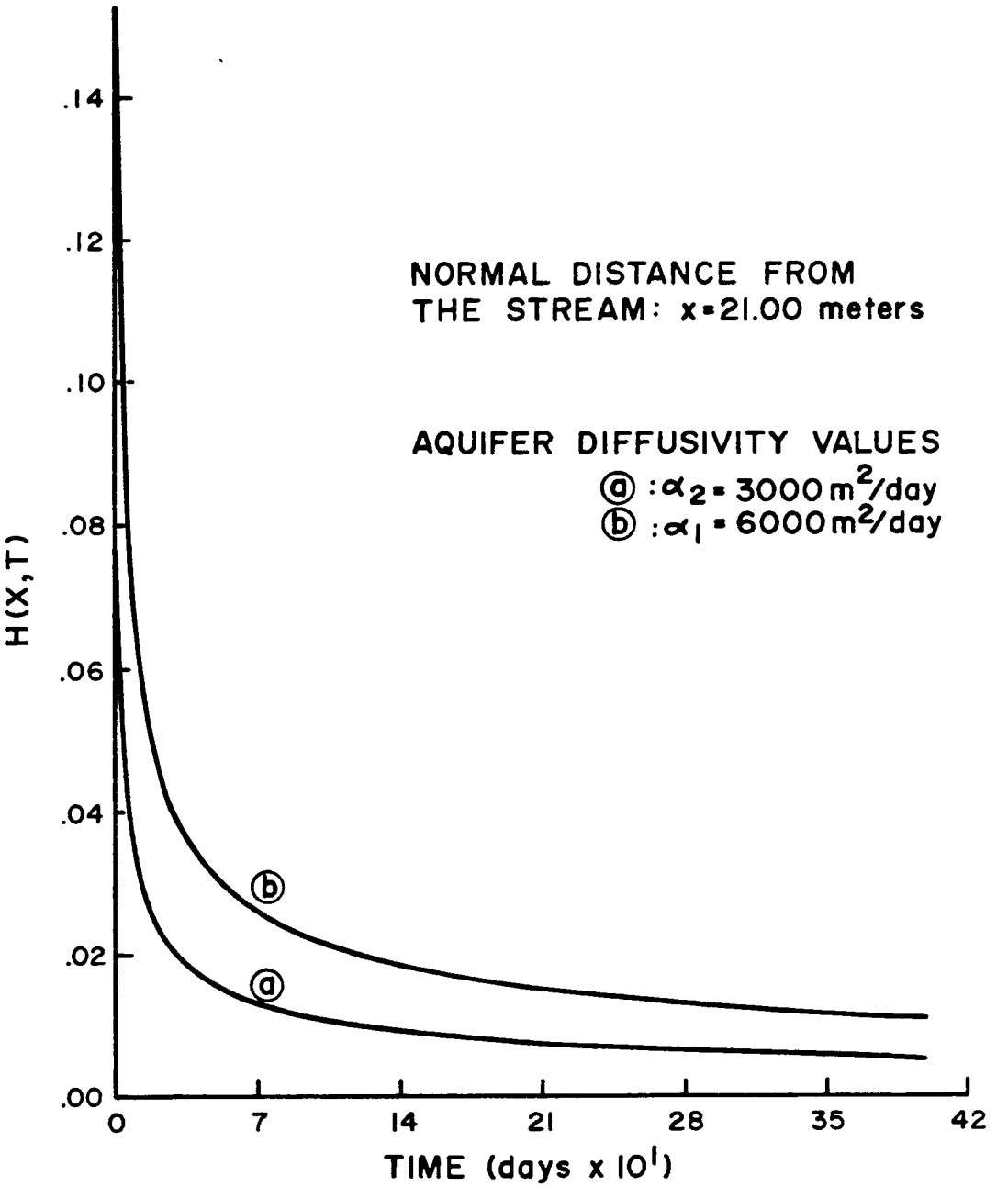

Figure B-2. Impulse response functions for well Erwing #4.

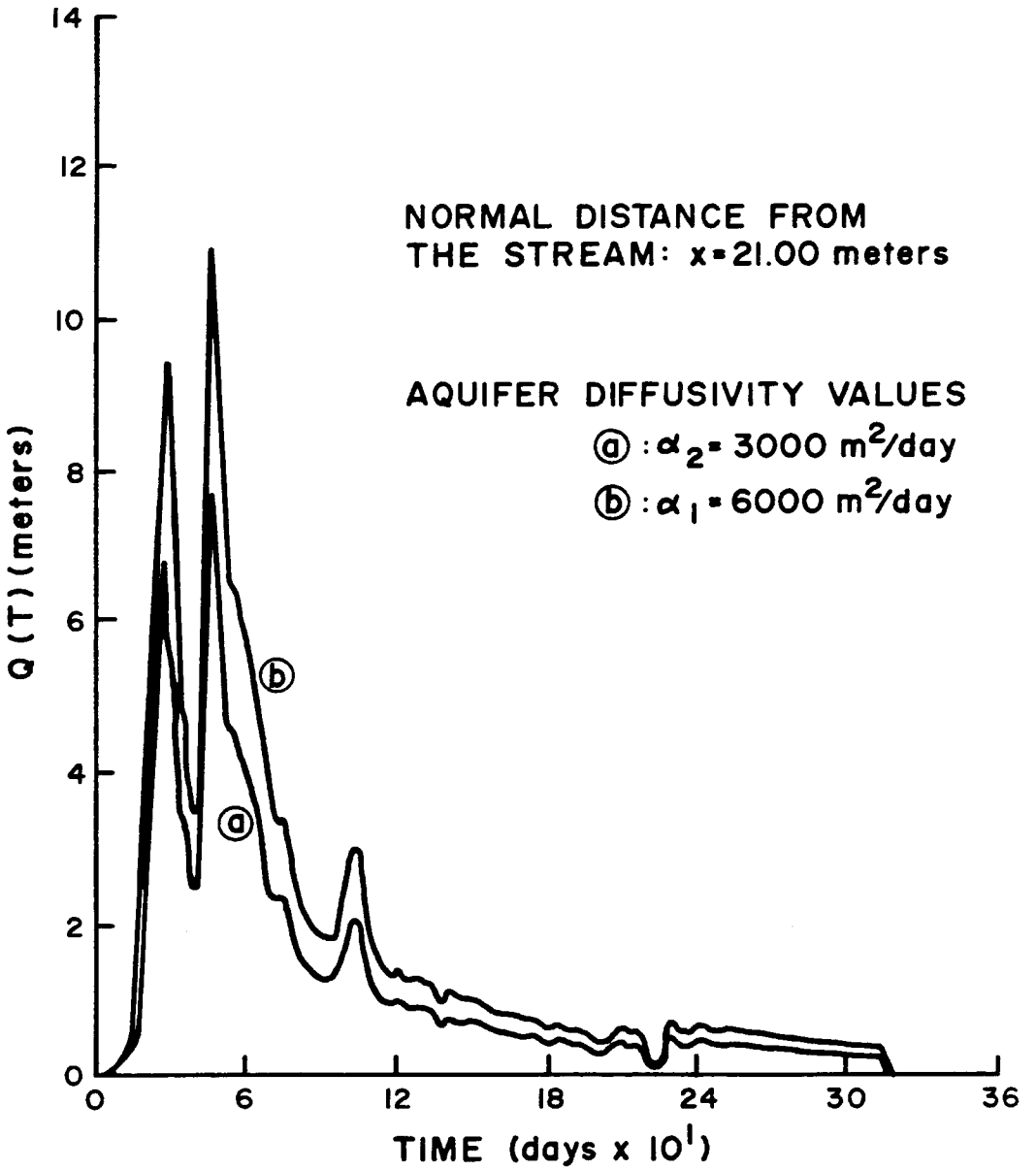

Figure B-3. System input function for Erwing #4.

Table B-3. Well Murphy #5, daily elevations of water table above mean sea level (January 1960 to December 1960).

Date	Water Level (feet)	Water Level (meters)	Date	Water Level (feet)	Water Level (meters)
1/14/60	2289.13	697.72	2/21/60	2315.25	705.68
1/15/60	2290.83	698.24	2/22/60	2315.22	705.68
1/16/60	2292.16	698.65	2/23/60	2314.80	705.55
1/17/60	2293.54	699.07	2/24/60	2314.77	705.54
1/18/60	2297.52	700.28	2/25/60	2314.56	705.48
1/19/60	2298.92	700.71	2/26/60	2314.46	705.45
1/20/60	2302.92	701.93	2/27/60	2314.08	705.33
1/21/60	2305.70	702.78	2/28/60	2313.74	705.23
1/22/60	2308.04	703.49	2/29/60	2313.91	705.28
1/23/60	2308.49	703.63			
1/24/60	2310.89	704.36	3/01/60	2213.52	705.16
1/25/60	2312.66	604.90	3/02/60	2313.46	705.14
1/26/60	2313.29	705.09	3/03/60	2313.36	705.11
1/27/60	2314.28	705.39	3/04/60	2313.02	705.01
1/28/60	2314.98	705.60	3/05/60	2312.54	704.86
1/29/60	2315.58	705.79	3/06/60	2312.30	704.79
1/30/60	2316.11	705.95	3/07/60	2312.55	704.86
1/31/60	2316.55	706.08	3/09/60	2313.08	705.02
			3/11/60	2313.81	705.24
2/01/60	2316.67	706.12	3/12/60	2313.83	705.25
2/02/60	2317.37	706.33	3/13/60	2314.44	705.44
2/03/60	2317.95	706.51	3/14/60	2314.69	705.52
2/04/60	2317.65	706.42	3/15/60	2314.82	705.56
2/05/60	2318.13	706.56	3/16/60	2314.90	705.58
2/06/60	2317.94	706.51	3/17/60	2314.50	705.46
2/07/60	2317.66	706.42	3/18/60	2314.04	705.32
2/08/60	2317.22	706.29	3/19/60	2313.83	705.25
2/09/60	2316.69	706.13	3/20/60	2313.67	705.20
2/10/60	2316.60	706.10	3/21/60	2313.48	705.15
2/11/60	2316.43	706.05	3/22/60	2313.16	705.05
2/12/60	2316.67	706.12	3/23/60	2312.87	704.96
2/13/60	2316.75	706.14	3/24/60	2313.00	705.00
2/14/60	2316.87	706.18	3/25/60	2312.94	704.98
2/15/60	2316.84	706.17	3/26/60	2312.96	704.99
2/16/60	2316.63	706.11	3/27/60	2312.48	704.84
2/17/60	2316.12	705.95	3/28/60	2312.42	704.82
2/18/60	2315.86	705.87	3/29/60	2312.07	704.72
2/19/60	2315.78	705.85	3/30/60	2311.72	704.61
2/20/60	2315.53	705.77	3/31/60	2311.56	604.56

Table B-3 -- continued

Date	Water Level (feet)	Water Level (meters)	Date	Water Level (feet)	Water Level (meters)
4/01/60	2311.48	704.54	7/25/60	2294.05	699.22
4/03/60	2311.47	704.53	7/29/60	2294.31	699.30
4/04/60	2311.04	704.40			
4/05/60	2310.71	704.30	8/05/60	2293.03	698.91
4/06/60	2310.19	704.14	8/10/60	2293.95	699.19
4/07/60	2309.78	704.02	8/11/60	2292.03	698.61
4/08/60	2310.19	704.19	8/17/60	2292.74	698.83
4/09/60	2309.83	704.03	8/22/60	2293.52	699106
4/10/60	2309.83	704.03	8/23/60	2293.57	699.08
4/11/60	2309.45	703.92	8/25/60	2293.31	699.00
4/12/60	2310.26	704.17	8/27/60	2292.77	698.83
4/13/60	2310.21	704.15			
4/14/60	2310.10	704.12	9/03/60	2292.26	698.68
4/15/60	2310.06	604.10	9/19/60	2292.01	698.60
4/25/60	2308.40	703.40	9/26/60	2291.37	698.41
5/02/60	2305.80	702.81	10/03/60	2291.11	698.33
5/09/60	2305.67	702.77	10/10/60	2291.27	698.38
5/16/60	2303.81	702.20	10/17/60	2291.36	698.40
5/23/60	2302.18	701.70	10/24/60	2289.91	697.96
5/31/60	2300.54	701.20			
			11/01/60	2290.22	698.06
6/06/60	2299.75	700.96	11/07/60	2290.25	698.07
6/13/60	2298.50	700.58	11/14/60	2290.40	698.11
6/20/60	2297.73	700.36	11/22/60	2289.80	697.93
6/27/60	2296.80	700.06			
			12/01/60	2287.74	697.30
7/05/60	2295.97	699.81	12/10/60	2289.59	697.87
7/17/60	2294.67	699.41	12/23/60	2289.58	697.86

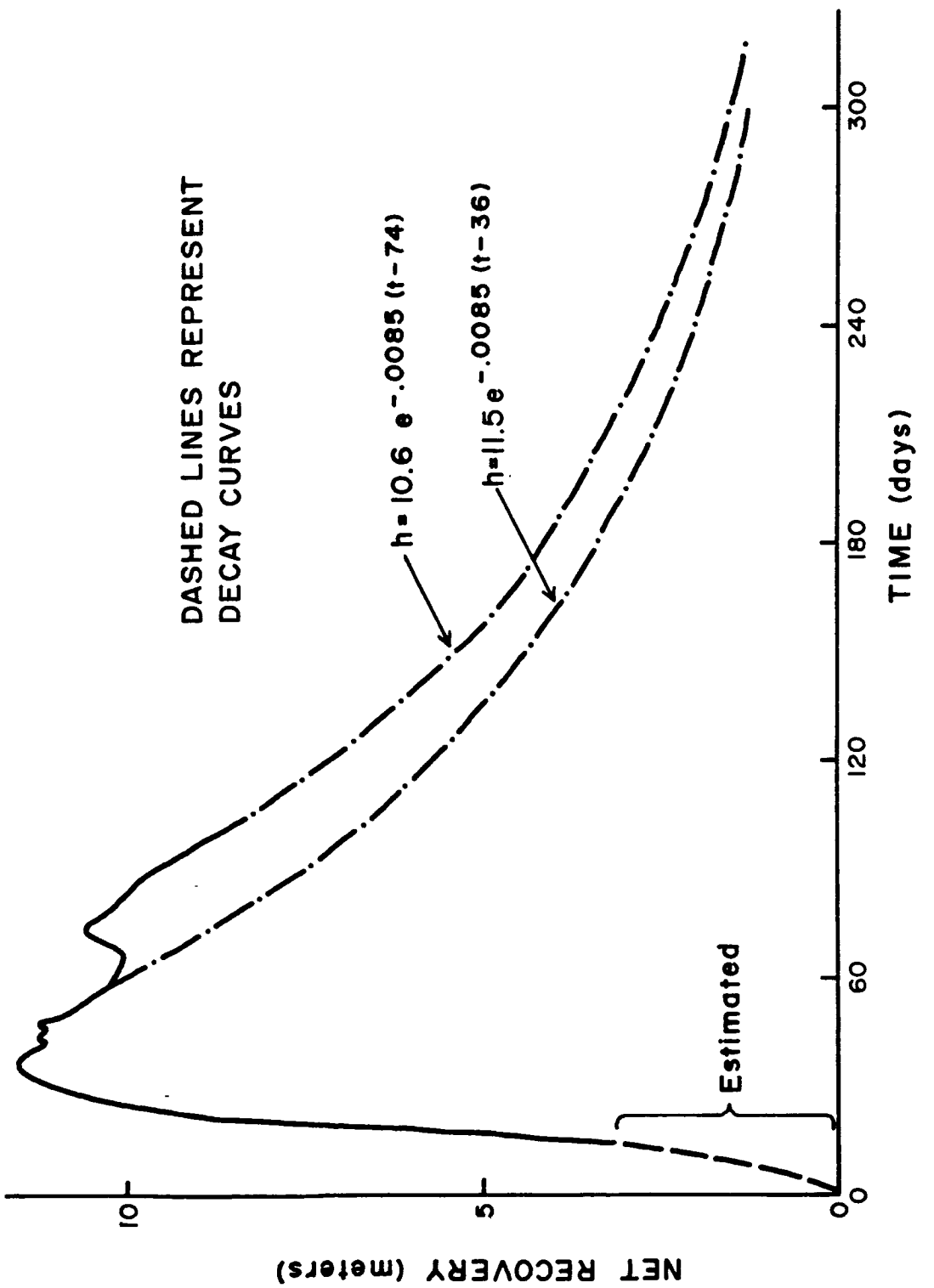

Figure B-4. Well hydrograph for Murphy #5.

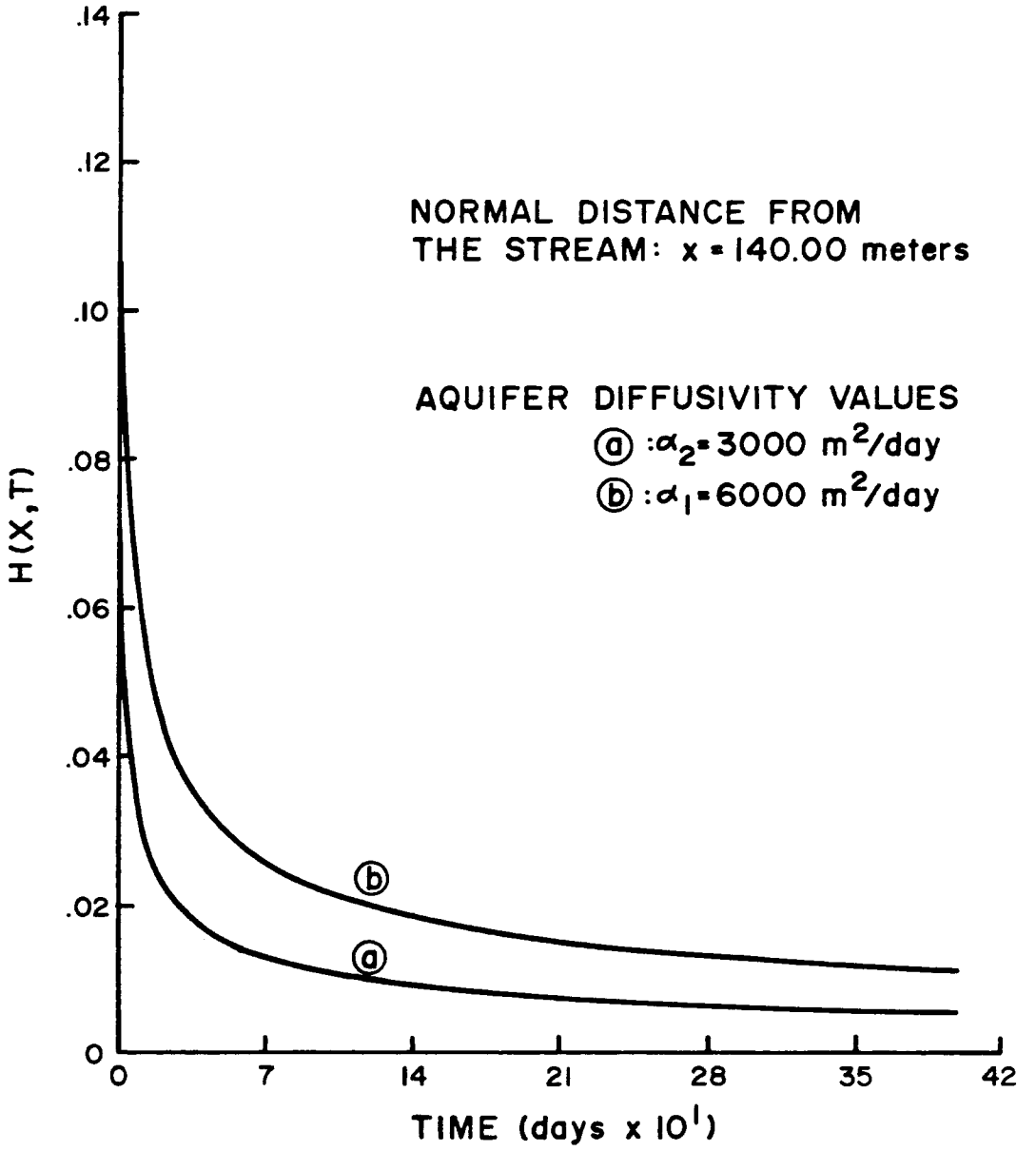

Figure B-5. Impulse response functions for Murphy #5.

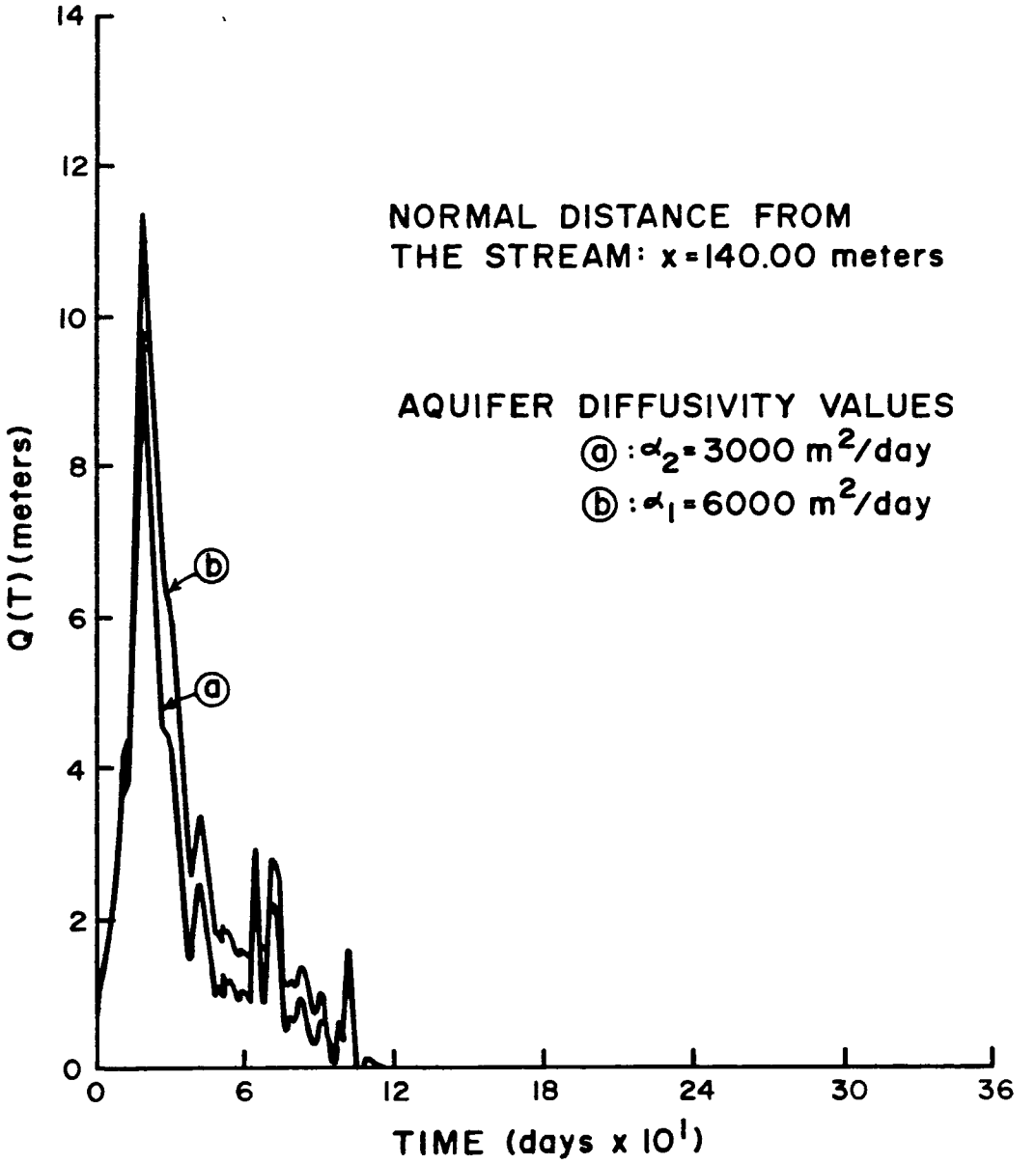

Figure B-6. System input function for Murphy #5.

Table B-4. Well Murphy #4, daily elevations of water table above mean sea level (January 1960 to December 1960).

Date	Water Level (feet)	Water Level (meters)	Date	Water Level (feet)	Water Level (meters)
1/15/60	2288.46	697.52	2/24/60	2313.88	705.26
1/16/60	2289.17	697.74	2/25/60	2313.63	705.19
1/17/60	2290.77	698.22	2/26/60	2313.66	705.20
1/18/60	2291.86	698.56	2/27/60	2313.40	705.12
1/19/60	2294.02	699.22	2/28/60	2313.04	705.01
1/20/60	2295.14	699.56	2/29/60	2313.21	705.07
1/21/60	2299.10	700.76			
1/22/60	2299.59	700.91	3/01/60	2312.92	704.98
1/24/60	2302.31	701.74	3/02/60	2312.84	704.95
1/25/60	2306.10	702.90	3/03/60	2312.75	704.92
1/26/60	2308.02	703.48	3/04/60	2311.43	704.52
1/27/60	2309.02	703.79	3/06/60	2311.74	704.62
1/28/60	2309.99	704.08	3/07/60	2311.99	704.69
1/29/60	2311.04	704.40	3/09/60	2312.21	704.76
1/30/60	2311.88	704.66	3/11/60	2312.68	704.90
1/31/60	2312.48	704.84	3/12/60	2312.46	704.84
			3/13/60	2313.18	705.06
2/01/60	2313.23	705.07	3/14/60	2313.21	705.07
2/02/60	2313.71	705.22	3/15/60	2313.47	705.14
2/03/60	2314.62	705.49	3/16/60	2313.56	705.17
2/04/60	2314.29	705.39	3/17/60	2313.40	705.12
2/05/60	2315.24	705.68	3/18/60	2313.27	705.08
2/06/60	2315.16	705.66	3/19/60	2312.92	704.98
2/07/60	2315.20	705.67	3/20/60	2312.76	704.93
2/08/60	2315.13	705.65	3/21/60	2312.66	704.90
2/09/60	2314.64	705.50	3/22/60	2312.47	704.84
2/10/60	2314.68	705.51	3/23/60	2312.20	704.76
2/11/60	2314.36	705.42	3/24/60	2312.41	704.82
2/12/60	2314.80	705.55	3/25/60	2312.50	704.85
2/13/60	2314.96	705.60	3/26/60	2312.32	704.79
2/14/60	2315.13	705.65	3/27/60	2311.90	704.67
2/15/60	2315.19	705.67	3/28/60	2311.85	704.65
2/16/60	2315.11	705.64	3/29/60	2311.59	704.57
2/17/60	2314.74	705.53	3/30/60	2311.31	704.49
2/18/60	2314.60	705.49	3/31/60	2311.09	704.42
2/19/60	2314.58	705.48			
2/20/60	2314.41	705.43	4/01/60	2311.02	704.40
2/21/60	2314.20	705.37	4/03/60	2311.02	704.40
2/22/60	2314.19	705.36	4/04/60	2310.72	704.31
2/23/60	2313.90	705.27	4/05/60	2310.53	704.25

Table B-4 -- continued

Date	Water Level (feet)	Water Level (meters)	Date	Water Level (feet)	Water Level (meters)
4/06/60	2309.97	704.08	8/05/60	2293.95	699.19
4/07/60	2309.59	603.96	8/10/60	2294.27	699.29
4/08/60	2309.95	704.07	8/17/60	2293.19	698.96
4/09/60	2309.56	703.95	8/22/60	2293.74	699.13
4/10/60	2309.28	603.87	8/23/60	2293.63	699.09
4/11/60	2309.34	703.88	8/25/60	2293.65	699.10
4/12/60	2309193	704.07	8/27/60	2293.33	699.01
4/13/60	2310.03	704.09			
4/14/60	2309.88	704.05	9/03/60	2292.75	698.83
4/15/60	2309.67	703.99	9/19/60	2292.33	698.70
4/25/60	2308.01	703.48	9/26/60	2291.32	698.39
5/02/60	2307.11	703.21	10/03/60	2291.01	698.30
5/09/60	2304.95	702.55	10/10/60	2291.08	698.32
5/16/60	2303.52	702.11	10/17/60	2291.19	698.35
5/23/60	2301.95	701.63	10/24/60	2290.50	698.14
5/31/60	2300.36	601.15			
			11/01/60	2290.01	697.99
6/06/60	2299.61	700.92	11/07/60	2290.31	698.08
6/13/60	2298.07	700.45	11/14/60	2290.44	698.12
6/20/60	2297.57	700.30	11/22/60	2289.82	697.94
6/27/60	2296.80	700.06			
			12/10/60	2289.54	697.85
7/05/60	2295.75	699.74	12/23/60	2289.57	697.86
7/17/60	2294.49	699.36			
7/25/60	2294.81	699.46			
7/29/60	2294.81	699.46			

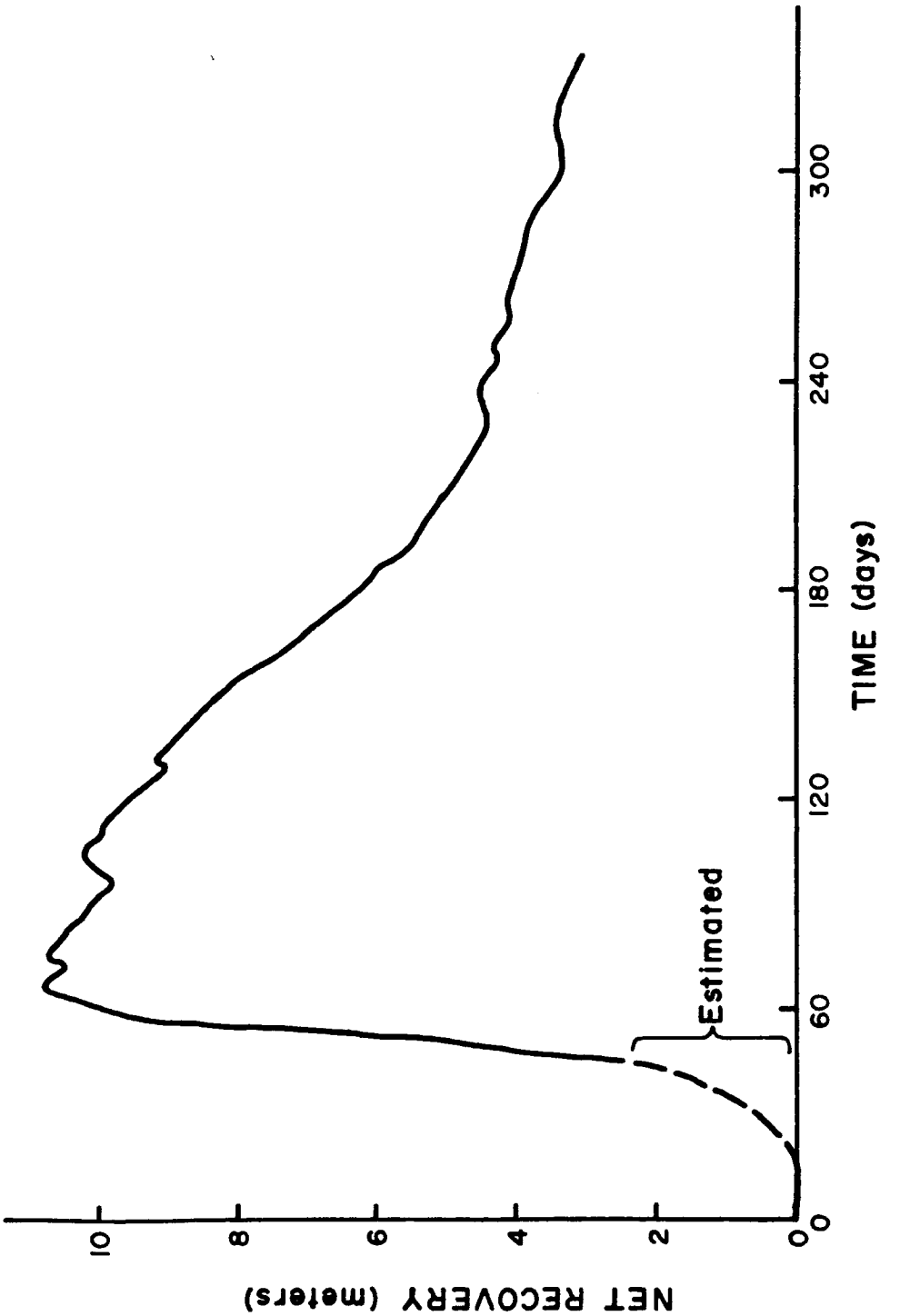

Figure B-7. Well hydrograph for Murphy #4.

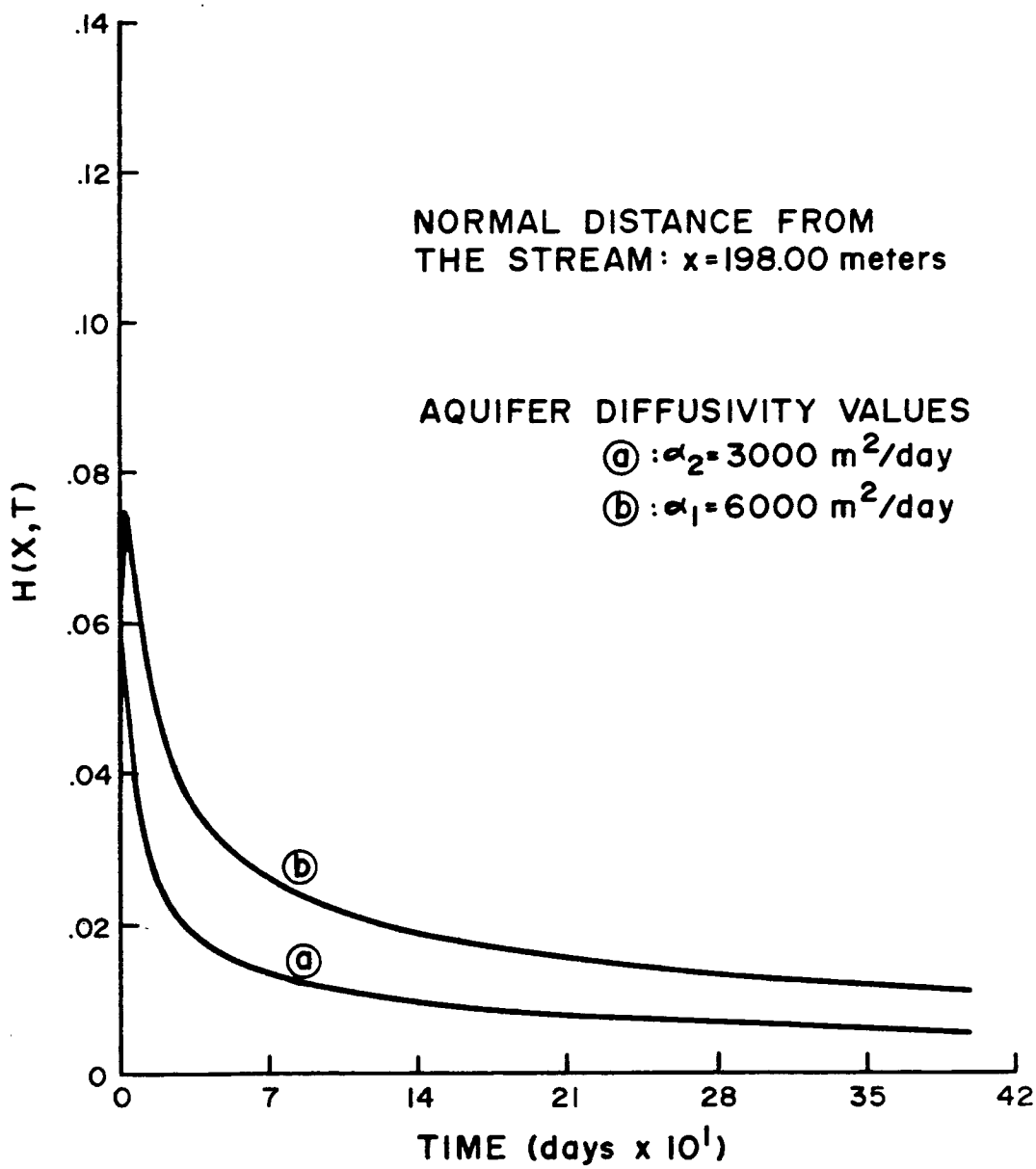

Figure B-8. Impulse response function for Murphy #4.

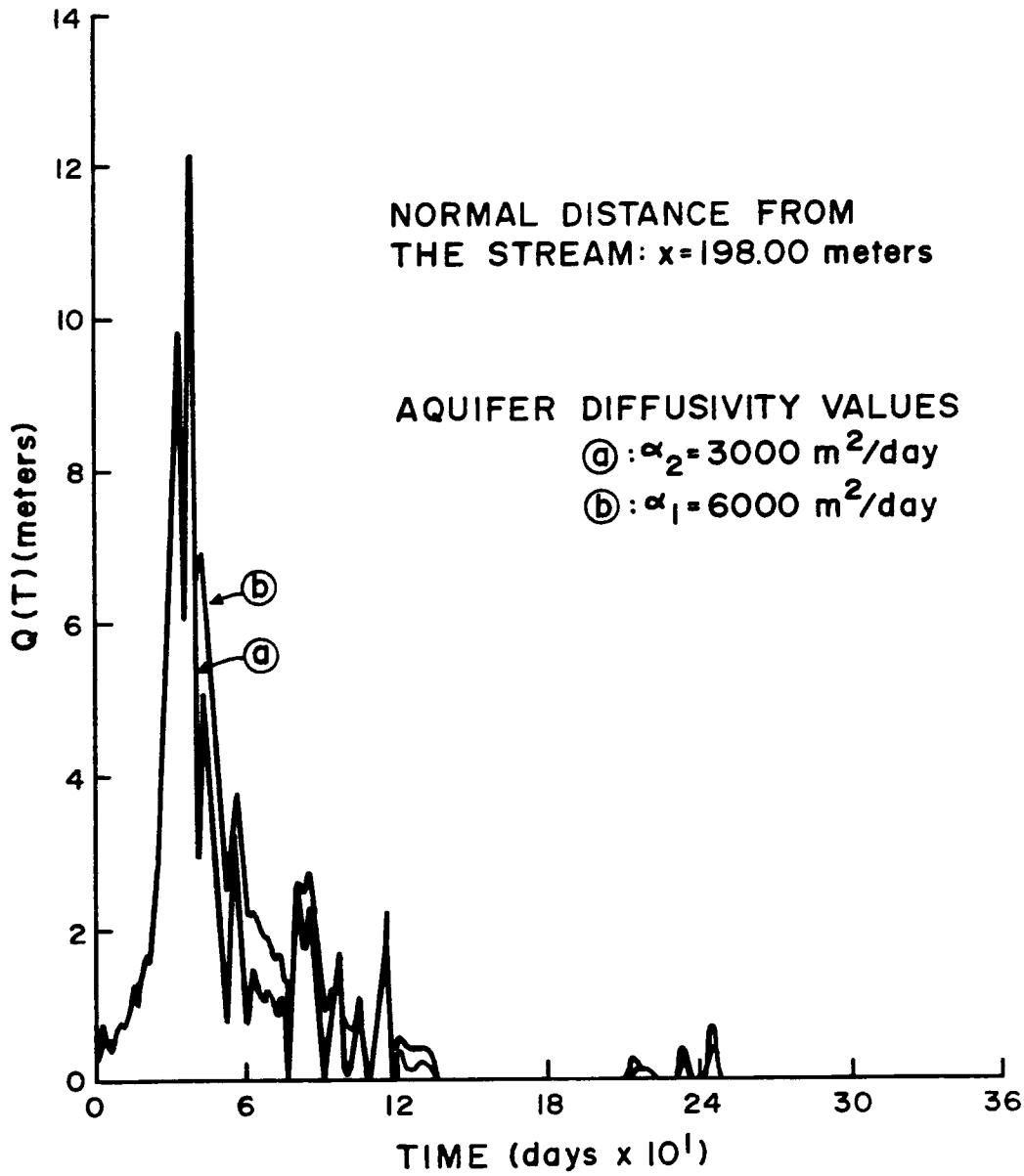

Figure B-9. System input function for Murphy #4.

Table B-5. Well Campbell #1, daily elevations of water table above mean sea level (January 1960 to December 1960)

Date	Water Level (feet)	Water Level (meters)	Date	Water Level (feet)	Water Level (meters)
1/14/60	2281.08	695.27	3/01/60	2308.66	703.68
1/15/60	2282.78	695.79	3/02/60	2308.47	703.62
1/16/60	2284.11	696.19	3/03/60	2308.50	703.63
1/17/60	2285.49	696.62	3/04/60	2308.47	703.62
1/18/60	2289.47	697.83	3/05/60	2308.31	703.66
1/19/60	2290.87	698.26	3/06/60	2308.12	703.51
1/20/60	2294.87	699.47	3/07/60	2308.06	703.49
1/22/60	2299.47	700.88	3/08/60	2308.02	703.48
1/25/60	2302.56	701.82	3/09/60	2308.12	703.51
1/29/60	2306.05	702.88	3/10/60	2308.32	703.57
1/30/60	2307.18	703.23	3/11/60	2308.66	703.68
1/31/60	2307.75	703.40	3/12/60	2308.77	703.71
			3/13/60	2308.99	703.78
2/01/60	2308.27	703.56	3/14/60	2309.18	703.84
2/02/60	2309.23	703.85	3/15/60	2309.36	703.89
2/03/60	2309.59	703.96	3/16/60	2309.53	703.94
2/04/60	2310.13	704.13	3/17/60	2309.53	703.94
2/07/60	2310.66	604.29	3/18/60	2309.52	703.94
2/08/60	2310.97	704.38	3/19/60	2309.59	703.96
2/09/60	2310.96	704.38	3/21/60	2309.33	703.88
2/11/60	2311.06	704.41	3/22/60	2309.31	703.88
2/12/60	2310.83	704.34	3/23/60	2309.04	703.79
2/14/60	2311.27	704.47	3/24/60	2308.95	703.77
2/15/60	2311.00	704.39	3/25/60	2309.69	703.99
2/16/60	2311.17	704.44	3/26/60	2308.47	703.62
2/17/60	2310.89	704.36	3/27/60	2308.39	703.59
2/18/60	2311.04	704.40	3/28/60	2308.45	703.61
2/19/60	2310.98	704.38	3/29/60	2308.08	703.50
2/20/60	2310.44	704.22	3/31/60	2307.54	703.34
2/21/60	2310.48	704.23			
2/22/60	2310.46	704.22	4/01/60	2307.39	703.29
2/23/60	2309.90	704.06	4/02/60	2307.29	703.29
2/24/60	2309.64	703.98	4/03/60	2307.11	703.21
2/25/60	2309.50	703.93	4/04/60	2307.28	703.26
2/26/60	2309.31	703.88	4/05/60	2306.97	703.16
2/27/60	2309.02	703.79	4/06/60	2306.81	703.11
2/28/60	2308.88	703.74	4/07/60	2306.98	703.17
2/29/60	2308.93	703.76	4/08/60	2306.68	703.07

Table B-5 -- continued

Date	Water Level (feet)	Water Level (meters)	Date	Water Level (feet)	Water Level (meters)
4/09/60	2306.45	703.00	6/20/60	2297.58	700.30
4/10/60	2306.28	702.95	6/27/60	2296.64	700.01
4/11/60	2306.48	703.01			
4/12/60	2306.06	702.89	7/25/60	2294.65	699.41
			7/29/60	2294.55	699.38
5/02/60	2303.69	702.16			
5/23/60	2301.23	701.41	11/22/60	2292.36	698.7o
5/31/60	2300.00	701.04			
			12/01/60	2291.07	698.32
			12/10/60	2291.42	698.42

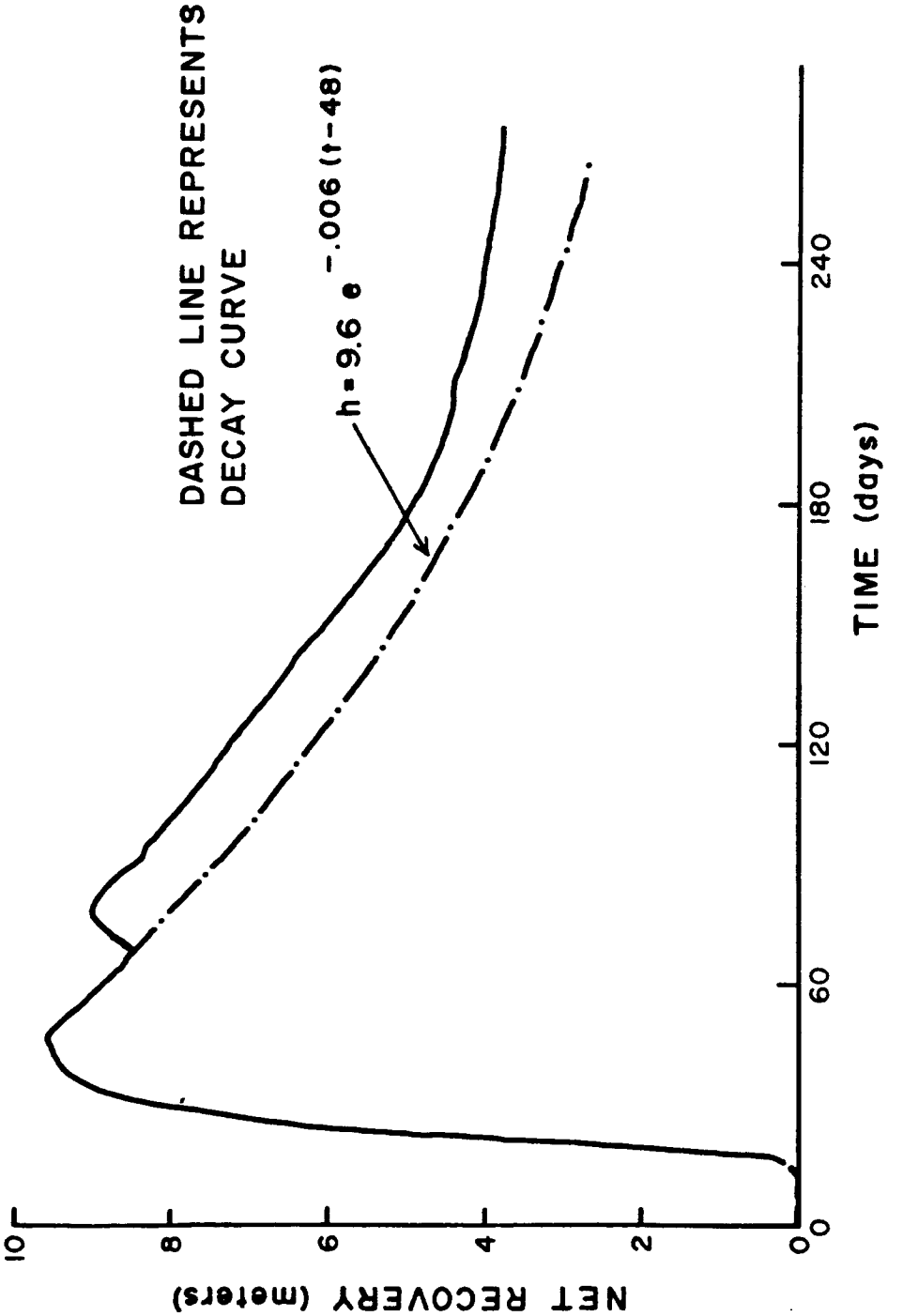

Figure B-10. Well hydrograph for Campbell #1.

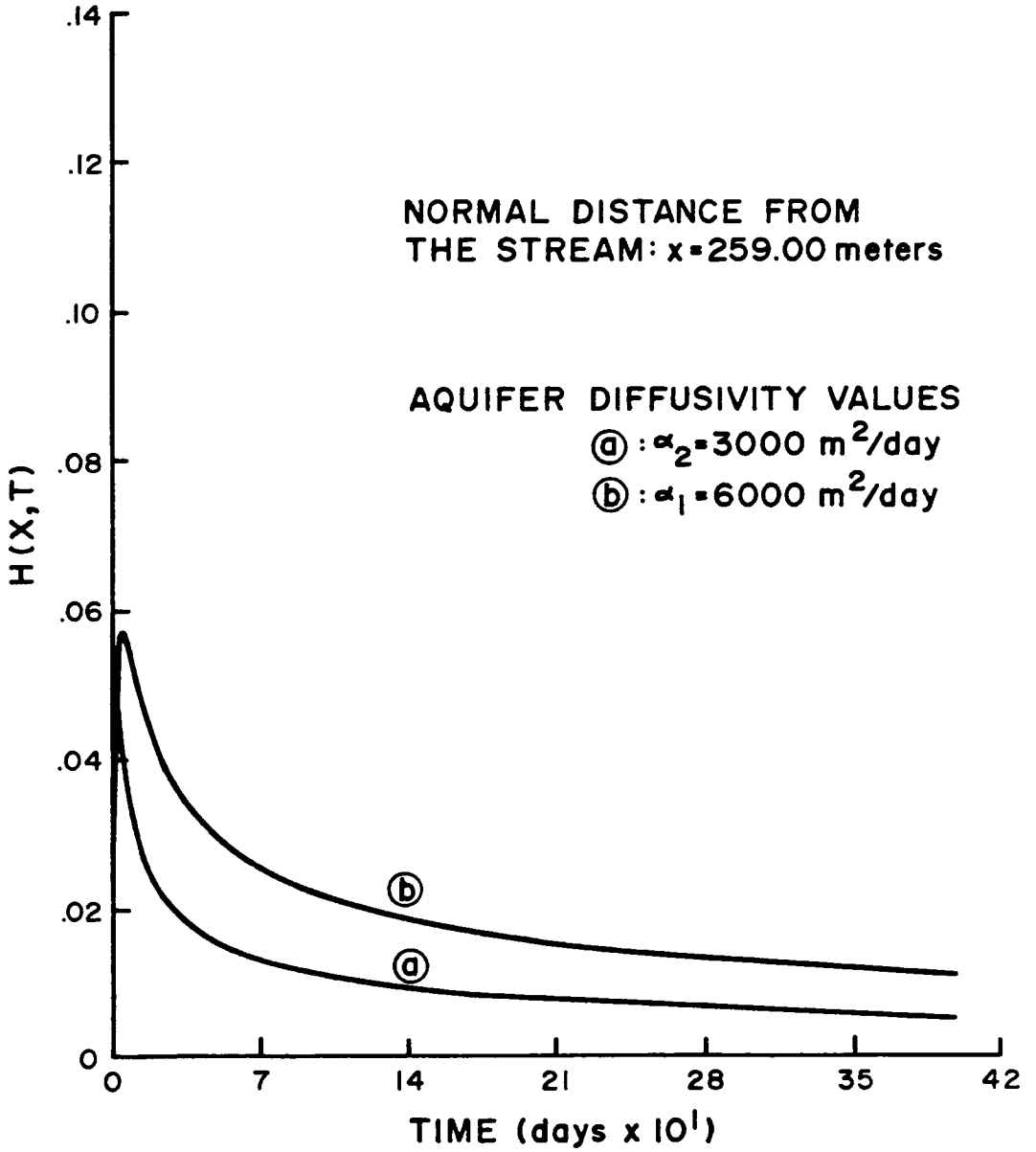

Figure B-11. Impulse response function for Campbell #1.

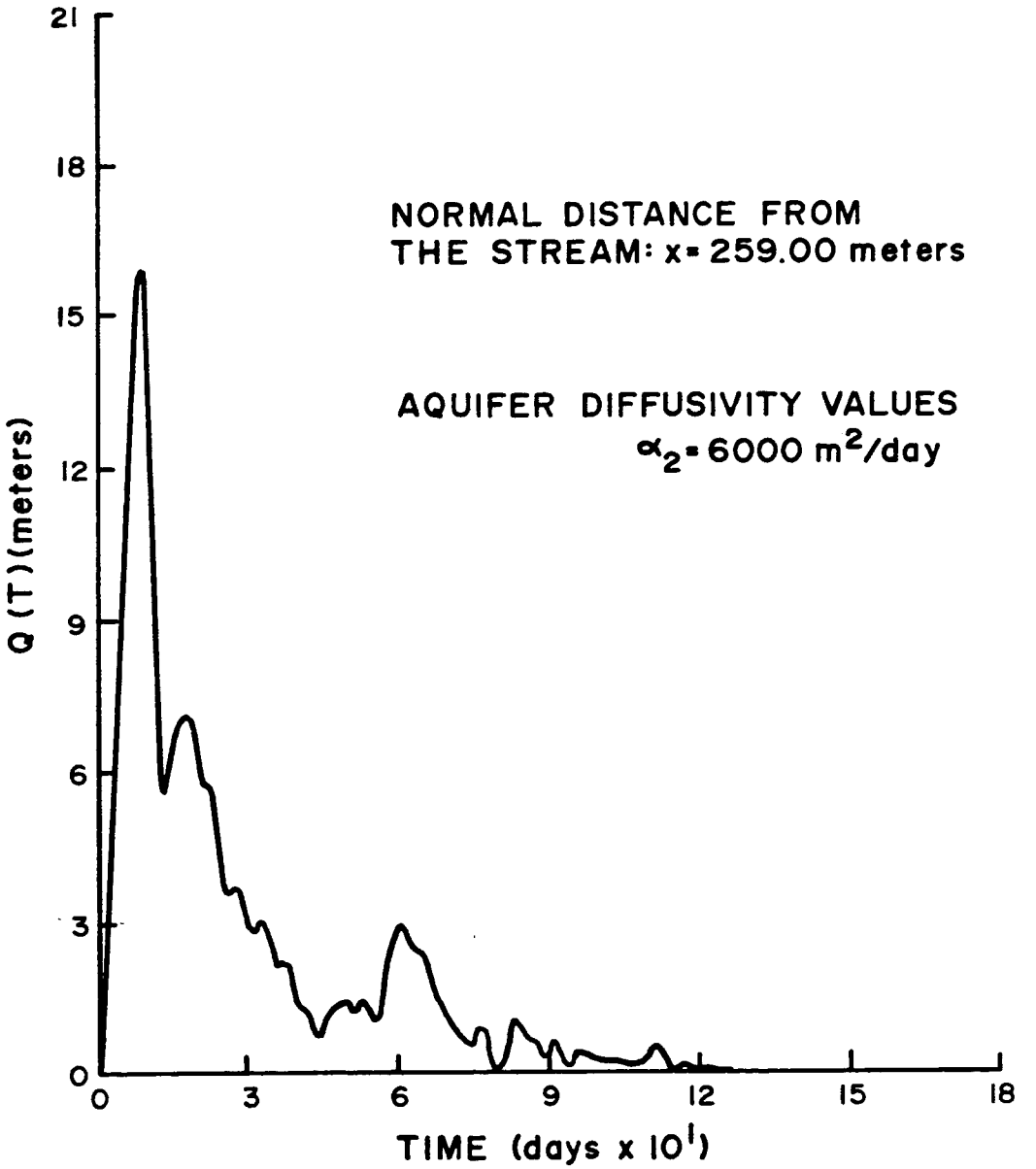

Figure B-12. System input function for Campbell #1.

Table B-6. Well Erwing #2, daily elevations of water table above mean sea level (December 1959 to October 1960).

Date	Water Level (feet)	Water Level (meters)	Date	Water Level (feet)	Water Level (meters)
12/26/59	2290.13	698.03	2/04/60	2306.17	702.92
12/27/59	2290.18	698.04	2/05/60	2306.75	703.09
12/28/59	-	-	2/06/60	2307.37	703.38
12/29/59	2290.30	698.08	2/07/60	2307.77	703.41
12/30/59	2290.47	698.13	2/08/60	2308.02	703.48
12/31/59	2290.53	698.15	2/09/60	2308.45	703.61
			2/10/60	2308.53	703.64
1/01/60	2290.56	698.16	2/11/60	2308.76	703.10
1/02/60	2290.88	698.26	2/12/60	2309.01	703.78
1/03/60	2291.16	698.37	2/13/60	2309.32	703.88
1/04/60	2291.28	698.38	2/14/60	2309.45	703.92
1/05/60	2290.58	698.17	2/15/60	2309.56	703.95
1/06/60	2291.78	698.53	2/16/60	2309.77	704.02
1/07/60	2292.16	698.65	2/17/60	2310.04	704.10
1/08/60	2291.85	698.55	2/18/60	2310.33	704.19
1/09/60	2291.88	698.56	2/19/60	2309.97	704.08
1/10/60	2291.99	698.60	2/20/60	2309.52	703.94
1/11/60	2292.06	698.62	2/21/60	2309.79	704.02
1/12/60	2292.23	698.67	2/22/60	2309.88	704.05
1/13/60	2292.37	698.71	2/23/60	2309.69	703.99
1/14/60	2292.48	698.75	2/24/60	2309.62	703.97
1/15/60	2292.76	698.83	2/25/60	2309.30	703.87
1/16/60	2293.07	698.93	2/26/60	2309.28	703.87
1/17/60	2293.52	699.06	2/27/60	2309.13	703.82
1/18/60	2294.25	699.29	2/28/60	2309.02	703.79
1/19/60	2294.63	699.40	2/29/60	2309.17	703.83
1/20/60	2294.59	699.39			
1/21/60	2295.o8	699.57	3/01/60	2309.03	703.79
1/22/60	2295.98	699181	3/02/60	2308.77	703.7o
1/23/60	2296.46	699.96	3/03/60	2308.72	703.70
1/24/60	2297.33	700.22	3/04/60	2308.65	703.67
1/25/60	2298.11	700.46	3/06/60	2308.30	703.57
1/26/60	2298.83	700.68	3/07/60	2308.58	703.65
1/27/60	2300.02	701.04	3/08/60	2308.41	703.60
1/28/60	2300.92	701.32	3/09/60	2308.51	703.63
1/29/60	2301.87	701.61	3/10/60	2308.49	703.62
1/30/60	2302.68	701.85	3/11/60	2308.54	703.61
1/31/60	2303.51	702.11	3/12/60	2308.80	703.72
			3/13/60	2308.96	703.77
2/01/60	2304.31	702.35	3/14/60	2309.06	703.80
2/02/60	2305.13	702.60	3/15/60	2309.07	703.80
2/03/60	2305.74	702.79	3/16/60	2309.48	703.93

Table B-6 -- continued

Date	Water Level (feet)	Water Level (meters)	Date	Water Level (feet)	Water Level (meters)
3/17/60	2309.42	703.91	5/02/60	2306.18	702.92
3/18/60	2309.57	703.95	5/09/60	2305.33	702.66
3/19/60	2309.72	704.00	5/16/60	2304.57	702.43
3/20/60	2309.62	703.97	5/23/60	2303.82	702.20
3/21/60	2309.58	703.96	5/31/60	2303.28	702.04
3/22/60	2309.51	703.94			
3/23/60	2309.46	703.92	6/06/60	2302.83	701.90
3/24/60	2309.38	703.90	6/13/60	2301.88	701.61
3/25/60	2309.08	703.81	6/20/60	2300.45	701.18
3/26/60	2308.93	703.76	6/27/60	2300.77	701.27
3/27/60	2308.64	703.67			
3/28/60	2309.02	703.79	7/05/60	2300.32	701.14
3/29/60	2308.77	703.71	7/12/60	2299.60	700.92
3/30/60	2308.80	703.72	7/17/60	2299.26	700.81
3/31/60	2308.57	703.65	7/25/60	2298.87	700.69
			7/29/60	2299.14	700.78
4/01/60	2308.57	703.65			
4/02/60	2308.42	703.60	8/05/60	2296.01	699.82
4/03/60	2308.04	703.49	8/10/60	2298.64	700.62
4/04/60	2308.33	703.58	8/11/60	2298.41	700.55
4/05/60	2308.18	703.53	8/12/60	2298.49	700.58
4/06/60	2308.17	703.53	8/15/60	2298.80	700.67
4/07/60	2308.27	703.56	8/17/60	2298.50	700.58
4/08/60	2308.13	703.52	8/22/60	2298.25	700.50
4/09/60	2307.94	703.46	8/23/60	2298.24	700.50
4/10/60	2307;92	703.45	8/25/60	2298.28	700.51
4/11/60	2307.99	703.47	8/27/60	2298.20	700.49
4/12/60	2307.80	703.42			
4/13/60	2307.55	703.34	9/03/60	2297.86	700.39
4/14/60	2307.19	703.23	9/20/60	2297.07	700.04
4/15/60	2306.73	703.09			
4/25/60	2307.80		10/03/60	2297.01	700.03
			10/24/60	2296.07	699.84

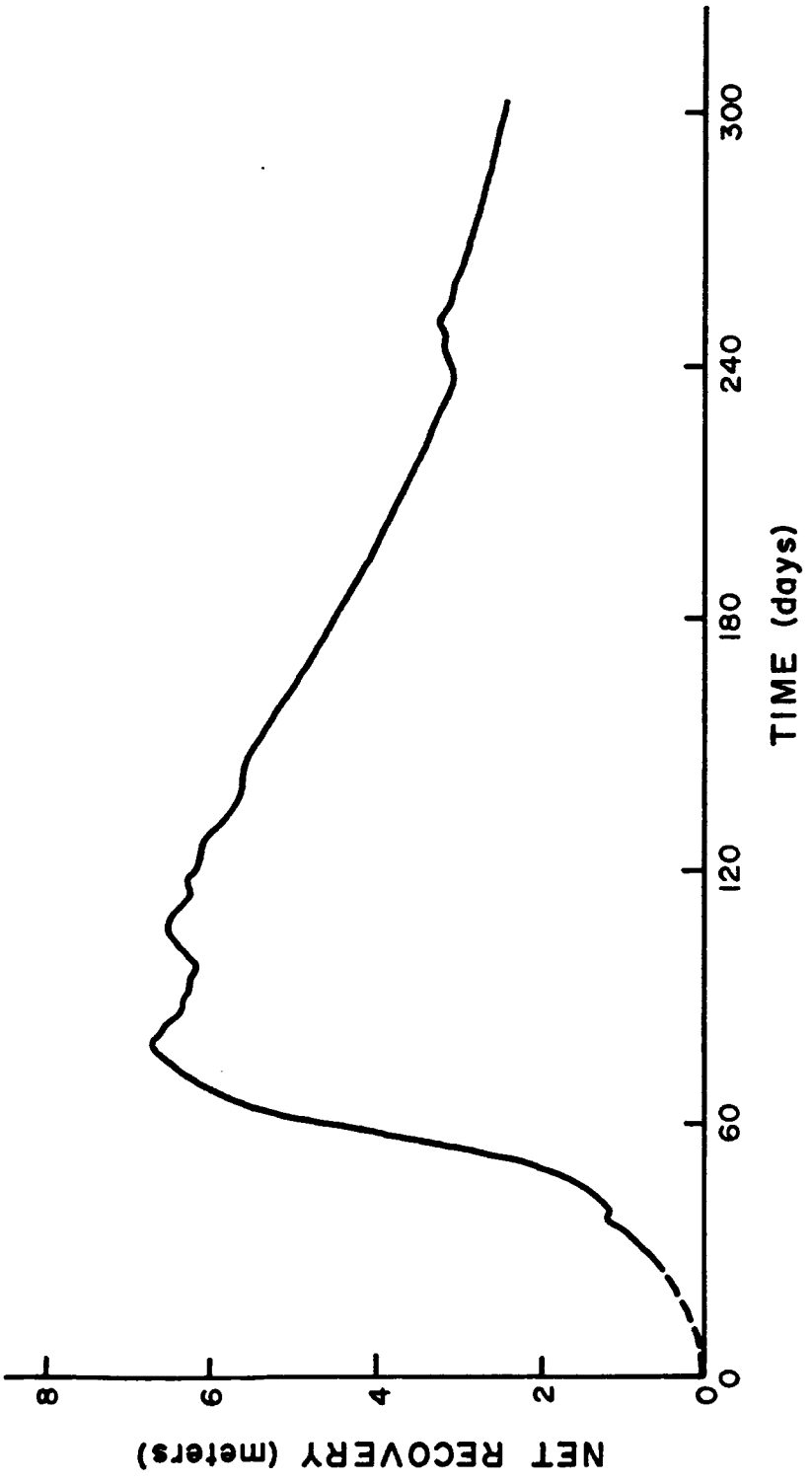

Figure B-13. Well hydrograph for Erwing #2.

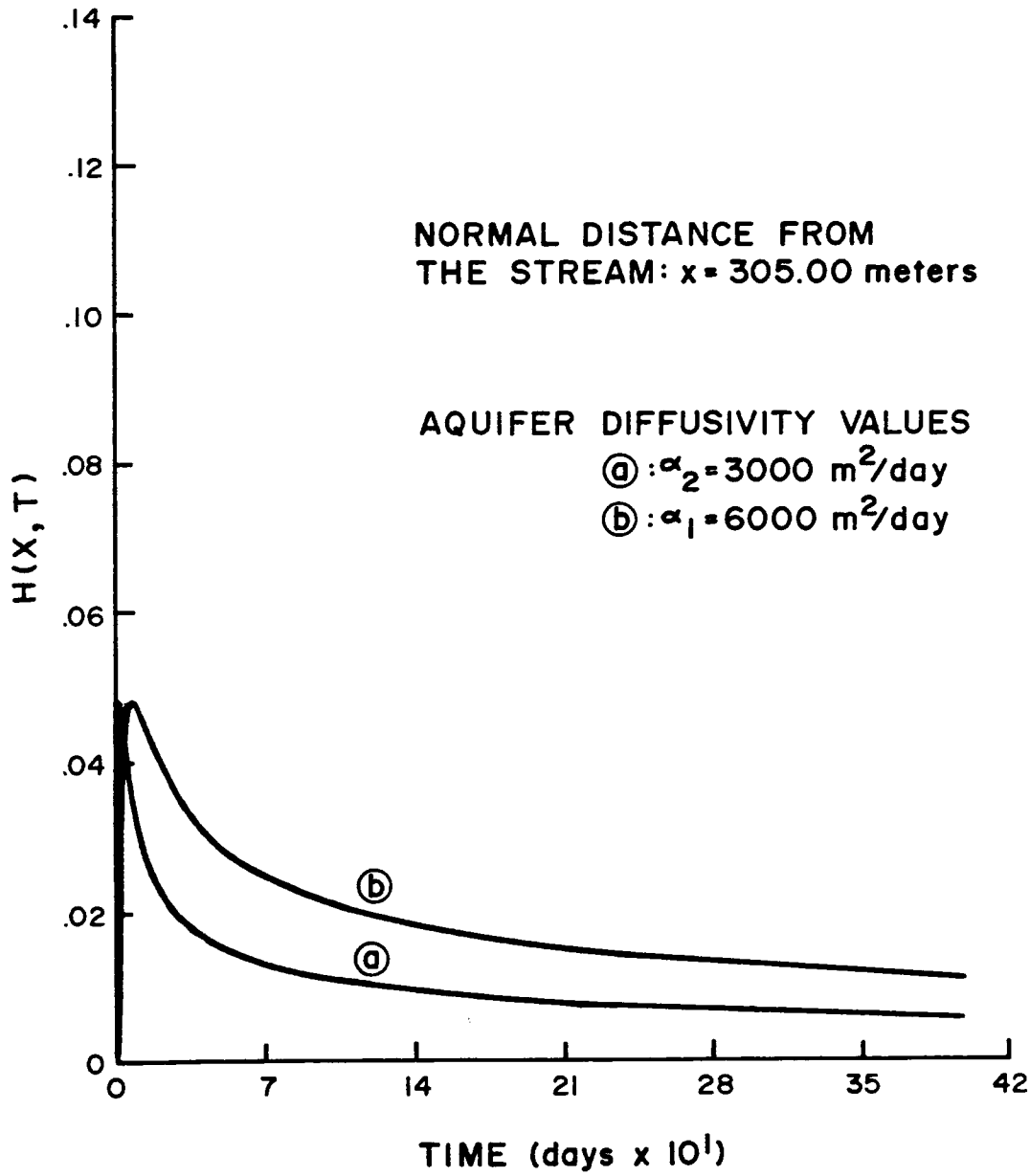

Figure B-14. Impulse reponse function for Erwing #2.

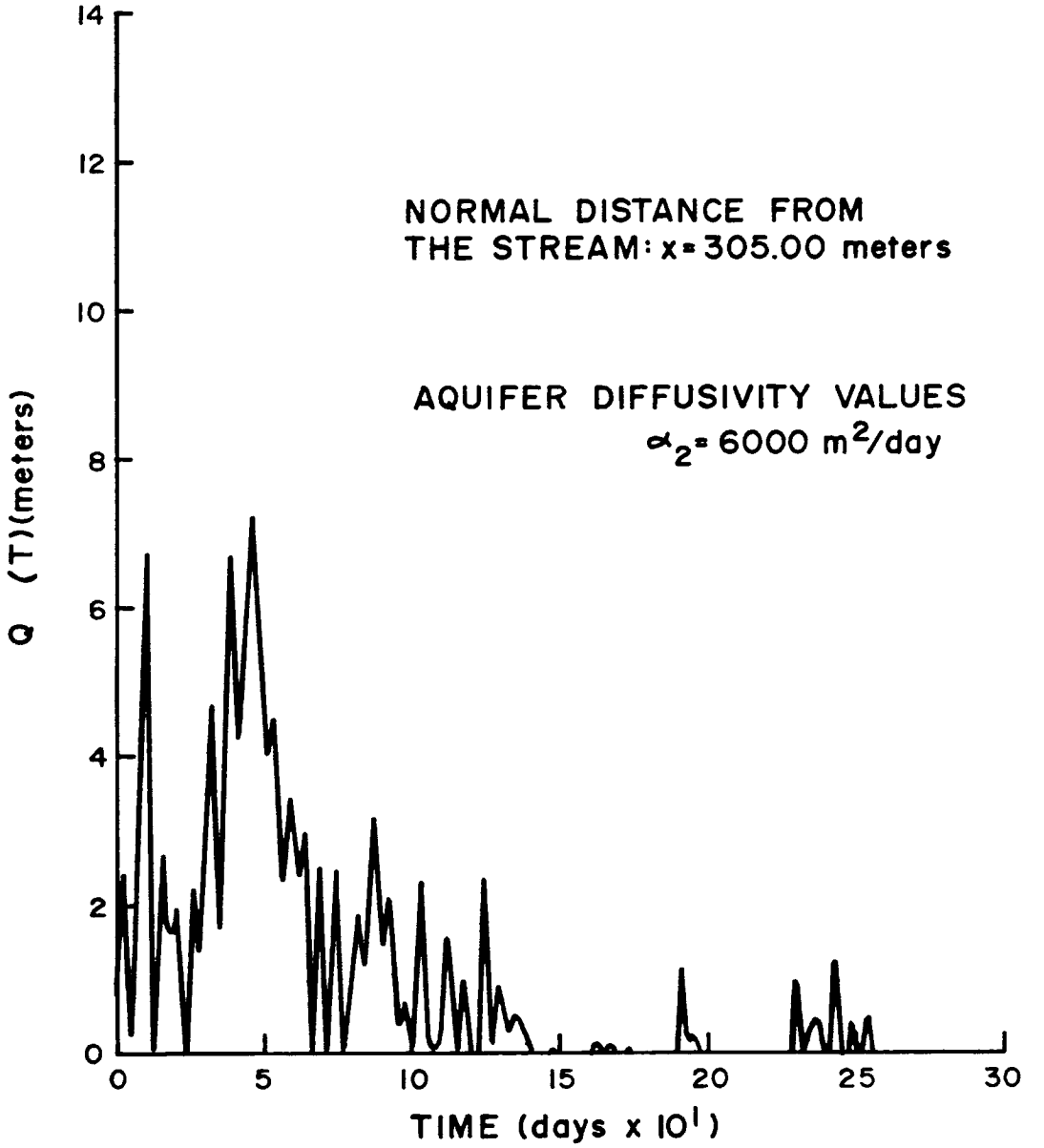

Figure B-15. System input function for Erwing #2.

Table B-7. Well Campbell #4, daily elevations of water table above mean sea level (December 1959 to November 1960)

Date	Water Level (feet)	Water Level (meters)	Date	Water Level (feet)	Water Level (meters)
12/26/59	2285.89	696.74	2/05/60	2301.64	701.54
12/27/59	2286.11	696.80	2/06/60	2301.83	701.60
12/29/59	2296.44	699.95	2/07/60	2302.20	701.71
12/30/59	2286.42	696.90	2/08/60	2302.66	701.85
12/31/59	2286.54	696.94	2/09/60	2302.78	701.89
			2/10/60	2302.78	701.89
1/01/60	2286.63	696.96	2/11/60	2302.99	701.95
1/02/60	2286.78	697.01	2/12/60	2303.16	702.00
1/03/60	2287.02	697.08	2/13/60	2303.47	702.10
1/05/60	2287.28	697.16	2/14/60	2303.71	702.17
1/06/60	2287.46	697.22	2/15/60	2303.97	702.25
1/07/60	2287.59	697.26	2/16/60	2304.07	702.28
1/08/60	2287.73	697.30	2/17/60	2303.96	702.25
1/09/60	2287.85	697.33	2/18/60	2304.26	702.34
1/10/60	2287.99	697.38	2/19/60	2304.24	702.33
1/11/60	2288.21	697.44	2/20/60	2303.94	702.24
1/12/60	2288.25	697.46	2/21/60	2304.21	702.32
1/13/60	2288.62	697.57	2/22/60	2304.47	702.40
1/14/60	2288.73	697.60	2/23/60	2304.15	702.30
1/15/60	2289.16	697.73	2/24/60	23-4.07	702.28
1/16/60	2289.16	697.73	2/25/60	2304.08	702.28
1/17/60	2290.04	698.00	2/26/60	2304.08	702.28
1/18/60	2290.68	698.20	2/27/60	2303.89	702.22
1/19/60	2291.35	698.40	2/28/60	2303.85	702.21
1/20/60	2291.98	698.59	2/29/60	2304.04	702.27
1/21/60	2292.69	698.81			
1/22/60	2293.43	699.04	3/01/60	2303.90	702.23
1/23/60	2294.20	699.27	3/02/60	2303.74	702.18
1/24/60	2295.03	699152	3/03/60	2303.78	702.19
1/25/60	2295.70	699.73	3/04/60	2303.85	702.21
1/26/60	2296.23	699.89	3/05/60	2303.78	702.19
1/27/60	2297.00	700.12	3/06/60	2303.59	702.13
1/28/60	2297.63	700.32	3/07/60	2303.42	702.08
1/29/60	2298.29	700.52	3/08/60	2303.56	702.12
1/30/60	2298.94	700.71	3/09/60	2302.70	702.17
1/31/60	2299.49	700.89	3/10/60	2303.77	702.19
			3/11/60	2303.85	702.21
2/01/60	2299.96	701.03	3/12/60	2303.95	702.24
2/02/60	2300.55	701.21	3/13/60	2304.01	702.26
2/03/60	2300.83	701.29	3/14/60	2303.13	701.99
2/04/60	2301.27	701.43	3/15/60	2304.23	702.33

Table B-7 -- continued

Date	Water Level (feet)	Water Level (meters)	Date	Water Level (feet)	Water Level (meters)
3/16/60	2304.60	702.44	5/02/60	2301.67	701.55
3/17/60	2304.53	702.42	5/09/60	2300.82	701.29
3/18/60	2304.57	702.43	5/16/60	2300.05	701.05
3/19/60	2304.48	702.40	5/23/60	2299.46	700.87
3/20/60	2304.39	702.38	5/31/60	2298.60	700.61
3/21/60	2304.53	702.42			
3/22/60	2304.60	702.44	6/06/60	2298.02	700.43
3/23/60	2304.55	702.42	6/13/60	2297.13	700.16
3/24/60	2304.52	702.41	6/20/60	2296.73	700.04
3/25/60	2304.31	702.35	6/27/60	2295.97	699.81
3/26/60	2304.26	702.34			
3/27/60	2304.20	702.32	7/05/60	2295.62	699.70
3/28/60	2304.35	702.36	7/12/60	2294.70	699.42
3/29/60	2304.10	702.29	7/17/60	2294.28	699.29
3/30/60	2303.43	702.08	7/25/60	2294.15	699.25
3/31/60	2303.79	702.19	7/29/60	2294.15	699.25
4/01/60	2303.69	702.16	8/05/60	2293.48	699.05
4/02/60	2303.73	702.17	8/10/60	2293.55	699.07
4/03/60	2303.49	702.10	8/11/60	2293.65	699.10
4/04/60	2303.72	702.17	8/12/60	2293.74	699.03
4/05/60	2303.55	702.12	8/15/60	2294.06	699.23
4/06/60	2303.39	702.07	8/17/60	2293.93	699.19
4/07/60	2303.42	702.42	8/22/60	2293.23	698.97
4/08/60	2303.36	702.36	8/23/60	2293.46	699.04
4/09/60	2303.22	702.02	8/25/60	2293.56	699.08
4/10/60	2303.13	701.99	8/27/60	2293.49	699.05
4/11/60	2303.22	702.02			
4/12/60	2303.88	702.22	9/03/60	2293.02	698.91
4/13/60	2302.27	701.73	9/10/60	2292.46	698.74
4/14/60	2302.10	701.68			
4/15/60	2302.09	701.68	10/03/60	2291.25	698.37
4/25/60	2302.22	701.71	10/24/60	2292.38	698.72
			11/7/60	2291.06	698.31

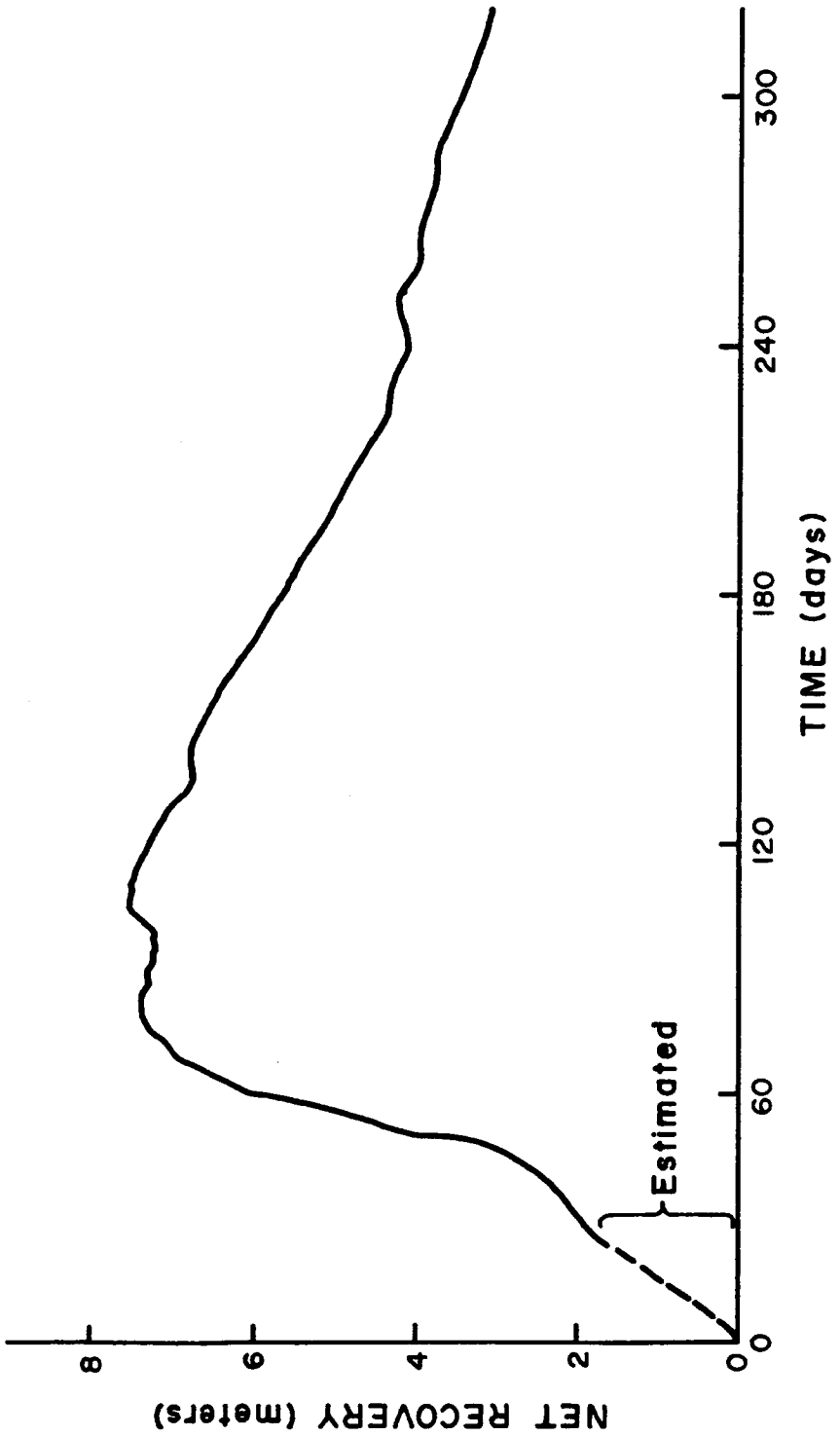

Figure B-16. Well hydrograph for Campbell #4.

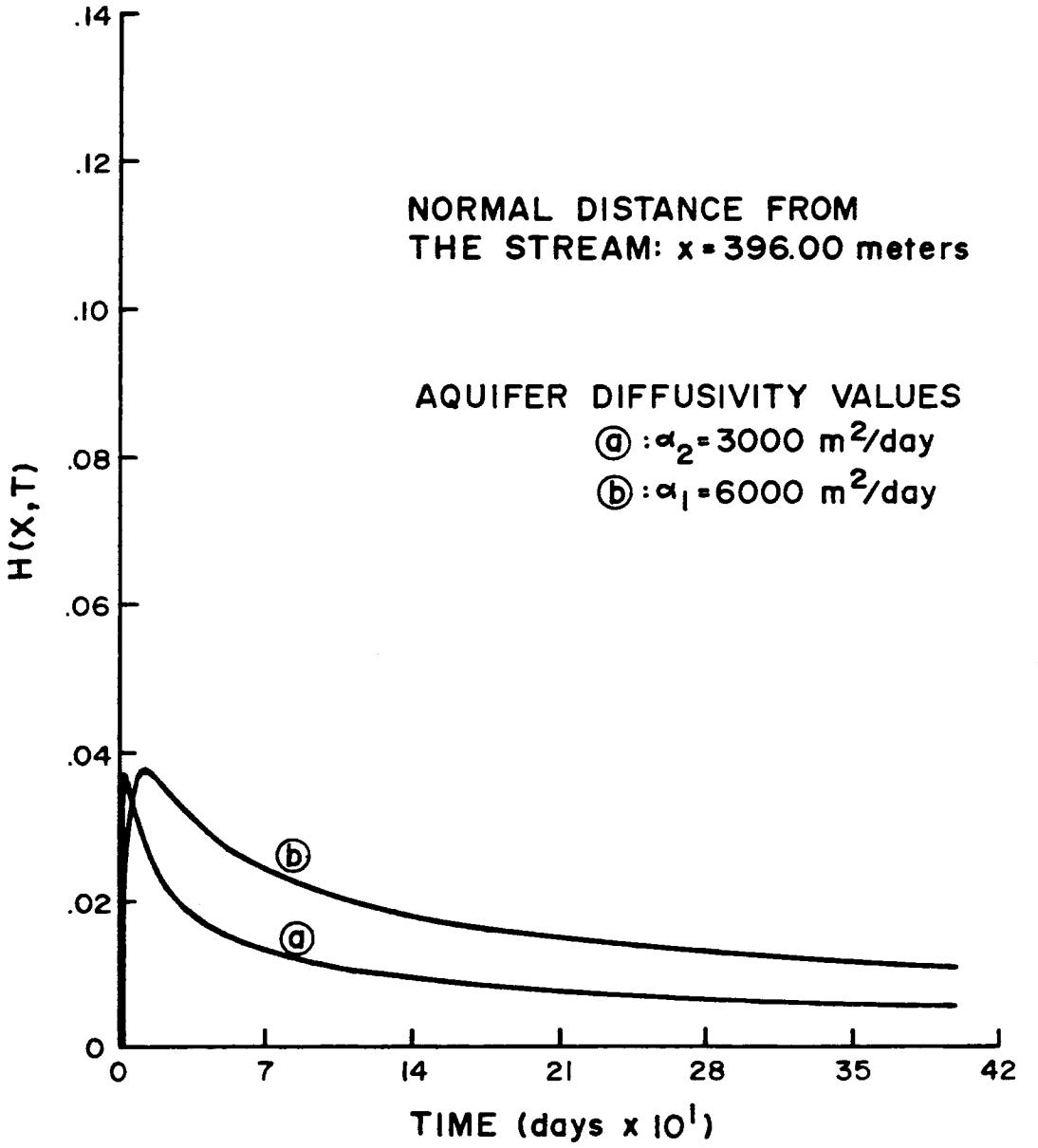

Figure B-17. Impulse response function for Campbell #4.

Table B-8. Well Nurphy #1, daily elevations of water table above mean sea level (February 1960 to December 1960)

Date	Water Level (feet)	Water Level (meters)	Date	Water Level (feet)	Water Level (meters)
2/02/60	2302.65	701.85	3/14/60	2313.77	705.24
2/03/60	2304.21	702.32	3/15/60	2313.86	705.26
2/04/60	2305.53	702.72	3/16/60	2313.99	705.30
2/05/60	2306.82	703.12	3/17/60	2314.07	705.33
2/06/60	2308.02	703.48	3/18/60	2314.11	705.34
2/07/60	2308.75	703.71	3/19/60	2314.17	705.36
2/08/60	2310.29	704.17	3/20/60	2314.12	705.34
2/09/60	2310.71	704.30	3/21/60	2314.13	705.34
2/10/60	2311.50	704.54	3/22/60	2314.10	705.33
2/11/60	2312.02	704.70	3/23/60	2314.05	705.32
2/12/60	2312.63	704.89	3/24/60	2314.00	705.31
2/13/60	2313.05	705.02	3/25/60	2314.00	705.31
2/14/60	2313.47	705.14	3/26/60	2313.95	705.29
2/15/60	2313.84	705.26	3/27/60	2313.91	705.28
2/16/60	2313.96	705.29	3/28/60	2313.78	705.24
2/17/60	2314.62	705.49	3/29/60	2313.66	705.20
2/18/60	2314.47	705.45	3/30/60	2313.56	705.17
2/19/60	2314.69	705.52	3/31/60	2313.43	705.13
2/20/60	2314.72	705.52			
2/21/60	2314.79	705.55	4/01/60	2313.28	705.09
2/22/60	2314.89	705.58	4/02/60	2313.01	705.00
2/23/60	2314.90	705.58	4/03/60	2313.00	705.00
2/24/60	2314.81	705.55	4/04/60	2312.94	704.98
2/25/60	2314.91	705.58	4/05/60	2312.77	704.93
2/26/60	2314.93	705.59	4/06/60	2312.70	704.91
2/27/60	2314.76	705.54	4/07/60	2312.53	704.86
2/28/60	2314.69	705.52	4/08/60	2312.41	704.82
2/29/60	2314.61	705.49	4/09/60	2312.21	704.76
			4/10/60	2312.01	704.70
3/01/60	2314.56	705.48	4/11/60	2311.88	704.66
3/02/60	2314.41	705.42	4/12/60	2311.79	704.63
3/03/60	2314.28	705.39	4/13/60	2311.62	704.58
3/04/60	2314.25	705.38	4/14/60	2311.57	704.50
3/05/60	2314.09	705.33	4/15/60	2311.38	704.51
3/06/60	2313.95	705.29	4/25/60	2310.26	704.17
3/07/60	2313.84	705.26			
3/08/60	2313.69	705.21	5/02/60	2309.05	703.79
3/09/60	2313.57	705.17	5/09/60	2308.66	703.68
3/10/60	2313.53	705.16	5/16/60	2308.01	703.48
3/11/60	2313.38	705.12	5/23/60	2307.39	703.29
3/12/60	2313.37	705.11	5/31/60	2306.42	702.99
3/13/60	2313.72	705.22			

Table B-8 -- continued

Date	Water Level (feet)	Water Level (meters)	Date	Water Level (feet)	Water Level (meters)
6/06/60	2305.65	702.76	8/23/60	2298.96	700.72
6/13/60	2303.68	702.16	8/25/60	2298.96	700.72
6/20/60	2304.00	702.26	8/27/60	2298.85	700.69
6/27/60	2303.10	701.98			
			9/19/60	2298.15	700.47
7/05/60	2302.29	701.74	9/26/60	2296.40	699.94
7/12/60	2302.42	701.78			
7/17/60	2301.02	701.35	10/03/60	2295.94	699.80
7/25/60	2300.53	701.20	10/10/60	2296.36	699.93
7/28/60	2300.30	701.13	10/17/60	2296.45	699.96
7/29/60	2299.95	701.02	10/24/60	2296.18	699.87
8/05/60	2299.70	700.95	11/01/60	2295.83	699.77
8/10/60	2299.51	700.89	11/07/60	2295.33	699.61
8/11/60	2299.47	700.88	11/14/60	2295.37	699.62
8/12/60	2299.41	700.86	11/22/60	2295.08	699.54
8/15/60	2299.26	700.81			
8/17/60	2299.07	700.75	12/01/60	2294.33	699.31
8/22/60	2299.04	700.74	12/10/60	2294.59	699.39
			12/23/60	2294.31	699.30

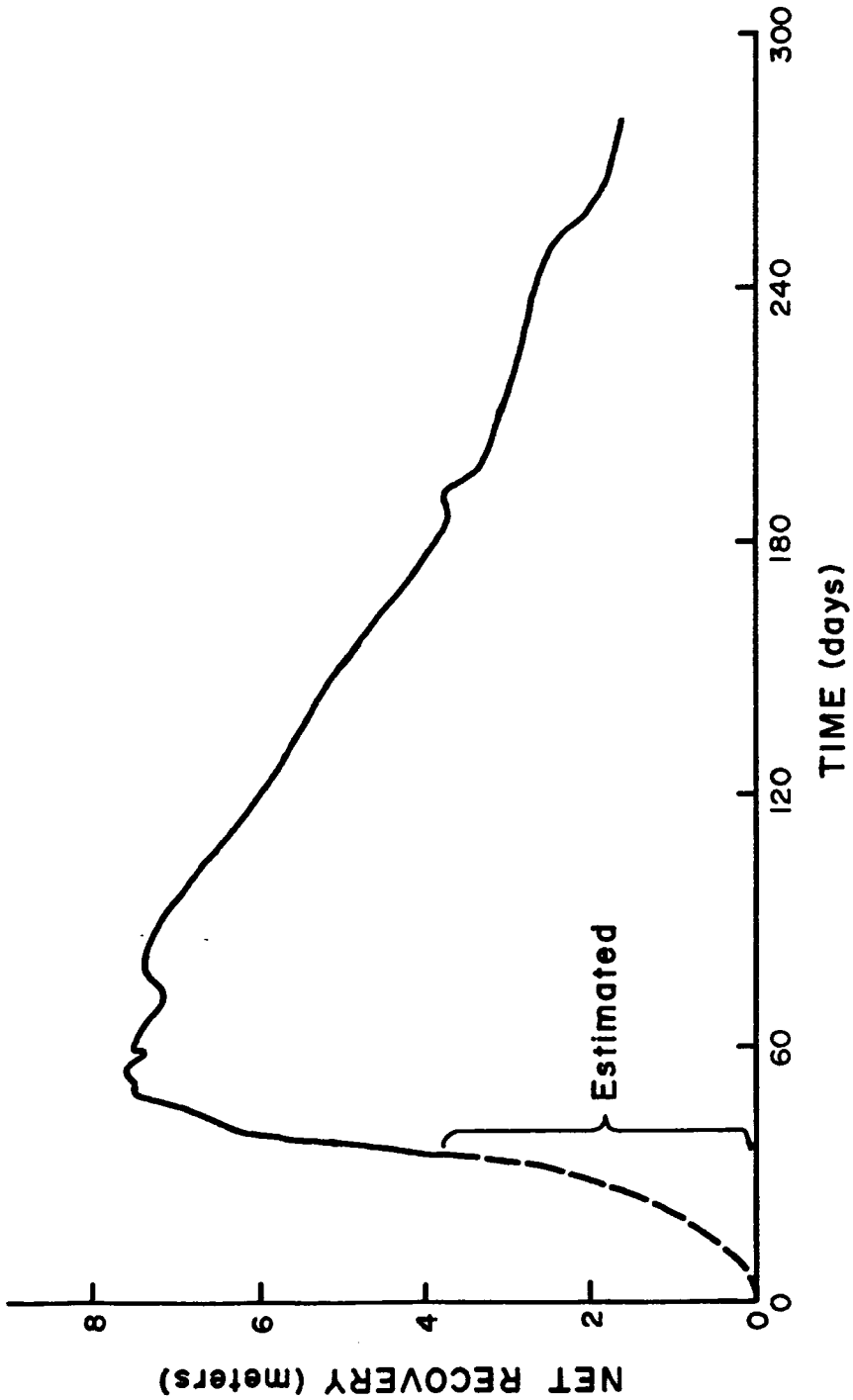

Figure B-18. Well hydrograph for Murphy #1.

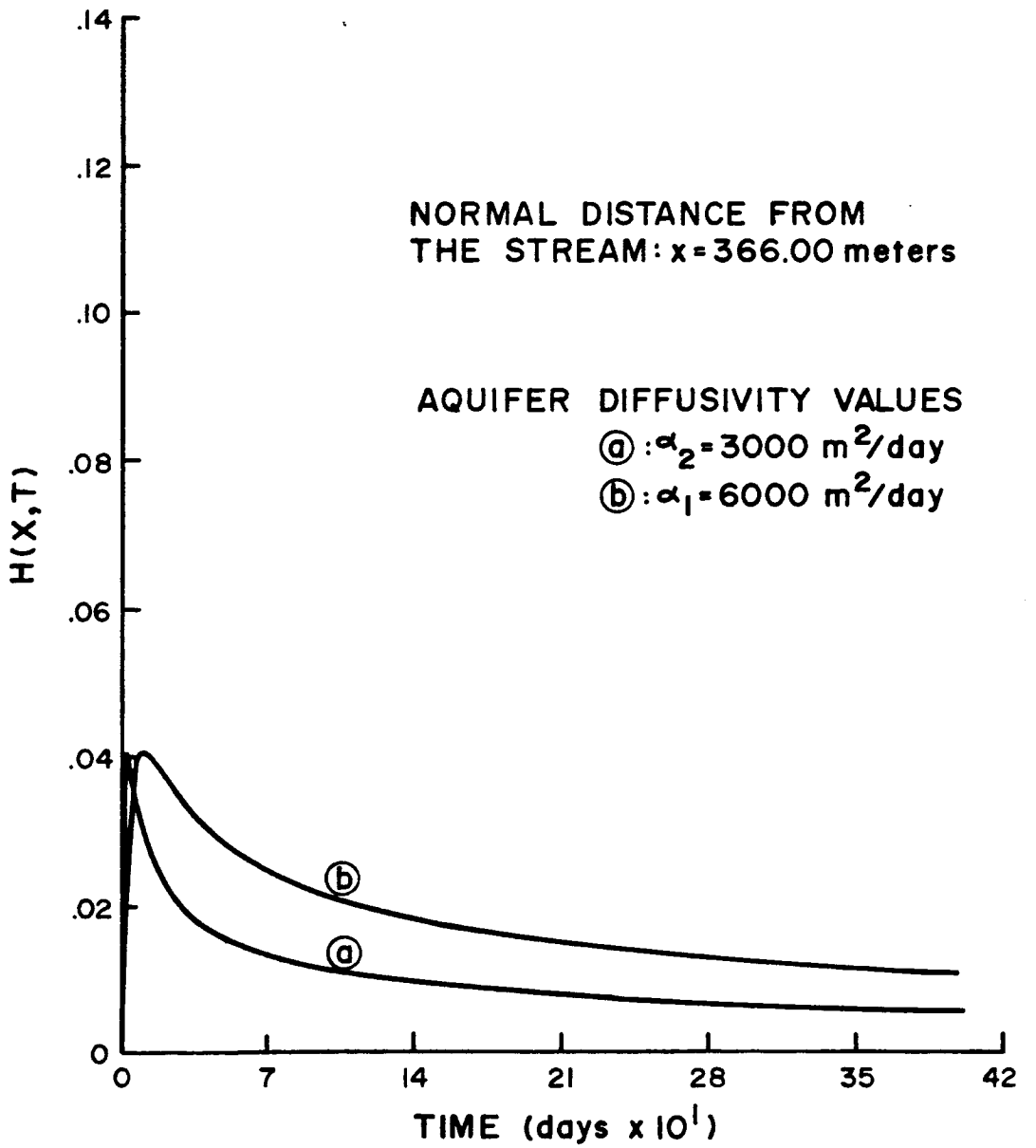

Figure B-19. Impulse response function for Murphy #1.

APPENDIX C

TRANSMISSION LOSS CALCULATIONS

From the U.S. Geological Survey gaging station records (1960), an average discharge (or inflow) is obtained for the days in which the flow rate was above 7 cubic feet per second (cfs). Seven cfs is taken as a threshold point. The transmission loss is calculated as follows:

Reach: Bear Creek to Point A

Q_{inflow} = 38.66 cfs

73 days above 7 cfs

Length of the reach = .8 miles

Substituting in Burkham's equation

$$Q_f = 0.18L(Q_{inflow})^{0.8}$$

$$Q_f = 0.18(.8)(38.66)^{0.8} = 2.68 \text{ cfs}$$

Converting Q_f to acre-feet over the 73 days

TL = 388.10 acre-feet

The above value is the transmission loss for the reach, Bear Creek to Point A. Hence, the outflow at Point A from the above reach is the measured discharge above 7 cfs at Bear Creek gaging station minus the calculated transmission loss of this reach averaged over the 73 days.

Reach: Sabino Creek to Point A

Q_{inflow} = 56.52 cfs

136 days above 7 cfs

Length of the reach = 1.8 miles

Substituting in Burkham's equation

$$Q_f = 0.18L(Q_{inflow})^{0.8}$$

$$Q_f = 0.18(1.8)(56.52)^{0.8} = 8.17 \text{ cfs}$$

Converting Q_f to acre-feet over the 136 days

TL = 2,204.27 acre-feet

This value is retained as transmission loss for the reach, Sabino Creek to Point A. The outflow at Point A from the above reach is calculated in the same manner as mentioned earlier.

Reach: Point A to Point B

Q_{inflow} is the sum of the outflow from the above two reaches, Bear Creek to Point A and Sabino Creek to Point A. The duration of the Q_{inflow} is assumed to be the longest period of the previous two reaches. Finally, the transmission loss of this reach is computed exactly in the same manner as earlier.

Following the same process of computation, the transmission losses for the remaining reaches are calculated and reported in Table 4.

REFERENCES

Anderson, T. V., 1972, Electric-analog analysis of the hydrologic system, Tucson basin, southeastern Arizona: U.S. Geological Survey Water-Supply Paper 1939-C, 34 p.

Aslyng, H. C. et al., 1963, Soil physics terminology, Inter. Soc. of Soil Sci. Bull. 23, p. 7.

Besbes, M., 1978, L'estimation des apports aux nappes souterraines, Unpublished Thèse de Doctorat d'Etat, University Pierre et Marie Curie, Paris VI, France, 270 p.

Besbes, M., Delhomme, J. P., and De Marsily, G., 1978, Estimating recharge from ephemeral streams in arid regions: a case study at Kairouan, Tunisia. Water Resources Research, v. 14, No. 2, p. 281-290.

Biswas, T. D., Nielsen, D. R., and Biggar, J. W., 1966, Redistribution of soil water after infiltration, Water Resources Research, v. 2, No. 3, p. 513-524.

Bredehoeft, J. D., Papadopulous, S. S., Cooper, H. H., 1982, Groundwater: The water-budget myth, in Scientific Basis of Water-Resource Management, Studies in Geophysics, Washington, D.C., p. 51-57.

Burkham, D. E., 1970, Depletion of streamflow by infiltration in the main channels of the Tucson basin, southeastern Arizona: U.S. Geological Survey Water-Supply Paper 1939-B, 36 p.

Colman, E. A., 1944, The dependence of field capacity upon depth of wetting of field soils, Soil Sci., v. 58, p. 48-50.

Crank, J., 1975, The Mathematics of Diffusion. Second Ed., Oxford University Press, Ely House, London W.1.

Davidson, E. S., 1973, Geohydrology and water resources of the Tucson basin, Arizona: U.S. Geological Survey Water-Supply Paper 1939-E, 81 p.

Davis, J. C., 1967, A geophysical investigation of hydrologic boundaries in the Tucson basin, Pima County, Arizona. Unpublished Ph.D. dissertation, University of Arizona, Tucson, 49 p.

Davis, J. C., 1973, Statistics and data analysis in geology: John Wiley and Sons, New York, 550 p.

Davis, S. N., and De Wiest, R. J. M., 1966, Hydrogeology, John Wiley & Sons, New York.

Evans, D. D., and Warrick, A. W., 1970, Time in transient of water moving vertically for ground-water exchange, in Proceedings of the Southwestern and Rocky Mountain Division of A.A.A.S.: Tucson, Arizona Agricultural Experiment Station Tech. Paper 11, p. 87-97.

Flug, M., Abi-Ghamen, G. V., and Duckstein, L., 1980, An event-based model of recharge from an ephemeral stream, Water Resources Research, v. 16, No. 4, p. 685-690.

Foster, K. E., 1969, Mathematical analysis of a natural recharge mound. Unpublished M.S. thesis, University of Arizona, Tucson.

Freeze, R. A., 1969, The mechanism of natural ground-water recharge and discharge: 1. One dimensional, vertical, unsteady, unsaturated flow above a recharging or discharging ground-water flow system, Water Resources Research, v. 5, No. 1, p. 153-171.

Freeze, R. A., and Cherry, K. A., 1979, Groundwater: Englewood Cliffs, New Jersey, Prentice-Hall, Inc.

Glover, R. E., 1961, Mathematical derivations as pertain to groundwater recharge, Agricultural, Fort Collins, Colorado, Mines, 81 p.

Gray, H. J., ed., 1958, Dictionary of Physics: Longmans, Green & Co., London, 544 p.

Gross, G. W., Hay, R. N., and Duffy, C. J., 1976, Application of environmental tritium in the measurement of recharge and aquifer parameters in a semi-arid limestone terrain: Las Cruces, New Mexico, OWRR project No. B-041-NMEX, New Mexico State University Water Resources Research Institute, 212 p.

Hillel, D., 1971, Soil and water: physical principles and processes, Academic Press, New York, 287 p.

Keith, S. J. S., 1981, Stream channel recharge in the Tucson basin and its implications for ground water management. Unpublished M.S. thesis, University of Arizona, Tucson, 84 p.

Lane, L. J., Diskin, M. H., and Renard, K. G., 1971, Input-output relationships for an ephemeral stream channel system: Journal of Hydrology, v. 13, p. 22-40.

Matlock, W. G., 1965, The effect of silt-laden water on infiltration in alluvial channels. Unpublished Ph.D. thesis, University of Arizona, Tucson, 102 p.

Moench, A. F., and Kisiel, C. C., 1970, Application of the convolution relation to estimating recharge from an ephemeral stream, Water Resources Research, v. 6, No. 4, p. 1087-1094.

Neuman, S. P., and De Marsily, G., 1976, Identification of linear systems response by parametric programming, Water Resources Research, v. 12, No. 2, p. 253-262.

Olson, M. C., 1982, Mountain-front recharge to the Tucson basin from Tanque Verde, Arizona. Unpublished M.S. thesis, University of Arizona, Tucson, 145 p.

Pashley, E. F., 1966, Structure and stratigraphy of the central, northern, and eastern parts of the Tucson basin, Arizona. Unpublished Ph.D. thesis, University of Arizona, Tucson, 273 p.

Polubaninova-Kochina, P. Ya., 1962, Theory of ground water movement, translated by R. J. M. de Wiest, Princeton University Press, Princeton, New Jersey, 613 p.

Remson, I., and Randolph, J. R., 1962, Review of some elements of soil-moisture theory, U.S. Geological Survey Professional Paper 411-D, 38 p.

Richards, L. A., 1936, Capillary conductivity data for three soils, J. Am. Soc. Agron., v. 28, p. 297-300.

Richards, L. A., and Weaver, L. R., 1944, Moisture retention by some irrigated soils as related to soil tension, J. Agr. Res., v. 69, p. 215-235.

Schofield, R. K., 1935, The pF of the water in soil, Trans. Third Intern. Congr. Soil Sci., v. 2, p. 37-48.

Simpson, E. S., Thorud, D., and Friedman, I., 1970, Distinguishing seasonal recharge to groundwater by deuterium analysis in southern Arizona, in World Water Balance Proceedings of the Reading Symposium, July 1970: International Association of Scientific Hydrology, p. 112-121.

Smith, G. E., 1910, Groundwater supply and irrigation in the Rillito valley: Tucson, Arizona, Bulletin No. 64, University of Arizona Agricultural Experiment Station, p. 81-243.

Soil Science Society of America, 1956, Report of definitions approved by the Committee on Terminology: Soil Sci. Soc. America Proc., v. 20, No. 3, p. 430-440.

Sorey, M. L., 1967, Evaporation from streambed materials in the Tucson area, Unpublished M.S. thesis, University of Arizona, Tucson, 76 p.

Staple, W. J., 1962, Hysteresis effects in soil moisture movement, Can. J. Soil Sci., v. 42, p. 247-253.

Theis, C. V., 1940, The source of water derived from wells: Essential factors controlling the response of an aquifer to development, Civil Eng., v. 10, p. 277-280.

Turner, S. F., and others, 1943, Ground-water resources of the Santa Cruz Basin, Arizona: U.S. Geological Survey Open-File Report, 84 p.

U.S. Geological Survey, Water Resources Division, 1961, Surface water supply of the United States, 1960, Part 9, Colorado River Basin. Prepared in cooperation with the States of Arizona and with other agencies. Geological Survey Water-Supply Paper 1713.

van Hylckama, T. E. A., 1982, Personal communication: U.S. Geological Survey, Tucson, Arizona.

Water Resources Research Center, University of Arizona, 1980, Regional recharge research for southwest alluvial basins: Tucson, p. 5.1-5.51.

Wilson, L. G., and De Cook, K. J., 1968, Field observations on changes in the subsurface water regime during influent seepage in the Santa Cruz river, Water Resources Research, v. 4, No. 6, p. 1219-1234.

Youngs, E. G., 1958, Redistribution of moisture in porous materials after infiltration, 1, Soil Sci., v. 86, p. 117-125.